M-PM-Sym-1 MOLECULAR RECOGNITION AND THE IMMUNOGLOBULIN GENE SUPERFAMILY. Leroy E. Hood, Division of Biology, California Institute of Technology, Pasadena, CA 91125.

M-PM-Sym-2 THE THREE-DIMENSIONAL STRUCTURES OF ANTIGEN-ANTIBODY COMPLEXES.
David R.Davies, National Institutes of Health, Bethesda MD 20892
The crystal structures of two lysozyme:anti-lysozyme complexes are described. (Sheriff et al 1987 PNAS 84 9075; Davies et al 1988 J.Biol.Chem. 263 10541; Padlan et al 1989 PNAS). The interaction between the antibody and the lysozyme is tight in both cases, excluding almost all water molecules and covering an area of about 700A^2. In both cases all six CDRs contribute at least one side chain to the interface. A third such such lysozyme complex has also been reported. (Amit et al 1986 Science 233 747). Together, these complexes cover half the surface area of the lysozyme, and provide a basis for analyzing the nature of lysozyme antigenicity. Data will be presented summarizing the nature of the epitopes in terms of properties such as complementarity, charge interactions, mobility and accessibility. It has been proposed that conformational change can also occur upon antigen binding (Colman et al 1987 Nature 326 358). This will be discussed by reference to the present data.

M-PM-Sym-3 CATALYTIC ANTIBODIES. Richard A. Lerner. Department of Molecular Biology, Research Institute of Scripps Clinic, 10666 North Torrey Pines Road, La Jolla, CA 92037

Monoclonal antibodies have been elicited to haptens in which an organophosphorus moiety imparts the stereoelectronic properties of an esterolytic transition state for analogous carboxylic esters. Some of these antibodies were found to react specifically and stoichiometrically with activated esters that share certain structural features with the hapten. Studies on the effect of chemical modification of amino acids in the protein implicate the involvement of a histidine and a tyrosine residue of the combining site in the acyl transfer mechanism. One of these residues is presumed to be acylated in the reaction. These same antibodies are also shown to behave as enzymic catalysis with the appropriate ester substrates. These substrates are distinguished by the structural congruence of both hydrolysis products with haptenic fragments, as well as the correspondence of the acyl center with the phosphono group of the hapten. The divergent mechanisms are based on the difference in leaving group ability between the hydrolysis substrates and esters which covalently combine with the antibody. The antigenic phosphonates are potent inhibitors of the reactions in accord with their assigned role as transition state analogs. These experiments demonstrate that antibody-antigen binding may be directed to chemical processis, according to the prevailing theory which relates binding energy to enzyme function. The generation of artificial enzymes through transition state stabilization by antibodies has long been expected as a corollary to Pauling principle catalysis. These observations provide evidence towards the fullfillment of that prediction.

M-PM-Sym-4 MOLECULAR KINETICS OF IMMUNE RECOGNITION, Harden M. McConnell and Scheherazade S. Nasseri, Stauffer Laboratory for Physical Chemistry, Stanford, CA 94305

We have studied the binding and dissociation kinetics of an antigenic peptide p (pigeon cytochrome c 88-104) and a membrane protein M in a planar lipid bilayer on a glass slide. Here M is an affinity purified class II protein of the murine major histocompatibility complex (IE^k). These kinetics have been measured using fluorescence techniques, and the N-terminal fluorescinated peptide. The kinetics have also been studied by measuring the specific production of interleukin-2 (IL-2) by a T-helper cell hybridoma 2B4 in the presence of complexes of p and M in planar bilayers. For references to the use of supported bilayers to study T-cell triggering, see (1). The kinetics have been interpreted in terms of a two-step reaction

$$p + M \underset{k_{io}}{\overset{k_{oi}}{\rightleftharpoons}} (pM)_i \underset{k_{ti}}{\overset{k_{it}}{\rightleftharpoons}} (pM)_t$$

where $(pM)_i$ is an intermediate complex that shows peptide and IE^k specificity. Our estimated rate constants for the four steps are

$k_{oi} \sim 10^2$ ℓ/mol-sec, $k_{it} \sim 4 \times 10^{-4}$ sec^{-1}, $k_{ti} = 6.3 \times 10^{-6}$ sec^{-1}, and $k_{io} = 1.2 \times 10^{-3}$ sec^{-1}.

These experiments and results will be discussed with special reference to peptide specificity and the molecular structures of class I and class II molecules of the major histocompatibility complex (2). Supported by NIH. (1) T.H. Watts & H.M. McConnell, Ann. Rev. Immunol. 5, 461-475 (1987).
(2) P.J. Bjorkman et al. Nature 329, 506-512; 512-518 (1987); J.H. Brown et al. Nature 332, 845-850 (1988).

M-PM-Sym-5 B AND T EPITOPES ON THE NICOTINIC RECEPTOR MOLECULE. Bianca M. Conti-Tronconi, Dept. of Biochemistry, CBS, University of Minnesota, St. Paul, MN 55108. The nicotinic acetylcholine receptor(AcChR) is formed by four homologous subunits($\alpha_2\beta\gamma\delta$). In the disease myasthenia gravis(MG) autoantibodies against AcChR are produced, under the control of specific T-helper cells. We studied the structure of the surface domains recognized by anti-AcChR autoantibodies, and the sequence segments forming epitopes recognized by anti-AcChR T-helper cells. Two important epitopes on the AcChR α subunit recognized by antibodies in MG patients are the so-called Main Immunogenic Region(MIR), and the binding site(s) for cholinergic ligands. The binding of anti-MIR monoclonal antibodies(mAbs) was studied using panels of synthetic peptides, corresponding to the complete sequences of the human and Torpedo α-subunits. A main constituent loop of the MIR was localized between residues 67 & 76. Binding of anti-MIR mAbs to peptides containing single residue substitutions of the native sequence allowed identification of residues directly involved in antibody binding. We studied the binding to the same synthetic peptides of snake toxin cholinergic antagonists and of anti-AcChR mAbs able to inhibit the binding of cholinergic ligands. Both the toxins and the antibodies recognized peptides containing the sequence α185-200, and two other peptides in the aminoterminal part of the α-subunit. A similar approach was used to identify a sequence segment of neuronal AcChR forming the binding site for cholinergic ligands. AcChR specific T-helper cell lines obtained from different MG patients recognized primarily the α-subunit. Synthetic peptides corresponding to the sequence segment α1-22, which has a strong propensity to form an amphipatic α-helix, elicited up to 30% of the response induced by native AcChR. Different peptides were recognized by the autoreactive T cells of different patients. This suggests that the NH_2-terminal region of the AcChR α subunit contains important T cell epitopes, and that the T cell response in MG is heterogeneous.

M-PM-Min-1 ACTIN-BINDING PROTEINS - FUNCTIONAL INSIGHTS FROM THE PRIMARY STRUCTURE AND GENE DISRUPTION EXPERIMENTS IN DICTYOSTELIUM DISCOIDEUM. Angelika Noegel, Max-Planck-Institute for Biochemistry, 8033 Martinsried, FRG.

Dictyostelium discoideum is a motile organism which exhibits a polarized movement under the influence of chemotactic factors. The ease of cultivation of D.discoideum has facilitated the isolation of proteins that are associated with the actin filament system. cDNA clones coding for several of these proteins have been isolated and their sequence has been determined. Sequence comparison revealed a high homology to actin-binding proteins isolated from other organisms. The knowledge of primary structures led to the identification of an F-actin binding site in cross-linking proteins and of putative regulatory sites (e.g. EF-hand structures in α-actinin).
Dictyostelium is a haploid organism which is amenable to genetic manipulation since the description of a transformation system. For investigation of the in vivo role of actin-binding proteins, the corresponding genes can be specifically inactivated by gene disruption via homologous recombination or by the anti-sense RNA technique. Mutants lacking several actin-binding proteins have been generated and analysed. In addition, development of an extrachromosomal vector allows introduction into and expression in D.discoideum of in vitro modified genes coding for actin-binding proteins.

M-PM-Min-2 PROFILIN - LESSONS FROM THE 3-DIMENSIONAL STRUCTURE. Thomas D. Pollard, Department of Cell Biology and Anatomy, Johns Hopkins Medical School, Baltimore, MD.

The profilins are small actin monomer binding proteins consisting of 125 to 140 residues that also interact with acidic phospholipids and polyproline. The primary structures of profilins from Acanthamoeba, yeast and vertebrates established that all of the proteins named profilin had a common ancestor, but all have diverged from each other during evolution. Karen Magnus has determined the structure of Acanthamoeba profilin at 2.4 A resolution by x-ray crystallography and is refining the structure. (See poster by Magnus, Lattman and Pollard at this meeting.) The N-terminal half consists of 2 layers of aligned beta sheets. The C-terminal half is folded into 5 alpha-helices on the top of the molecule. The bottom is largely uncharged while the top is rich in basic residues. In the complex of amoeba profilin and actin, lys-115 of profilin can be chemically crosslinked to glu-364 of actin through a zero length bond. Acidic phospholipids such as PIP_2 compete with actin for binding to profilin, most likely because they too bind to the positively charged top of the molecule. The region surrounding lys-115 has sequence homology with the larger actin filament capping proteins including gelsolin and fragmin, suggesting that they share a common actin binding structure (Ampe and Vandekerckhove, 1987). The domain structures of these larger proteins to be presented by the other speakers provides evidence that this family of proteins evolved through gene duplication from a small ancestral protein about the size of profilin. Profilin is generally believed to function as an actin-monomer buffer in the cell, but both in platelets and amoeba the affinity of profilin for actin and the molar ratio to actin are so low that other factors are necessary to account quantitatively for the pool of unpolymerized actin. Consequently, it is worth considering that profilin may have another primary function such as regulating lipid metabolism.

M-PM-Min-3 GELSOLIN: FUNCTIONAL INSIGHTS FROM PROTEOLYTIC FRAGMENTS AND EXPRESSED cDNA SEQUENCES. D.J. Kwiatkowski, P.A. Janmey, and H.L. Yin. Hematology-Oncology Unit, Massachusetts General Hospital and the Department of Medicine, Harvard Medical School, Boston, MA 02114.

Gelsolin belongs to a family of Ca^{2+}-regulated actin modulating proteins found throughout the animal kingdom, which can sever actin filaments, nucleate actin filament assembly and cap the fast growing end of actin filaments. We report here studies designed to delineate critical domains within gelsolin by deletional mutagenesis, using Cos cells to secrete truncated plasma gelsolin after DNA transfection. Deletion of 11% of gelsolin from the C-terminus resulted in a major loss of its ability to promote the nucelation step in actin filament assembly, suggesting that a C-terminal domain is important in this function. In contrast, the polyphosphoinositide (PPI)-regulated actin filament severing activity of gelsolin was retained in a derivative containing only 21% of the N-terminal sequence. Combined with previous results using proteolytic fragments, we deduce that an eleven amino acid sequence in the N-terminus mediated PPI-regulated binding of gelsolin to the sides of actin filaments prior to severing. Deletion of only 3% of the C-terminal sequence, including a dicarboxylic acid sequence similar to the N-terminus of actin, resulted in a loss of Ca^{2+}-requirement for filament severing and monomer binding. Since this region in actin has been implicated as a binding site for gelsolin, our results suggests that this C-terminal sequence may act as a Ca^{2+}-regulated pseudosubstrate. Unexpectedly, deletion of 69% of the C-terminal residues led to the reappearance of a Ca^{2+} requirement for severing. Although this site may be cryptic in gelsolin, it is likely to mediate the Ca^{2+}-regulation of severing by related proteins such as villin, severin and fragmin, because these proteins lack the C-terminal gelsolin-like regulatory site.

M-PM-A1 TIME COURSE OF CARDIAC Ca^{2+} CURRENT AFTER A CONCENTRATION JUMP OF ISOPROTERENOL. A. Yatani, K. Okabe and A.M. Brown. Department of Physiology and Molecular Biophysics, Baylor College of Medicine, One Baylor Plaza, Houston, TX 77030.

Previously we reported that the G protein stimulatory regulator of adenylyl cyclase, G_s, regulates cardiac Ca^{2+} channels not only through a cascade of intermediary cytoplasmic events but also through direct membrane delimited events as in the case of the G protein, G_k and muscarinic K^+ channels. If G_s directly activates Ca^{2+} channels one might expect that β-agonist effects would have a latency of 50 to 150 ms similar to the latency for activation of K^+ channels following application of muscarinic agonists. To test this, we measured the latency of the action of Isoproterenol (ISO) on whole-cell Ca^{2+} currents (I_{Ca}) of single guinea pig atrial myocytes using the concentration-clamp technique which produced concentration jumps with a time constant of ~3 ms. Results: (1) ISO at 10 nM to 10 μM, increased I_{Ca} within 50 msec after application. Activation by ISO had two phases that were fitted with the sum of two exponentials. At 10 μM of ISO, the time constants were 200 msec and 30 sec. (2) In contrast to ISO, activation of I_{Ca} by Forskolin had a single exponential time course with a time constant of 40 sec. (3) GDPβS at 840 μM in the pipette blocked the fast phase of the ISO effect completely and the slow phase by about 80%. (4) GDPβS had no effects on the Forskolin response. (5) Preincubation of the β-blocker propranolol at 5 μM blocked both fast and slow phases of ISO effects. These results show that G_s activates cardiac Ca^{2+} channels through direct and cytoplasmic pathways.

M-PM-A2 ACETYLCHOLINE INHIBITS MOSTLY A SUSTAINED RATHER THAN AN INACTIVATING COMPONENT OF THE CALCIUM CURRENT IN RAT SYMPATHETIC NEURONS. Diomedes E. Logothetis, Mark R. Plummer, Peter Hess, and Bernardo Nadal-Ginard, Depts. of Cardiology at Children's Hospital and Physiology at Harvard Medical School, Boston MA. 02115.

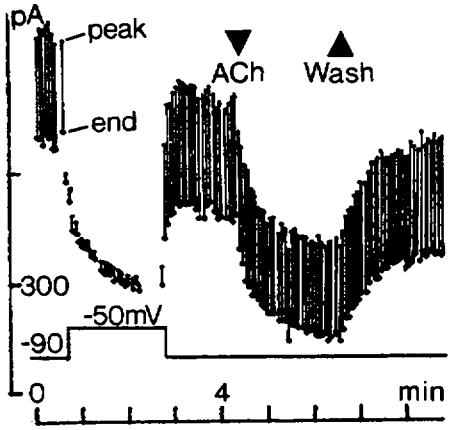

Sympathetic neurons mechanically dissociated from the superior cervical ganglion (SCG) of 1 to 4-day-old rats were studied by whole-cell patch clamp.
It has been recently reported (Wanke et al (1987) PNAS 84, 4313-4317) that Acetylcholine (ACh) acting via GTP-binding proteins selectively inhibits a rapidly inactivated Ca current in SCG cells. Under our experimental conditions ACh inhibited mostly a long-lasting component of the Ca current rather than an inactivating one. We obtained the same result using 10, 50, or 100uM ACh. Intracellular perfusion with nonhydrolyzable guanine nucleotide analogs (100uM GTPgS) on the other hand abolished the inactivating current and also inhibited a long-lasting component of the Ca current. These results suggest that in SCG cells modulation of Ca channels by GTP binding proteins is not selectively targeted towards the inactivating component of the Ca current.

M-PM-A3 AN ENDOGENOUS PURIFIED GLYCOPEPTIDE MODIFIES Ca^{2+} CHANNELS IN CARDIAC MYOCYTES AND NEURONS. G. Callewaert, *I. Hanbauer and M. Morad. Department of Physiology, University of Pennsylvania, Philadelphia, PA and *NHLBI, NIH, Bethesda, MD.

An endogenous glycopeptide (EM) with a molecular weight of 1100 Daltons was recently extracted and purified from rat brain. EM inhibited specifically and reversibly ^{3}H-nitrendipine binding and $^{45}Ca^{2+}$-uptake in neuronal cells. Acid hydrolysis of EM decreased its inhibitory effect on $^{45}Ca^{2+}$-uptake and on ^{3}H-nitrendipine binding. The amino-acid composition of the hydrolysate was: 55% Asp, 25% Glu, 5% Gly, 5% Thr and two unidentified peaks. To substantiate the role of EM in modulating Ca^{2+} channel activity, we examined its effect on i_{Ca} in cardiac and neuroblastoma cells using the patch-clamp technique. In guinea pig ventricular myocytes 1-2 units EM (1 unit displaces 50% of ^{3}H-nitrendipine) caused a 100-300% increase in i_{Ca} with little effect on its time course. This was observed at all potentials and was slowly and partially reversible. The effect of EM was unaltered by cAMP, GTP-γ-S or GDP-β-S in the pipette or by perfusing the cell with α_1- or β-adrenergic blockers, indicating that the effect of EM was not mediated through a G-protein-dependent pathway. EM-effect was not mimicked by GABA, L-glutamate or glycine. After acid hydrolysis EM had no effect on i_{Ca}. In neuroblastoma cells, on the other hand, 1-2 units of EM caused a reversible depression of both $i_{Ca(L)}$ and $i_{Ca(T)}$. Acid hydrolysis of EM reduced this inhibitory effect. Our results, therefore, suggest that EM regulates the Ca^{2+} channel activity in cardiac and neuronal cells. Supported by NIH #RO1 HL16152.

M-PM-A4 **MODE 2 BEHAVIOR OF CARDIAC L-TYPE Ca CHANNELS FAVORED BY A cAMP DERIVATIVE**

David T. Yue, Stefan Herzig, and Eduardo Marban[1]. Depts. of Biomedical Engineering and Medicine[1] (Cardiology), The Johns Hopkins University School of Medicine, Baltimore, MD 21205

The regulation of L-type Ca channel activity has been proposed to involve shifts of the channel between 3 distinct gating modes (Hess, Lansman, and Tsien, 1984). While MODE 2 gating behavior, characterized by long-lasting openings, is promoted by the Ca channel agonist Bay K 8644, no endogenous factor has yet been shown to favor this striking pattern of gating. We now report that addition of the membrane permeant cAMP derivative 8-Br-cAMP increases the occurrence of MODE 2 behavior. Cell-attached recordings of single L-type Ca channels were obtained from guinea-pig ventricular myocytes, with 70 mM $BaCl_2$ in the pipette. Bath application of a high concentration of 8-Br-cAMP (1 mM) not only produced an increase in the proportion of active sweeps (0.39+.10 vs 0.78+.13), but also a striking enhancement of the fraction of active sweeps exhibiting MODE 2 behavior from 0.0094+.001 to 0.156+.09 (mean ± SEM, n=3), as illustrated by the representative traces (right). For purposes of quantitation, MODE 2 behavior was defined by periods lasting > 20 ms with mean open probability > 0.7. Our results suggest that ultra-long-lasting openings are caused by high levels of cAMP-dependent channel phosphorylation, and that enhancement of MODE 2 gating constitutes one mechanism by which the Ca channel is regulated by adrenergic stimulation.

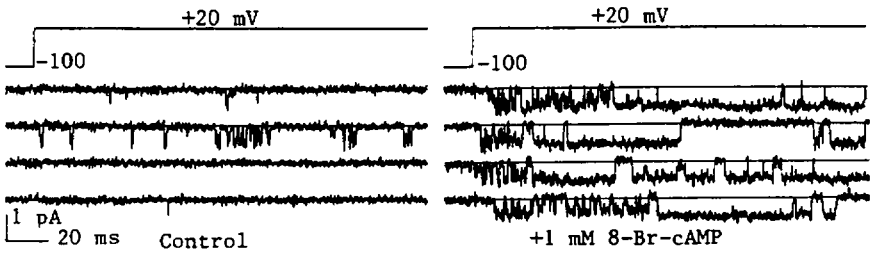

M-PM-A5 **ENDOTHELIN MODULATES CA^{2+} CHANNELS IN CORONARY ARTERY SMOOTH MUSCLE CELLS.** S.D. Silberberg, T.C. Poder, A.E. Lacerda and A.M. Brown. (Intr. by J.M. Caffrey). Dept. of Physiology and Molecular Biophysics, Baylor College of Medicine, One Baylor Plaza, Houston, TX 77030.

Endothelin is the most potent vasoconstrictor presently known. Its action on voltage-dependent calcium channels conducting sodium ions was studied in single, freshly dissociated, porcine coronary artery smooth muscle cells using the cell-attached mode of the patch clamp technique. The patch of membrane under the pipette was voltage clamped to -100 mV and stepped to -50 or to -30 mV for 700 ms, every 3 sec. Endothelin at 50 nM, applied outside the pipette, increased channel activity by increasing the frequency with which bursts occurred (n=3). P_o increased by 22% to 685%. Channel open time and conductance were not altered. Single channel currents were identified as high-threshold (L-type) calcium channel currents by their voltage-dependence, time characteristics and dihydropyridine sensitivity. Furthermore, in whole-cell voltage clamp experiments, only high-threshold calcium currents were detected in these cells. Bay K 8644 (50 nM) increased I_{Ca} 2-5 fold while Nitrendipine (10^{-6} M) blocked I_{Ca} by 50%. The ability of bath-applied endothelin to increase single channel calcium currents in the cell-attached mode shows that the peptide acts via a second messenger system. These findings may account for the dependence of endothelin-induced vasoconstriction on extracellular calcium. (Supported by HL36930 and HL37044.)

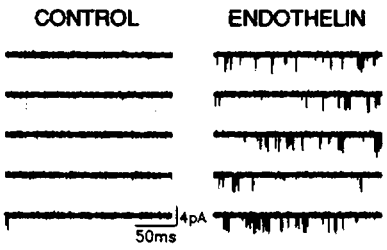

M-PM-A6 PHOTO-RELEASE OF GTP-γ-S INHIBITS T-TYPE CALCIUM CHANNEL CURRENTS IN RAT DORSAL ROOT GANGLION (DRG) NEURONES.

R.H. Scott, A.C. Dolphin and J.F. Wootton* Dept. of Pharmacology, St George's Hospital Medical School, London SW17 0RE, UK and *Dept. of Physiology, Cornell University, Ithaca, USA (intro by T. Bolton).

We have shown that photo-release of GTP-γ-S or GMP-PNP within DRGs differentially inhibits the transient component of the high threshold Ca^{2+} channel current. The photosensitive (O- and S-caged) nitrophenylethyesters of GTP-γ-S (100μM) were included in the intracellular solution in patch pipettes (1-4MΩ) and experiments were performed in very low illumination. Cells were voltage clamped at -90mV and T-type Ca^{2+} channel currents carried by Ba^{2+} were activated between -60 and -20mV. The T-type current was further isolated by abolition of high threshold currents with 1μM ω-conotoxin, which also shifted the voltage for T-type current activation to the left by 10mV. This current was inhibited by 1-octanol (1μM). A light flash (300-380nm, 63mJ to 20mm^2) in the absence of caged compound did not affect the T-type current. Liberation of 6μM free GTP-γ-S by the same light flash increased the T-type current by about 20% (n=5) and it was subsequently decreased compared to control by liberation of a further 6μM GTP-γ-S. The T-type current was abolished with a $t_{\frac{1}{2}}$ of about 1 minute after liberation of 20μM GTP-γ-S (n=5). Single T-type Ca^{2+} channels were recorded from inside out patches and had a saturating probability of opening of about 0.08, application of 50μM GTP-γ-S completely abolished T-type channel activity in the isolated patches. The dual effects of GTP-γ-S on the T-type current suggest that more than one G-protein may be involved in regulation of these Ca^{2+} channels.

M-PM-A7 MODULATION OF THE CALCIUM CURRENT BY INTERNAL GTP-γS IN CHICK SENSORY NEURONS. Carla Marchetti, Istituto di Cibernetica e Biofisica, Consiglio Nazionale delle Ricerche, Genova, Italy.

Neurotransmitters, such as noradrenaline and dopamine, inhibit the voltage-dependent calcium current in dorsal root ganglion (DRG) cells and slow down its activation kinetics. This effect is mimicked by internal perfusion with GTP-γS, and is abolished by pre-treatment with pertussis toxin (Holz et al., 1984), suggesting an involvement of a GTP-binding protein. I have studied the modification in the time course of the calcium current in chick DRG induced by internal GTP-γS. Whole-cell currents were measured in an external bath containing TEA-Cl and 2 mM $CaCl_2$. The pipette filling solution contained (mM): 124 CsCl, 1 $CaCl_2$, 11 EGTA and 2 Mg-ATP. Cells were held at -50 mV to minimize the transient components of the calcium current. The activation of the current at +10 mV could be fitted by a single exponential curve with τ=2.0±0.7 ms. With 100μM GTP-γS in the pipette, the current waveform changed with time and after 1-3 minutes could be fitted by a double exponential curve with τ_1=2.0±0.5 ms and τ_2=20±5 ms. The time to peak was prolonged from 8 msec in control to >80 ms with GTP-γS. The effect was very similar to that of 10 μM Dopamine added to the bath and was reduced at higher depolarizations. It was interpreted by a simple model: when the G protein is active, the channel switches to a different closed state from which it still can open, but with different kinetics. The resulting current is the sum of an unmodified component and a slower component, which does not appear in control.

M-PM-A8 MU OPIOIDS INHIBIT CALCIUM CHANNELS. Jean E. Schroeder, Peter S. Fischbach, Mulubrhan Mamo, E.W. McCleskey. Washington University, 660 S. Euclid Ave., St. Louis, MO 63110.

The opioid mu receptor mediates the action of morphine but effects upon ion channels are incompletely understood. Previous reports show the mu receptor coupled to potassium channels [Werz and MacDonald, J. Pharmacol. Exp. Ther. 234, 49 (1985); North, et al., PNAS 84, 5487, (1987)]. We find a link between the mu receptor and calcium channels in adult rat dorsal root ganglion neurons grown in tissue culture from 0 to 2 days.

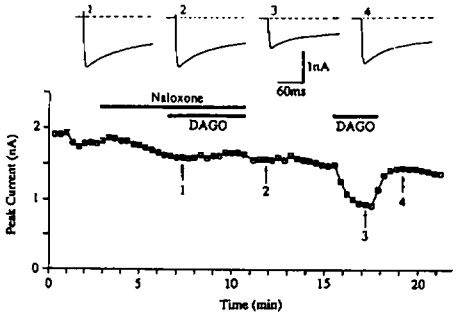

The traces in the figure are whole cell patch clamp recordings of Ca currents elicited by steps from -70 mV to +10 mV at the indicated times. The graph shows the peak current amplitude as a function of time. 10 μM naloxone, an opioid-receptor antagonist, inhibits the effect of 100 nM DAGO (Tyr-D-Ala-Gly-MePhe-Gly-ol), a mu-receptor agonist. DAGO, applied in the absence of naloxone, reversibly reduces the Ca current.

These cells have a clearly distinguishable T-type Ca current and two components of high threshhold current. The high threshhold currents have different inactivation kinetics and steady-state availability curves. All three Ca currents are reduced by DAGO.

M-PM-A9 TWO COMPONENTS OF HIGH THRESHOLD CA^{2+} CURRENT MODULATED DIFFERENTIALLY BY PHYSIOLOGICAL STIMULI. Richard, S.[1,2], Tiaho, F.[2], Charnet, P.[2], Nargeot, J.[2], Nerbonne, J.M.[1] [1]Pharmacology Dept., Wash. Univ. Med. Sch., St. Louis, MO, [2]CNRS LP8402, INSERM, Montpellier France (Intr. by Jonathan Cohen).

In isolated adult rat ventricular myocytes, voltage-gated inward Ca^{2+} currents (I_{Ca}), evoked during depolarizations from a holding potential (HP) of -90mV, begin to activate at ≈-40mV, peak at ≈ 0mV and reverse positive to +70mV; at all test potentials, current decay follows a biexponential time course. The waveforms of I_{Ca} are attributed to the activation of a novel type of High-Threshold Ca^{2+} current which comprises two distinct components, I_{Ca}(fc) and I_{Ca}(sc) with differing decay time constants: at -10mV, tau_{fc} and tau_{sc} (mean±SD, n=17) are 6.6±2.1 and 63±23 ms, respectively. The voltage-dependences of I_{Ca}(fc) and I_{Ca}(sc) activation are also distinct: I_{Ca}(fc) begins to activate at ≈ -30mV, peaks at -10mV and is negligible positive to ≈+40mV; I_{Ca}(sc), in contrast, peaks ≈+10mV and dominates at potentials positive to ≈0mV. I_{Ca} waveforms also vary with HP: I_{Ca} amplitude is larger and current decay is slower for currents evoked from a HP of -50mV. In addition, I_{Ca}(sc) amplitudes increase as the HP is depolarized from -90 to -50mV and subsequently decrease at more positive HPs. When the time between successive depolarizations (from the same HP) is reduced, similar changes are observed. Hyperpolarized potentials and low frequencies, therefore, reveal preferential activation of I_{Ca}(fc); depolarized potentials and high frequencies, in contrast, favor I_{Ca}(sc). These results are interpreted in terms of a scheme involving bimodal (voltage- and frequency-dependent) gating of a single Ca^{2+} channel type, rather than as reflecting activation of distinct Ca^{2+} channels. In response to β-adrenergic agonists, I_{Ca} (peak) amplitudes increase owing to the specific augmention of I_{Ca}(fc); there is little or no effect on I_{Ca}(sc) amplitudes. The Ca^{2+} agonist BayK 8644, in contrast, increases I_{Ca}(sc) and decreases of I_{Ca}(fc). In addition to voltage- and time-dependent regulation, therefore, Ca^{2+} channel gating can be modulated differentially by distinct, physiologically-relevant, stimuli. (Support: American Heart Association, NIH #HL34161 and the Fondation de France).

M-PM-A10 THE CALCIUM ACTION POTENTIAL IN PARAMECIUM IS MODULATED BY G-PROTEINS. Juan Bernal and Barbara E. Ehrlich. Departments of Medicine and Physiology, University of Connecticut, Farmington CT.

When the voltage-dependent calcium channels of Paramecium are activated, the cell swims backward. The duration of this behavior is correlated with the magnitude of the calcium current. After compounds known to activate G-proteins were incorporated into intact cells, backward swimming was markedly prolonged (Biophys. J. 53, 21a, 1988). To determine if this modulation was on membrane properties of the cell, we studied the effect of G-proteins on the calcium action potential in the marine ciliate Paramecium calkinsi. The calcium action potential was induced in Na-free solutions containing high TEA and Ca using current clamp conditions. The amplitude of the action potential increased as extracellular calcium was increased from 0.5 to 90 mM and was blocked reversibly by 2 uM W(12)Br. Compounds of interest were injected into the cell by pressure. When GTPγS, a non-hydrolyzable analogue of GTP which activates G-proteins, was injected, the duration of the calcium action potential increased by 300%. This effect was maintained over 20 min. GDPβS, which inhibits G-proteins, reduced the duration and amplitude of the calcium action potential. Five min after injection of GDPβS the voltage response to a current pulse was reduced to the passive properties of the cell. The effect of GTP was similar to that of GTPγS, but the effect reversed within 5 min. These results support the hypothesis that G-proteins are able to modulate membrane channels.

Supported by NIH grant GM 39092. BEE is a PEW scholar in the Biomedical Sciences.

M-PM-A11 REGULATION OF CALCIUM CURRENT IN CARDIAC MYOCYTES BY CYCLIC GMP REGULATED PHOSPHODIESTERASES. H. C. Hartzell, R. Fischmeister & F. Sullivan. Dept. of Anatomy and Cell Biology, Emory Univ. School of Medicine, Atlanta, GA 30322.

Two cyclic nucleotide phosphodiesterases (PDE) in heart are regulated by cGMP: PDE II is stimulated by micromolar concentrations of cGMP, whereas PDE IV is inhibited by cGMP. We have previously hypothesized a role for PDE II in regulation of Ca current (I_{Ca}) in frog heart (*Nature* 323, 273-275: 1986; *Mol. Pharmacol.* 33, 664-671: 1988). To investigate further the role of PDEs in regulation of I_{Ca}, we have examined the effects of several PDE inhibitors on I_{Ca} in isolated myocytes from frog ventricle. Neither 1-methyl, 3-isobutyl xanthine (MIX) nor milrinone (MIL) had significant effects on basal I_{Ca}. In contrast, 10 μM MIX increased I_{Ca} about 140% when I_{Ca} was elevated by submaximal concentrations of internally-perfused cAMP (<5 μM) or externally-applied isoproterenol (0.1 μM). Significant stimulation was seen with concentrations as low as 0.3 μM MIX. Since the K_i for inhibition of PDE II by MIX is 20 μM, as measured by hydrolysis of ^{32}P-cAMP, the effects of MIX on I_{Ca} occured at concentrations much lower than required to inhibit this enzyme. MIL, which is a selective inhibitor of PDE IV, produced similar effects to those of low concentrations of MIX. This supports the conclusion that low concentrations of MIX and MIL stimulate I_{Ca} by inhibiting PDE IV. When applied internally, MIX produced minimal effects on I_{Ca}, which suggests that MIX may inhibit the enzyme from the external surface of the membrane. MIL, in contrast, was equally effective from the internal and external surfaces, suggesting that MIL acts on the interior surface and is membrane-permeable. Further support for the conclusion that MIL and low concentrations of MIX inhibit PDE IV was provided by experiments in which PDE IV was inhibited by internal perfusion with cGMP (in the presence of cAMP). Under these conditions, neither MIL nor concentrations of MIX <10 μM had any effects on I_{Ca}. However, higher concentrations of MIX (>100 μM) stimulated I_{Ca}, presumably by inhibiting PDE II.

M-PM-A12 AN ENDOGENOUS COMPOUND MODULATES THE VOLTAGE-DEPENDENT CALCIUM CURRENT. Edwin C. Johnson, James B. Becker and Mark A. Simmons. Marshall University School of Medicine, Huntington, West Virginia 25755. We have previously isolated a "hypertensive factor", tentatively identified as a small peptide, from rat erythrocytes. This factor increases blood pressure when injected into normotensive rats and increases sensitivity of aortic muscle to contractile stimuli. We have now purified this substance by monoclonal antibody affinity chromatography and have examined its effects on the voltage dependent calcium current (I_{Ca}). Whole cell recordings were made from ventricular myocytes dissociated from the heart of adult *rana catesbiana*. I_{Ca} was activated by 200 msec pulses from a holding potential of -80 mV. Extracellular TTX was applied to block I_{Na} and Cs was applied both extra- and intracellularly to block K currents. I_{Ca} was measured as the difference between the peak inward current and the current at the end of the pulse. When the purified "hypertensive factor" was applied to single cells, an increase in the peak amplitude of I_{Ca} following pulses to 0 mV was observed. Furthermore, both the rate of activation of I_{Ca} and the rate of inactivation of I_{Ca} were accelerated. The factor also shifted the peak of the I_{Ca} current-voltage relationship slightly to the hyperpolarizing direction. We examined the steady-state inactivation curve for I_{Ca} between -80 and 0 mV in the presence of the factor and observed a 9 mV hyperpolarizing shift compared to control. The reactivation, or recovery from inactivation, of the calcium current was unchanged by the compound. We conclude that this endogenous compound increases calcium channel activity in a manner similar to that of the dihydropyridines.

M-PM-B1 EFFECT OF NUCLEOTIDES, TEMPERATURE AND ACTIN ON THE DIGESTION OF MYOSIN S1 BY THERMOLYSIN. Andras Muhlrad and Nathalie Chaussepied, CVRI, University of California, San Francisco and Dept. of Oral Biology, Hebrew University, Jerusalem, Israel.

Chymotryptic subfragment 1 (S1) from rabbit skeletal muscle myosin was digested by thermolysin. Thermolysin cuts the S1 heavy chain preferentially 26 kDa from the N-terminus (Applegate & Reisler, PNAS *80:* 736, 1983 and Mornet et al., PNAS *81:* 7109, 1984). The speed of the digestion increased significantly in the presence of MgATP or MgADP at 25°C, but the nucleotides had no effect when the digestion was carried out at 12°C or 0°C. The results can be explained by assuming that there are two S1 conformers (Shriver & Sykes, Biochemistry *20:* 6357, 1981) and that both the addition of nucleotides and the lowering of the temperature shifts the transconformational equilibrium in the direction of the conformer that is more susceptible to thermolysin. Actin inhibits the thermolysin digestion of the S1 heavy chain at all temperatures employed, indicating that actin shifts the equilibrium in the direction of the less susceptible conformer. Actin inhibition prevails also when S1 in ternary complex with nucleotides and actin both in the actin·S1·ADP strongly attached and in the actin·S1·ATP weakly attached states. This indicates that the S1 structure at the 26 kDa/70 kDa junction is similar in rigor, strongly and weakly attached states. (Supported by HL-16683, MDA, and BSF).

M-PM-B2 COMPARISON OF THE REACTION OF DTNB WITH MYOSIN S1 AND TRYPTIC S1. K. N. Rajasekharan and M. Burke. Department of Biology, Case Institute of Technology, Case Western Reserve University, Cleveland, OH 44106.

The reaction of DTNB with S1 and tryptic S1 in the presence of MgADP has been investigated by reverse phase HPLC. For native S1 the protein, freed from residual DTNB was subjected to trypsinolysis at 4°C for 30 min prior to analysis by HPLC. By monitoring the eluate at 214 and 340 nm, the amounts of the separated three heavy chain fragments and light chain and the location of the mixed TNB disulfides among these peptides could be determined. For both S1 and tryptic S1, the initial reaction (30 min) appears to be confined to the formation of mixed TNB disulfides in the 21-kDa peptide with limited modification of the light chain. In the subsequent reaction intramolecular disulfide exchange occurs in both proteins and for S1 these disulfides appear to be localized within the 21-kDa segment and probably involve SH1 and SH2 as proposed by Wells and Yount [Biochemistry 19, 1711-1717 (1980)] although low levels of disulfide formation between the 21-kDa and 50-kDa segments can also be detected. For tryptic S1 the major intramolecular disulfide exchange appears to be between the 21-kDa and 50-kDa segments. Since tryptic digestion increases the segmental flexibility in S1 [Highsmith and Eden, (1987) Biochemistry 26, 2747-2750], the present data indicate that this enhanced flexibility involves regions containing the thiols in the 21-kDa and 50-kDa segments. Because these thiols are close to regions identified with actin binding, it is proposed that the decrease in actin affinity accompanying tryptic digestion may be due to a loss in the structural integrity of the actin binding domain. (Supported by NIH grant NS151319)

M-PM-B3 Gln-488 & 489 ARE CLOSE TO SH-1 of MYOSIN S1 IN THE PRESENCE OF Mg^{2+}-NUCLEOTIDE. Renné Chen Lu & Anna Wong, Dept. of Muscle Res., Boston Biomed. Res. Inst. & Dept. of Neurology, Harvard Med. Sch., Boston, MA 02114

It has been documented that the most reactive thiol, SH-1, of S1 is not directly involved in the binding of nucleotide. Nevertheless, the possibility remains that SH-1 region is involved in maintaining the conformation of the ATPase site and that would explain the effect on ATPase activities when SH-1 is modified. We have reported that benzophenone iodoacetamide (BPIA) can be selectively incorporated into SH-1 and upon photolysis an intramolecular crosslink is formed between SH-1 and the 25 kDa region of S1. If a Mg^{2+}-nucleotide is present during photolysis, crosslinks can be formed either with the 25 kDa or the 50 kDa region (Lu et al., PNAS 83 6392, 1986). To determine the residues that are close to SH-1, S1 was crosslinked with radioactive BPIA and degraded with proteolytic enzymes. Peptides containing crosslinks were isolated by liquid chromatography and subjected to amino acid sequence analyses. The results show that Glu-88, Asp-89 and Met-92 are the three sites in the 25 kDa region that are close to SH-1 independent of the presence of nucleotide (Lu & Wong, Biophys. J. 53, 175a, 1988). Similar studies on S1 that has been photolyzed in the presence of Mg^{2+}- nucleotide indicated that Gln-488 and Gln-489 in the 50 kDa region are also crosslinkable to SH-1. Comparison of the amino acid sequences of myosin S1 from different species shows that certain regions with functional importance have high percentage of homology. The findings that the primary structure of the segment from Asn-473 to Tyr-503 is extremely conserved among various species (Warrick & Spudich, Ann. Rev. Cell Biol. 3, 379, 1987) and that Gln-488 & 489 are close to SH-1 only in the presence of nucleotide suggest that this region may play a dynamic role during ATP hydrolysis. Supported by NIH AR28401 & RR03370.

M-PM-B4 HYDROPHOBIC SURFACES ON MYOSIN by Stefan Highsmith, Department of Biochemistry, University of the Pacific, San Francisco, CA 94115.

The non-ionic detergent dodecyl nonaoxyethylene ether ($C_{12}E_9$) increases the MgATPase activity of rabbit skeletal myosin subfragment-1 (S1) from 0.041 s^{-1} to 0.12 s^{-1} at 22°C in 10 mM KCl, pH 7. Myosin, S1A1, S1A2, trypsinized S1 and actoS1 MgATPase activities (V_{max}) were all increased about three-fold. Neither ATP nor actin binding to S1 appear to be effected. The dependence of the increase in S1 activity on [$C_{12}E_9$] shows a smooth transition that was 50% complete at 45 uM $C_{12}E_9$. Between 10^{-4}M and 10^{-2} M $C_{12}E_9$, the activity is constant. Normal MgATPase activity is regained when the detergent is removed. The dependence of [$C_{12}E_9$] for 50% activation on [S1] indicated that about forty $C_{12}E_9$ molecules are bound to S1. Other molecules that had single long straight saturated hydrocarbon moieties also increased S1 activity.

These results for myosin, S1 and actoS1 indicate that at [$C_{12}E_9$] less than its critical micelle concentration, about forty molecules of $C_{12}E_9$ reversibly and non-cooperatively bind to S1 to lower its energy of activation for MgATP hydrolysis. Forty $C_{12}E_9$ molecules are less than one half the size of a micelle but are one fifth the volume of S1. This somewhat novel observation suggests that S1 has a substantial hydrophobic surface. A speculative S1 structure consistent with these results is one with two tertiary structural subdomains that share a hydrophobic interface about which the two subdomains rotate relative to one another. Rotation is hypothesized to be part of the catalytic cycle, and the intramolecular intersubdomain forces that inhibit rotation to be weakened by the binding of many long chain hydrocarbons to the hydrophobic interface. Other interpretations are possible. (NIH Grant AM 37499).

M-PM-B5 CIRCULAR DICHROISM (CD) AND DIFFERENTIAL SCANNING CALORIMETRIC (DSC) STUDY OF THE THERMAL UNFOLDING OF THE DOUBLE-STRANDED α-HELICES IN MYOSIN ROD, LMM AND LONG S-2. Antonio Bertazzon & Tian Y. Tsong, Department of Biochemistry-CBS, University of Minnesota, St. Paul, MN 55108

Previous work shows that S1 and Rod of myosin can undergo autonomous structure transition. Here we examine whether within the Rod independent domains also exist. It is known that the double-coiled coil structures of myosin Rod, LMM and Long S-2 undergo helix-to-coil transition in the temperature range 35-60°C. The DSC thermogram of Rod can be resolved into 6 quasi-two state transitions. CD spectrum exhibit nearly identical melting features. Comparison of the DSC thermograms of isolated Long S-2, LMM and Rod allows us to assign the melting temperatures of structure domains. DSC shows that Long S-2 melts at 45±1°C in 0.5 M KCl, pH 7.0. With additional information on the pH dependence of the 6 components of the Rod and of LMM and S-2, we tentatively assign transitions I, IV, V and VI to LMM and III to S-2. S-2 may also contain Transition II and a part of Transition I. The total ΔH of transitions are, respectively, 1050±50 kcal/mol, 745±65 kcal/mol and 300±10 kcal/mol for Rod, LMM and S-2. The ΔH/residue are, respectively, 478 cal, 602 cal, and 322 cal for Rod, LMM and S-2. These results indicate that S-2 and LMM of Rod melt independent of each other and the end effect of the fragmentation is small. Different parts of myosin Rod have different thermal stability. ΔH/residue of these quasi-independent domains are also different.

[This work has been supported by NIH Grant.]

M-PM-B6 SUBUNIT EXCHANGE BETWEEN THICK FILAMENTS OF VERTEBRATE SKELETAL MYOSIN. Julien S. Davis. Department of Biology, The Johns Hopkins University, Baltimore, MD 21218.

Mechanisms that require subunit exchange rather than de novo filament synthesis are favored for the incorporation of new myosin into extant A-band structure. Generally muscle function is fully retained. Mechanisms have been proposed for the related process of in vitro exchange of subunits into thick filaments of myosin. A random mechanism in which myosin exchange occurs with equal probability along the length of the filaments is favored by Tan, I., Ziotchenko, E. & Saad, A. D. (1988) Biophys. J. 53:176a on the basis of fluorescence energy transfer and radioactive label exchange data. A different mechanism in which exchange occurs far more rapidly at the filament ends with the rate progressively slowing as the center of the filament is approached is implicit in the kinetic mechanism of thick filament assembly (see Davis, J. S. (1988) Ann. Rev. Biophys. Biophys. Chem. 17: 217-239). Stochastic stimulation was used to compute the time dependence of subunit exchange in a population 2000 filaments (~ the number per sarcomere) at equilibrium. Transition probabilities were calculated from deterministic rate and cooperativity parameters obtained from experiments on the kinetics of filament growth. The results are interpreted as follows: 1) Three rate constants and the two cooperativity parameters generate an equilibrium distribution of thick filament sizes similar to that measured in experiments. 2) Exchange occurs first at the filament tips and then spreads gradually towards the center of the filament. 3) Significant exchange occurs in milliseconds full exchange of subunits takes considerably longer - a direct consequence of the cooperativity inherent in the kinetics and thermodynamics of thick filament assembly and length regulation. 4) Experimental and computed time courses of exchange are of similar form, indicative of a shared mechanism.

M-PM-B7 *Acanthamoeba* Myosin-II Minifilaments: Mechanism of Assembly. Walter F. Stafford, John H. Sinard and Thomas D. Pollard. Department of Muscle Research, Boston Biomedical Research Institute, Boston, Massachussets and The Department of Cell Biology and Anatomy, The Johns Hopkins University School of Medicine, Baltimore, Maryland.

The mechanism of assembly *Acanthamoeba* Myosin-II minifilaments was investigated by analytical ultracentrifugation, light scattering and electron microscopy. The mode of association was deduced to be monomer-dimer-tetramer-octamer. Small amounts of hexadecamer were observed under some conditions. The sedimentation velocity profiles were depedendent on salt and protein concentration indicating a reversible equilibrium between monomer and the various polymeric species. At 50mM KCl, a single boundary with a sedimentation coefficient of 21S was observed. In either 200mM or 300mM KCl a single boundary with a sedimentation coefficient of 6-7S was observed. At intermediate salt concentrations (100-200mM) multiphasic boundary profiles were observed. By varying the protein concentration, we were able to demonstrate that these were reaction boundaries arising from a rapidly reversible chemical equilibrium involving several intermediate species. The 21S species is most likely an octamer. A 13S component appears to correspond to tetramer while the 6-7S component appears to arise from a monomer-dimer interaction. Polymers with these apparent stoichiometries could be observed in the electron microscope. The results of light scattering studies under the same range of conditions were consistent with sedimentation analysis.

M-PM-B8 PURIFICATION AND CHARACTERIZATION OF DROSOPHILA CYTOPLASMIC MYOSIN LIGHT CHAINS. Xiao-jia Chang and Dan Kiehart (Intr. by Daniel Branton), Harvard University, Cambridge, MA 02138.

Two polypeptides with apparent molecular weight 18 KD and 16 KD co-purify with Drosophila cytoplasmic myosin heavy chain (DCM-HC) by column chromatography (Kiehart and Feghali, 1986, J. Cell Biol. 103:1517-1525) and by immunoprecipitation with antibodies against DCM-HC. The purified 18 KD and 16 KD polypeptides, tentatively called light chains (LC-1 and LC-2, respectively), have been protease digested and peptide-mapped by HPLC. Selected peptides were further analyzed by amino acid sequencing. The peptide profiles of HPLC indicate that the LC-1 and LC-2 are not proteolytically related to each other. The partial protein sequence data indicate that both LC's of the cytoplasmic myosin are distinct from those of muscle myosin in Drosophila. A fragment of 31-amino acids from LC-1 shows the best sequence match to the position 92-123 of the chicken smooth muscle myosin regulatory LC (65% identical, 75% similar match). A 14- and a 12-amino acid sequence from LC-2 shows best match to position 119-133 and 137-149 of the chicken muscle myosin alkaline LC (46% identical, 77% similar match). These results establish that the 18 and 16 KD polypeptides are indeed Drosophila cytoplasmic myosin light chains and suggest that the 18 KD is likely to be the regulatory LC, the 16 KD to be the alkaline LC. A detailed analysis of the structural features of these LC's and their function in regulation is underway. Supported by NIH GM 33830.

M-PM-B9 PHOSPHORYLATION AND REGULATION OF MACROPHAGE MYOSIN BY MYOSIN LIGHT CHAIN KINASE ISOLATED FROM AVIAN SMOOTH MUSCLE. M.A.L.Atkinson and J.A.Trotter, Dept.of Biochemistry, Univ. of Texas Health Center, Tyler, Tx 75710 and Dept. of Anatomy, Univ. of New Mexico, Albuquerque, NM 87131.

Myosin purified from rabbit alveolar macrophages is phosphorylated on the 20 k-Da light chains and on the 220 k-Da heavy chain (Biochem. Biophys. Res. Commun. (1982) 106, 1071). It is known that the phosphorylation of the light chain modulates the actin-activated Mg^{2+}ATPase activity of the molecule (J.Biol.Chem. (1979), 254, 8781) but it is not known whether this is through an effect on the affinity of the myosin for actin or on the rate of ATP hydrolysis. In this study we have used myosin light chain kinase (MLCK) purified from chicken gizzard smooth muscle. This enzyme phosphorylates the purified macrophage myosin to a stoichiometry of 2 mols of phosphate per mol of myosin. All the phosphate is associated with serine in a single tryptic peptide derived from the 20 k-Da light chain. This is the same site that is phosphorylated *in vivo*. The actin-activated Mg^{2+}ATPase activity of dephosphorylated myosin (20 nmols/min/mg) is enhanced five fold by phosphorylation with smooth muscle MLCK apparently through an effect on Vmax rather than by an alteration of Kapp. Since these ATPase activities are relatively low we are exploring alternative purification protocols.

(Supported by NIH grant GM40423 to MALA)

M-PM-B10 IDENTIFICATION OF THE CASEIN KINASE II PHOSPHORYLATION SITE IN BOVINE BRAIN MYOSIN HEAVY CHAIN. Noriko Murakami, Gregory Healy-Louie, and Marshall Elzinga, Department of Path. Biochemistry, Institute for Basic Research, Staten Island, NY 10314

The heavy chain (HC) of bovine brain myosin is phosphorylated by casein kinase II (CK II) [Murakami et al., J. Biochem. 95 651 (1984)] in a region located within 5 kDa of the carboxyl terminus [Barylko et al., Eur. J. Biochem. 158 271 (1986)]. In the experiments described here, we have attempted to identify the exact location of this phosphorylation site. Myosin was isolated from fresh steer brains. It contained 1.1 moles of endogenous phosphate per mole of HC. CK II treatment of this myosin in the presence of ^{32}P-ATP led to incorporation of 0.8-1.0 mole of additional phosphate per mole of myosin. Incubation with acid- and alkaline-phosphatases reduced the endogeneous phosphate to about 0.17 mol/mol of HC, and when the dephosphorylated myosin was incubated with CK II, 1.8-2.0 mol of phosphate were incorporated per mole of myosin; this stoichiometry suggests that one site was phosphorylated per heavy chain. Only serine was phosphorylated by CK II. After proteolytic digestion of ^{32}P-phosphorylated myosin, one major and several minor phosphopeptides were isolated. These peptides are similar in composition, and probably arise from the same site, differing slightly in length because of incomplete digestion. Alternatively, they may arise from myosin heavy chain isozymes. The peptides are relatively acidic, and the presence of proline in them indicates that the phosphorylation site is located very near the carboxyl-terminus of the heavy chain. Amino acid sequencing of these peptides is in progress.

M-PM-B11 ANALYSIS OF MOLECULAR INTERACTIONS BETWEEN MYOSIN MOLECULES USING EXPRESSION IN *E.COLI* AND OLIGONUCLEOTIDE-DIRECTED SITE-SPECIFIC MUTAGENESIS.
Simon J.Atkinson,R.D.Moir,S.R.Clarke and Murray Stewart.MRC Laboratory of Molecular Biology,Hills Rd.,Cambridge CB2 2QH,England.

To investigate the molecular interactions between myosin molecules that are responsible for filament structure and assembly we have cloned and expressed fragments of rabbit skeletal myosin rod in *E.coli*.A 1.7kb cDNA fragment coding for the C-terminal 559 amino acids of myosin was cloned into the pIN-II-A2 vector (Nakamura,K.and M.Inouye.1982.EMBO J.1,771-775) from which high levels of expression were obtained as a fusion protein with 5 amino acids of the *E.coli* prolipoprotein.Other fragments were produced by cloning smaller restriction fragments into the vector or by inserting artificial stop codons.The expressed protein fragments were recognized by polyclonal antisera to rabbit LMM and shadowed preparations showed the presence of rod-like particles that had the expected length for α-helical coiled-coil molecules of the appropriate size.Oxidative crosslinking indicated that the molecules renatured with their chains in register.The 559 amino acid fragment and fragments with 100 and 320 amino acids deleted from the N-terminal end were,like myosin,insoluble at low ionic strength.However,fragments which lacked 90 or more amino acids from the C-terminus did not precipitate under these conditions.Paracrystals with a characteristic repeat near 40 nm were formed in low salt.These fragments and paracrystals are also being used to investigate the effect of changes made to the sequence by site-directed mutagenesis.

M-PM-C1 SOME LIMITATIONS OF THE WHOLE CELL PATCH CLAMP TECHNIQUE IN THE STUDY OF MEMBRANE TRANSPORT R.T. Mathias, I. Cohen and C. Oliva, Physio & Biophys, SUNY Stony Brook, NY.

The whole cell patch clamp technique has been widely used to control both voltage and ion gradients across cell membranes. We recently showed (Oliva et.al. Biophys. J. 54) that the time for diffusion of substances from pipette to cell interior was primarily limited by the pipette tip. As a consequence, the intracellular concentration is essentially uniform at all time whereas the pipette concentration may have significant axial gradients.

In this report, we extend the analysis of Oliva et.al. to electro-diffusion of a substance transported across the cell membrane. In steady state, electrochemical gradients within the pipette drive a flux that equals net transmembrane transport rate. A simple approximate expression relating bulk pipette concentration, Cp, and intracellular concentration, Ci, is: $Ci = Cp - jR/r$, where j (moles/sec) is net transmembrane flux, R(Ohm) is pipette resistance, D (sq.cm/sec) is the diffusion coefficient of the substance and r (Ohm-cm) is resistivity of the pipette solution. This equation allows one to calculate a more accurate relationship between j and Ci, given an experimental value of j and Cp. We also find that time to reach steady state perfusion of a cell is reduced when the substance is transported. Oliva et.al. derived the time constant for a substance not transported: $T=VR/Dr$, where V(cu.cm) is cell volume. The major effect of membrane transport is to reduce the time constant to $T/(1+kR/Dr)$, where k (cu.cm/sec) is the change in membrane transport per unit change in intracellular concentration. We conclude that the pipette has important effects on measurement of membrane transport parameters. We will present some of these effects on Na/K transport, Na/Ca exchange and whole cell perfusion studies using isolated cardiac myocytes. NIH grants HL36075, EY06391, HL20558, PPGHL28958.

M-PM-C2 THE EFFECTS OF REPETITIVE STIMULATION ON THE SODIUM CURRENT OF CHICK HEART CELLS. M.R. Gold and G.R. Strichartz, Cardiac Unit, Mass. General Hospital and Anesthesia Research Laboratories, Brigham and Women's Hospital, Harvard Medical School, Boston, MA 02115.

The effects of repetitive stimulation on the TTX-sensitive sodium current of cultured embryonic chick atrial cells were studied using the whole cell patch clamp technique. Single cells (in 136 mM Na^+) were activated with 150 msec pulses to 0 mV (E_h -100), which produced a reversible, frequency-dependent decrement in the peak sodium current. At 1, 2 and 3 Hz stimulation rates the steady-state decreases were 10.8 ± 6.6, 22.5 ± 11.8 and 38.3 ± 11.5, respectively (mean ± SD, n=10). Membrane hyperpolarization, to remove resting inactivation (E_h -130 to -140 mV), markedly reduced this decrement at all frequencies. In contrast, removal of extracellular potassium (5.4 mM normal K^+) had no effect on the reduction of sodium current. Using a double pulse reactivation (reprime) protocol, we showed that recovery from inactivation followed a multi-exponential time course. At recovery times corresponding to the interstimulus intervals associated with stimulation frequencies of 1-3 Hz (i.e. 183-850 msec) there was incomplete recovery from inactivation. Membrane hyperpolarization accelerated the reactivation process significantly, enabling more complete recovery in the frequency range studied. In summary, slow inactivation underlies a decrement in sodium current observed with repetitive depolarization at heart rates in the physiologic range. (Supported by NIH GM15904 (GRS) and Postdoctoral support (MRG) from BWH Anesthesia Foundation.)

M-PM-C3 MECHANISM OF QUINIDINE BLOCK OF INWARD-RECTIFIER K^+ CHANNEL (K_1). R. Sato, I. Hisatome, J.A. Wasserstrom, and D. H. Singer, Northwestern U., Chicago, Illinois.

We have previously shown that quinidine blocks IK_1 channel activity from the inside of the membrane. Underlying mechanisms remain to be clarified. We, therefore, used single channel recording techniques to study the mechanisms of quinidine block of IK_1 in guinea pig ventricular myocytes under conditions of cell attached and inside-out patch. The pipette solution contained (in mM): 145 KCl and 5 HEPES (pH 7.4). In cell attached patch experiments, normal Tyrode's solution was used as bath solution. In inside-out patch experiments, the internal solution contained (in mM): 120 K-aspartate, 25 KCl, 3 Na_2 ATP, 5 EGTA, 5 HEPES, 1 Mg Cl_2 (pH 7.2). Under conditions of cell attached patch, 30 μM quinidine reduced open-probability and increased the probability of opening into a lower conductive state. Channel activity persisted even after a 30 min exposure. Under inside-out patch conditions, the same concentration of quinidine reduced unit amplitude as well as open probability, with virtual abolition of burst behavior. When unit amplitude had decreased to 70% of control, open probability also was reduced (from 0.27 to 0.044 at H.P = -50 mV). The blocking and unblocking rate constants were $1.12 \times 10^6\ M^{-1}\ S^{-1}$, $1.56\ S^{-1}$, ($K_d = 1.4 \times 10^{-6}$ M), respectively, under these conditions. Within 10 minutes, quinidine blocked IK_1 activity completely. When quinidine concentration was increased, interburst-interval prolonged in a dose dependent manner. In summary, quinidine blocked IK_1 channel activity by decreasing unit amplitude and open probability. The decrease in open probability, in turn, reflected an increase in interburst interval due to an increase in the drug binding non-conductive state and/or a decrease in mean open time.

M-PM-C4 **BARIUM ION BLOCKS INTERSTITIAL POTASSIUM ION ACCUMULATION DURING ACUTE MYOCARDIAL ISCHEMIA; ROLE OF INWARD RECTIFIER (IK1) AND ATP-SENSITIVE POTASSIUM CHANNELS.**

Karl P. Dresdner Jr. and Andrew L. Wit, Department of Pharmacology, Columbia University, College of Physicians & Surgeons, New York, NY 10032.

The causes of the increase in interstitial potassium ion, [K+]o, accumulation during the first 15 minutes of acute myocardial ischemia are still not established. Substantial effects of cellular acidosis, low ATP, and increased Ca++ upon K+ channels have been found from voltage and patch clamp studies of single cardiac cells and membrane patches. This improved understanding of cardiac potassium ion channels now allows us to study the basis of the net cellular K+ efflux occuring during acute myocardial ischemia using a well-characterized model, the isolated, coronary-perfused rabbit ventricular septum. Right ventricular endocardial muscle [K+]o was measured continuously with an extracellular, valinomycin, theta style, double-barrel K+ sensitive microelectrode (5-10 micron tip). [K+]o increased during 15 minutes of acute global ischemia from 4.0 mM to 11.2 mM (±1.8,SD,n=13) and was fully reversed by coronary reflow. 2.5 mM Ba++ was added to the perfusate to block the inward rectifier (IK1) and the ATP-sensitive K+ channels, and thereby, test the contribution of these K+ channels to the [K+]o accumulation. 2.5 mM Ba++ caused an 80% reduction in the [K+]o accumulation occurring during the first 15 minutes of acute ischemia. In control experiments, 2.5 mM Ba++ did not interfere with the K+ electrode's response to [K+]. **We conclude that the inward rectifier (IK1) K+ channel, and/or ATP-senstive K+ channel significantly contribute to the [K+]o increase during acute myocardial ischemia.**

M-PM-C5 RECEPTOR-MEDIATED CHANGES IN INTRACELLULAR Ca^{2+} CONCENTRATION OF QUIESCENT RAT VENTRICULAR MYOCYTES. V.K. Sharma, M. Korth, D.J. Williford, A. Moscucci, A.Q. Christie, R.T. Dirksen, and S-S. Sheu. Dept. of Pharmacology, University of Rochester, Rochester, NY 14642.

Activation of β-adrenergic, α_1-adrenergic, low affinity muscarinic, or purinergic receptors leads to a positive inotropic effect in rat heart. While the β-adrenergic receptors utilize cAMP as the intracellular second messenger, α_1-adrenergic, low affinity muscarinic and purinergic receptors operate via an increased turnover of phosphoinositides. We have studied the effect of receptor-activation on intracellular Ca^{2+} concentration ($[Ca^{2+}]_i$) in rat ventricular myocytes. As shown, isoproterenol causes a decrease, methoxamine causes no change, carbachol causes a slow increase, and ATP causes a biphasic increase in $[Ca^{2+}]_i$ in suspensions of quin-2 loaded myocytes. Some of these experiments have been repeated in fura-2 loaded single cells with fluorescence digital imaging microscopy. These results indicate that the receptor-mediated $[Ca^{2+}]_i$ changes in heart are quite different from other tissues such as endocrine cells despite similar biochemical second messenger systems. The mechanism for these receptor-mediated $[Ca^{2+}]_i$ changes will be discussed.

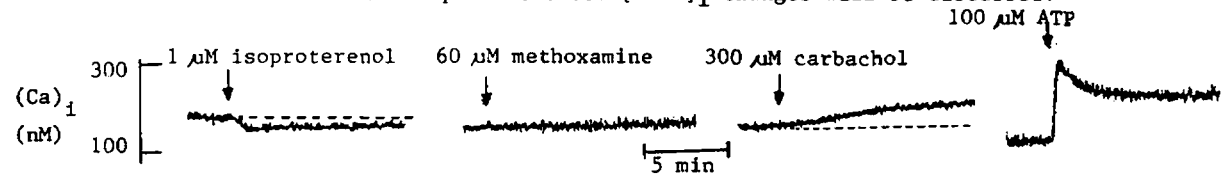

M-PM-C6 Ca^{2+}-DEPENDENT COMPONENT OF DELAYED OUTWARD K^+ CURRENT IN GUINEA PIG VENTRICULAR MYOCYTES

HIRAOKA, M. and FAN, Z., Dept. Cardiovasc. Dis., MRI, Tokyo Med. Dent. Univ., Tokyo-113 JAPAN

It is still controversial whether the delayed outward K^+ current (I_k) in ventricular cells is activated by increased internal Ca^{2+} or not. To clarify this problem, we studied the properties of I_k in the presence and absence of external Ca^{2+}, $[Ca^{2+}]_o$. Membrane currents were recorded from guinea pig ventricular myocytes using a patch clamp technique of the whole-cell configuration. In the absence of external K^+, Na^+ and Ca^{2+}, a time-dependent outward current was activated at potentials positive to -30 mV and increased its amplitude with depolarization, suggesting that I_k was basically controlled by voltage-dependent manner. The time-courses of activation and deactivation were well fitted to two exponential functions. The faster component had time constant about 500 msec and the slower one about 3 sec. The current activation examined by the envelope of the I_k tail was also expressed as the sum of two exponentials. In the presence of $[Ca^{2+}]_o$, the amplitude of the I_k tail increased and achieved faster activation than in its absence. Analyses of two components revealed that Ca^{2+} increased the fraction of the fast component without affecting the time constants and the slower components. When one order reaction between $[Ca^{2+}]_i$ and the activation of I_k plus a basal value was set, we could simulate the behaviors of I_k obtained experimentally. These result indicates that a portion of I_k is activated by increased internal Ca^{2+}, which can determine the action potential duration in ventricular cells.

M-PM-C7 DESCRIPTION OF CHARGE MOVEMENT IN ISOLATED GUINEA-PIG AND RAT VENTRICULAR MYOCYTES. Robert W. Hadley and W.J. Lederer, Dept. of Physiology, University of Maryland School of Medicine, Baltimore, MD 21201.

Nonlinear capacitative currents produced by voltage-sensors in the sarcolemma were studied in guinea-pig and rat ventricular myocytes using the whole-cell patch clamp technique. Ionic currents were minimized by the use of impermeant ions and the addition of organic and inorganic channel blockers to the solutions. Most experiments were done at 21° C, and at a holding potential of -100 mV. The current produced by a hyperpolarization (-100 to -140 mV) was used to subtract the linear capacitative current from all current records. The remaining current met the required criteria for charge movement. The threshold for charge movement appeared to be -60 mV, and it saturated at +40 mV, with a Q_{max} of 11 nC/uF. Inactivation (studied with 5 s clamp steps) occurred over a voltage range of -120 to +20 mV, and could immobilize up to 55% of the charge movement. The time course of Q_{on} decay could be described by a single exponential, which ranged from 1.76 ms at -40 mV to 0.93 ms at +40 mV. This time constant had a Q_{10} of 1.5. Comparison of charge movement in guinea-pig and rat myocytes revealed only minor differences in their properties.

M-PM-C8 THE ATP-DEPENDENCE OF K_{ATP} CHANNELS IN RAT VENTRICULAR MYOCYTES

C.G. Nichols & W.J. Lederer Dept. of Physiology, University of Maryland, School of Medicine, Baltimore, MD 21201.

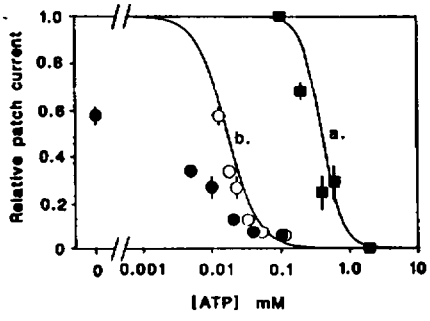

In inside-out (I-O) cardiac membrane patches, the reported K_i for inhibition of K_{ATP} channels by ATP is 15-100 uM. However, in the open-cell attached (O-C-A) patch configuration (on-cell patch formed and cell then permeabilized by exposure to saponin), the reported K_i is 500 uM (Kakei et al. 1985 J. Physiol, 363, 441- 462). The discrepancy between these results has not been explained. The figure shows the ATP-dependence of K_{ATP} channel activity in rat ventricular myocytes in O-C-A configuration (■). The data are fitted by the equation $1/(1+([ATP]/K_i)^H)$ where K_i = 400 uM and H = 3 (curve a). 10 mM creatine phosphate (CP) increased the sensitiviity to ATP (●) and reduced maximum channel activity (in 0 ATP) to about 60 % (relative to current in 0.1 ATP, 0 CP). 10 mM CP had no effect on K_i in I-O patches. (Curve b shows the best fit to I-O patch data, where K_i = 17 uM, H = 2, data not shown). The results suggest that permeabilized cells can be subject to [ATP] gradients between the "inside" of the cell and the bath. These gradients can be relieved by buffering the "internal" [ATP] by CP (i.e. cellular creatine phosphokinase stimulation of ADP + CP --> ATP + creatine). The CP-induced decrease in maximum activity (in 0 ATP) may be explained by CP generation of a small amount of ATP in addition to any added ATP. If it is assumed that CP generates 13 uM ATP (which in I-O patches reduces channel activity to 60 % of maximum), the resulting "corrected" data for O-C-A + CP (○) overlays the data obtained in I-O patches. This suggests that the K_i for I-O patches (17 uM) may also be the true K_i in the intact cell.

Supported by the N.I.H. and A.H.A. (Maryland Affiliate).

M-PM-C9 QUANTITATIVE DESCRIPTION OF THE DEPENDENCE OF THE Na,K-PUMP CURRENT ON INTRACELLULAR Na^+ IN ISOLATED GUINEA PIG VENTRICULAR MYOCYTES

David J. Mogul[1], Donald H. Singer[2,3], & Robert E. Ten Eick[3]
[1]Depts. of Elec. Engr., [2]Medicine, & [3]Pharmacology; Northwestern Univ. Chicago, IL

Na,K-pump current (I_{pump}) is a function of the intracellular Na^+ concentration ($[Na^+]_i$). We examined the quantitative relationship between I_{pump} and $[Na^+]_i$ in isolated guinea pig ventricular myocytes under steady state conditions. Membrane current was measured using the whole-cell-patch voltage-clamp technique. Steady state $[Na^+]_i$ was controlled using wide-tipped pipette microelectrodes. I_{pump} was determined by measuring the difference in steady state holding current between before and during exposure to dihydroouabain (1 mM). V_{hold} = -40 mV. I_{pump} was measured at ten different $[Na^+]_i$ (5 mM - 80 mM; n = 60) with only one measurement per cell and normalized to cell capacitance to account for differences in myocyte surface area. A nonlinear dependence of I_{pump} on $[Na^+]_i$ was found. Hill analysis of the relationship yielded a half-maximal $[Na^+]_i$ for pump stimulation = 23.13 mM and a Hill coefficient = 2.038. An alternative analysis of the experimental data was performed assuming that occupation of three internal binding sites by Na^+ is required for enzyme turnover. Regression analysis gave the best-fit when only two different binding affinities (K_D) are postulated; K_{D1} = 1 mM, $K_{D2} = K_{D3}$ = 29 mM. Using the latter model to analyze our data, the maximum level of I_{pump} when internal Na^+ binding sites are fully saturated closely approximated the theoretical saturation level calculated using published estimates of pump turnover rate and density. The maximum sensitivity of I_{pump} to changes in $[Na^+]_i$ occurred at normal physiological resting $[Na^+]_i$.

M-PM-C10 FLUORESCENT DETECTION OF MANGANESE INFLUX INTO CULTURED CHICK HEART CELLS. C.C. Freudenrich and M. Lieberman, Div. of Physiology, Dept. of Cell Biology, Duke University Medical Center, Durham, NC 27710

In recent years, Mn^{2+} (10 - 20 mM) has been used as a putative blocker of sodium/calcium exchange, even though the site of action has not been identified. We have detected the influx of Mn^{2+} into embryonic chick cardiac cells by exploiting the ability of Mn^{2+} to quench fura2 fluorescence. Cells were grown on coverslips, microinjected with fura2 free acid, and perfused at 37 °C with a Hepes/Tris buffered physiological salt solution on the stage of a microscope coupled to a SPEX fluorimeter. With this technique, the fluorescence from a single cell could be measured. Mn^{2+} (5 - 1000 μM) quenched the fluorescence of intracellular fura2; the rate of quenching was proportional to the Mn^{2+} concentration. The quenched signal was due to Mn^{2+} entry because it was not altered by perfusion with impermeant chelators (EDTA, DTPA), but was reversed by perfusion with a permeant chelator (TPEN). Ca^{2+} channel blockers (10 μM nifedipine + 10 μM verapamil) did not prevent Mn^{2+} from quenching the fura2 signal. Similarly, depletion of intracellular Na did not prevent the quenching action of Mn^{2+}. These results indicate that Mn^{2+} can be transported across the heart cell membrane by a mechanism that does not involve voltage-dependent Ca^{2+} channels or exchange with intracellular Na. [Supported in part by NIH grants HL27105, HL17670, and HL07101.]

M-PM-C11 CORRELATIONS BETWEEN FIBER STRUCTURE AND IMAGES OF VENTRICULAR ACTIVATION (A) AND REPOLARIZATION (R) FROM VOLTAGE-SENSITIVE DYES. Guy Salama, Anthony Kanai, and Richard Lombardi, Univ. of Pittsburgh, Dept. of Physiology, Pittsburgh, PA 15261.

Sheets of ventricular muscle from guinea pig hearts stained with the voltage-sensitive dye (di-4-ANEPPS) were pinned on a stretchable rack, attached to a tension transducer, stimulated at various sites and viewed with a rapid scan photodiode array (12x12), 1420 frames/s. Optical action potentials (APs) and thus A, R and APDs maps were measured from 124 adjacent sites (0.5x0.5 mm and 200μ deep) at various resting lengths. At the end of runs, tissues were marked with fiducial points, fixed, sectioned every 5μ as a function of depth. Fiber axis rotated less than 25° in the first 0.5 mm of epicardium and was superimposed on maps of A, R and APD. Fast and slow A and conduction velocities were aligned respectively to the $\parallel$ and $\perp$ orientation of the fibers regardless of stimulation site. R, like A appears to be an active process and APDs prolonged with fiber stretch in the steep region of the length-tension curve. Supported by the AHA and the Whitaker Foundation.

M-PM-C12 $[Na^+]_i$-DEPENDENCE OF THE CONTRACTILE PROPERTIES OF SINGLE CARDIAC MYOCYTES. Michael Näbauer, Robert Zanotti and Martin Morad. University of Pennsylvania, Department of Physiology, Philadelphia, PA and Mount Desert Island Biological Laboratory, Salsbury Cove, ME

Intracellular Na^+ is known to regulate contraction in cardiac muscle, but its effects on E-C coupling has not been studied directly in single cardiac myocytes. In internally dialyzed single isolated shark (Squalus acanthias) ventricular myocytes, we examined the dependence of tension development on $[Na^+]_i$. Membrane current and cell shortening were measured using the whole-cell patch-clamp method and a 256 element photodiode array. In cells dialyzed with 0 Na^+, the voltage-dependence of shortening and i_{Ca} were similar and bell-shaped. Contraction relaxed completely during 800 ms depolarizing pulses and there was little or no maintained tension. Cell shortening was completely suppressed by nifedipine (5 uM). With 60 mM Na^+ in the pipette solution, the voltage-dependence of shortening was sigmoid and contraction was maintained for the duration of depolarization. Block of the Ca^{2+} channel with nifedipine strongly reduced contraction at 0 mV but did not affect contraction at potentials positive to +60 mV. At both low and high $[Na^+]_i$, repolarization produced slowly decaying tail currents which were closely related to the degree of cell shortening and relaxation. These "tails" were suppressed by nifedipine only in cells dialyzed with 0 Na^+, were abolished by dialysis with 20 mM EGTA, and were unaffected by replacement of K^+_o by Cs^+. These currents may be therefore carried by the Na^+-Ca^{2+} exchanger. We conclude that Ca^{2+} channels transport the Ca^{2+} for contraction in the physiological ranges of membrane potential. Variation of $[Na^+]_i$ allows separation of a "tonic" and "phasic" component of contraction, with the "tonic" component being dependent on the presence of $[Na^+]_i$ and therefore most likely mediated by the Na^+-Ca^{2+} exchanger. Depending on $[Na^+]_i$, the Na^+-Ca^{2+} exchanger may contribute significantly to sequestration of Ca^{2+} and relaxation of tension, even at very positive potentials.

M-PM-D1 **HISTONE SUBUNIT INTERACTIONS AS DETERMINED BY PRESSURE AND SALT PERTURBATIONS.**
Suzanne F. Scarlata, Cornell University Medical College, 1300 York Ave., F231, New York, NY 10021; and Catherine A. Royer, Univ. of Illinois at U-C, Dept. of Physics, Laboratory for Fluorescence Dynamics, 1110 W. Green St., Urbana, IL 61801

We have studied histone-histone interactions for the various histone subunits (H_2A/H_2B and H_3/H_4) using fluorescence spectroscopy. The histones were labeled with a long-lived fluorescence probe (Dansyl) and the polarization and lifetimes were used to monitor changes induced in the associations by salt and pressure perturbations. The dimer form of H_2A/H_2B was found to be stable between 0.1 and 10 μm protein and between 0.100 and 2M NaCl. The H_3/H_4 complex was shown by polarization, lifetime, and gel exclusion chromatography to form dimers of tetramers above 10 μm protein and was entirely octameric at micromolar protein in 2M NaCl. The formation of the histone core particle $(H_2A/H_2B)_2(H_3H_4)_2$ by addition of salt was followed as a function of increasing ionic strength using the polarization and lifetime of the Dansyl dimer. Pressure destabilized all of the above complexes as evidenced by the reversible concentration dependent decreases in polarization. The stabilization of H_3/H_4 interactions by high salt was confirmed by a large shift of the dissociation curve to higher pressure. Addition of the unlabeled H_3/H_4 subunits to the solution of Dansyl-dimer also resulted in a net stabilization of the dimer in the core particle.

M-PM-D2 THE IMPORTANCE OF FLANKING SEQUENCES IN THE SEQUENCE SPECIFIC CLEAVAGE BY THE RESTRICTION ENDONUCLEASES Rsa I, Alu I and Hae III. Kumud Majumder, Molecular Biophysics Unit, Indian Institute of Science, Bangalore, India. (Present address : UNIDO – ICGEB, NII Campus, Shaheed Jeet Singh Marg, New Delhi-110 067, India).

Recent discoveries on the dependence in the sensitivity of some of the restriction enzymes (REs) on the conformational changes in DNA indicate a complex diversity in the nature of RE-DNA interaction. Although the bases around these recognition sequences are believed to be considerably important, not much data is available in this regard. We have studied the importance of flanking sequences in the sequence specific cleavage by the REs - RsaI, AluI and HaeIII. The oligomers d(ACGTACGT), d(CGTACGTACG), poly d(ACGT), d(AGCTAGCT), poly d(AGCT), d(GGCC) and d(CCGGCCGG) were used as the substrates for the relevant enzymes. We have found that in the absence of the flanking bases the REs - RsaI, AluI and HaeIII fail to cleave the corresponding recognition sites. The minimum number of such flanking bases (termed as flanking number or FN) has been found to be two (i.e., FN=2) for Rsa I. Preliminary indications showed that the flanking bases play important role in the case of several other REs also. It appears to us that in the sequence specific cleavage of DNA by RE the flanking bases play two roles viz. (i) provide better binding and improved kinetic stability to the enzyme-DNA complex formed prior to cleavage and (ii) stabilization of the local active conformation by buffering out the neighbouring influences like fraying or altered structure.

M-PM-D3 NUCLEOSOME RECONSTITUTION OF POLY dG·POLY dC AND POLY (rG-dC). Sumedha D. Jayasena and Michael J. Behe, Department of Chemistry, Lehigh University, Bethlehem, Pennsylvania 18015

The double stranded polypurine·polpyrimidine poly dG·poly dC and the mixed ribo-deoxyribo, A-form polynucleotide poly (rG-dC) have been successfully reconstituted into nucleosomes. The radioactively-labeled particles co-migrate in gel electrophoresis and sucrose-density gradient experiments with authentic nucleosomes derived from chicken erythrocyte chromatin. These results show that nucleosomes are able to accomodate a wider variety of polynucleotides than previously believed.

The ability of synthetic polydeoxynucleotides composed of oligoguanosine tracts of increasing length to form nucleosomes has also been determined by several reconstitution procedures. When the presence of nucleosomes is determined by resistance to nuclease digestion, polymers containing long tracts of contiguous guanosines fail to yield a protected band of ~150 base pairs. However, when assayed by a shift in the electrophoretic mobility of radiolabeled polymers exchanged at 0.8 M NaCl with authentic nucleosomes, all polymers tested are seen to form nucleosomes. Quantitative competitive reconstitution shows that the length of the tracts *per se* does not adversely affect their propensity to form nucleosomes since even 150 base pair poly dG·poly dC forms nucleosomes as well as heterogeneous-sequence DNA. However, the ability to form nucleosomes does depend on the length of the polymer repeating unit. Supported by NIH grants GM36343 and CA01159.

M-PM-D4 NEUTRON SCATTERING STUDIES OF DNA GYRASE AND ITS COMPLEX WITH DNA. S. Krueger, National Institute of Standards and Technology, Gaithersburg, MD 20899, G. Zaccai, Institut Laue-Langevin, A. Maxwell, U. of Leicester, A. Wlodawer, National Cancer Institute, and M. O'Dea and M. Gellert, National Institutes of Health, Bethesda, MD 20892.

Small angle neutron scattering (SANS) studies have been performed on bacterial DNA gyrase, which catalyzes the ATP-dependent supercoiling of DNA. The active enzyme consists of two proteins, A and B, of molecular weights 97,000 and 90,000, respectively, in an A_2B_2 complex. DNA readily binds to the enzyme in the absence of ATP. However, ATP hydrolysis is required in order to complete the supercoiling process.

The contrast variation technique was used in order to study gyrase and its complex with a 172 bp piece of DNA in both H_2O and D_2O solvents. The complex was also measured in the presence of the non-hydrolyzable ATP analog, ADPNP, which is known to support limited supercoiling. A radius of gyration, R_g = 67Å, was found for the gyrase alone. This is larger than would be expected from its known molecular weight and partial specific volume, suggesting a "hollow" particle. The entire H_2O scattering curve fits best to an oblate ellipsoid with semi-axes a:a:b in the ratio a/b = 2.5. R_g changes very little upon DNA binding, suggesting that the centers of mass for both the gyrase and DNA are close to each other. Increased aggregation of the complex upon addition of ADPNP prevents an accurate calculation of R_g. However, the D_2O scattering curve at higher angles fits best to an oblate ellipsoid with a/b = 2.0, implying that the gyrase enzyme is slightly more compact when ADPNP is bound. The SANS results were combined with those from biochemical and other structural techniques in order to construct a more complete model of DNA gyrase and its complex with DNA.

M-PM-D5 RECOGNITION OF SPECIFIC RNA SEQUENCES BY VIRAL COAT PROTEINS.
Gerald Stubbs and Rekha Pattanayek
Dept. of Molecular Biology, Vanderbilt University, Nashville, TN 37235

The structure of tobacco mosaic virus, which has been determined at 2.9Å resolution by fiber diffraction methods, offers a unique opportunity to study the basis for specificity in protein-nucleic acid recognition. Assembly of tobamoviruses is initiated at a hairpin loop in the viral RNA, either 400 or 900 nucleotides from the 3' end, depending on the virus. Five different viruses show a repeating pattern of GXX in this loop, regardless of the site used.

In the TMV structure, the protein-nucleic acid interactions are highly ordered and very clear. There are three base-binding sites on each protein subunit, and one of these sites appears to have a distinct specificity for guanine. The base sits between two intersubunit ion pairs, Arg 122 - Asp 88 and Asp 115 - Arg 113. Atom O6 forms a hydrogen bond with Arg 122; N2 with Asp 115. Asp 88, Arg 113 and Asp 115 are invariant in the many known tobamoviruses; Arg 122 changes to His in a few cases.

The hydrogen bond between N2 and Asp 115 is the most guanine-specific hydrogen bond in the structure. Indeed, consideration of base and amino-acid structures shows that a G-Asp hydrogen bond is the most base-specific hydrogen bond possible. It is thus not surprising that guanine is used repeatedly in the control of critical cellular processes; examples in addition to viral assembly include the range of mechanisms utilizing G proteins, switching of elongation factor states, and assembly of microtubules. In the few cases where the G binding sites are known, an Asp-N2 bond has either been observed or is consistent with present knowledge of the structure.

M-PM-D6 HIGH RESOLUTION CRYSTAL STRUCTURE OF E. COLI GLUTAMINYL-tRNA SYNTHETASE COMPLEXED WITH ITS COGNATE tRNA. Mark Rould, John J. Perona, and Thomas A. Steitz. Department of Molecular Biophysics and Biochemistry and Howard Hughes Medical Institute, Yale University, New Haven CT 06511.
Crystals of the ternary complex of glutaminyl-tRNA synthetase, its cognate tRNA, and ATP have been obtained which diffract beyond 2.8 angstroms. Four isomorphous heavy atom derivatives have been found; Iterations of solvent flattening and heavy atom parameter refinement have yielded a readily interpretable 2.8 A resolution electron density map. At present, the tRNA, as well as the amino terminal 350 of the 553 total residues comprising the synthetase have been fit to the map. Comparison of the bound tRNA-gln with uncomplexed phenylalanine tRNA suggests protein-induced distortion of the tRNA structure in the acceptor region and the anticodon loop. The amino terminal domain of the synthetase, containing the ATP and glutamine binding sites, intimately interacts with the acceptor end of the molecule, disrupting base pairing of U1 with A72 and directing the 3' terminus back toward the anticodon. Here the protein stabilizes an RNA conformation in which the base of C74 is looped out, allowing the bases of G73, C75 and A76 to stack. Fitting of the carboxyl-terminal domain of the protein is in progress, and has revealed interactions with the inside of the L-shaped structure extending from the D-loop to the anticodon loop. Specific interactions are seen between the C-terminal domain and the anticodon.

M-PM-D7 DIFFERENTIAL KINETICS AND SPECIFICITY OF recA BINDING TO RIGHT- AND LEFT-HANDED NUCLEIC ACID DOUBLE HELICES. Daniel S. Pilch[a], David A. Zarling[b,c], Hirak Basu[c], and Richard H. Shafer[d]. [a]Graduate Group in Biophysics, University of California, San Francisco, CA 94143, [b]Molecular Biology Department, SRI International, Menlo Park, CA 94025, [c]Department of Laboratory Medicine, [d]Department of Pharmaceutical Chemistry, University of California, San Francisco, CA 94143.

E. Coli recA protein catalyzes homologous recombination between single- and double-stranded nucleic acid sequences. In an SOS response, high levels of recA protein are induced by damage or perturbations to the nucleic acid helical structure, such as those resulting from adduction by certain chemical carcinogens. We have measured the kinetics of recA binding to right-handed (B- or A-form) and left-handed (Z-form) synthetic linear oligo- and polynucleotide sequences. The Z-sequences were stabilized by either modified base substitutions or chemical carcinogen adduction. RecA binds Z-form polydeoxynucleotides faster than the corresponding B-forms. The nature and magnitude of these kinetic differences is dependent on [ATPγS], [$MgCl_2$], [DNA]/[recA] ratio, temperature, pH, and [polyamine]. At concentrations precluding DNA aggregation, polyamines inhibit recA binding. We have previously shown that polyamines recognize determinants on the phosphate backbone of Z-DNA. Hence, polyamine inhibition of recA binding suggests recA recognition of phosphate backbone determinants as well. Studies with B- and Z-oligodeoxynucleotide substrates show that DNA length profoundly affects the equilibrium binding and kinetic preferences of recA. Furthermore, recA specifically binds Z-form polyribonucleotides compared to the A-forms, which it fails to recognize. Such differential binding affinities and kinetics suggest that Z-sequences, B-Z junctions, or adduct-induced regions of strand separation and distortion may act as nucleation sites for recA binding to double-stranded helices.

M-PM-D8 CRYO-ELECTRON MICROSCOPY OF CHROMOSOME FIBERS S. P. Williams, M. S. Smith, D. Rankert, and J. P. Langmore, University of Michigan, Ann Arbor, MI

Isolated chromatin fibers from erythrocytes of Necturus maculosus and sperm of Thyone briarius were examined in vitreous ice by energy-filtered cryo-electron microscopy. The microscopic results were directly correlated with results from x-ray scattering, performed in the same buffer (consisting of 60mM KCl, 15mM NaCl, 15mM PIPES, 3mM EDTA, pH 7.2). These data show that the diameter of the fibers is directly related to the linker length of the chromatin. For example, modified Guinier plots from x-ray data obtained at Stanford Synchrotron Radiation Laboratory indicate that the cross-sectional radii of gyration of the fibers are: 11 nm for Necturus (N = 48 bp); 12.2 nm for chicken erythrocytes (N = 66 bp); and 14.6 nm for Thyone (N = 88 bp). If the chromatin fibers are assumed to have constant density (as indicated by the microscopy) the scattering data indicate experimental diameters of 31 nm for Necturus, 34 nm for chicken, and 41 nm for Thyone chromatin in solution. The crossed-linker models predict diameters of 30 nm, 34 nm, and 40 nm, respectively. Reconstructions of the radial density distributions of frozen-dried and of frozen-hydrated fibers exhibit a core containing a high density of biological material rather than solvent-filled space. Fourier transforms of the frozen-hydrated fibers show consistent features indicative of helical symmetry. The structural data are consistent with the crossed-linker model for chromatin.

M-PM-D9 *IN VIVO* INTERACTION OF THE *LAC* REPRESSOR N-TERMINAL DOMAIN WITH THE *LAC* OPERATOR DNA Anastasia M. Khoury and Ponzy Lu, Dept. of Chemistry, University of Pennsylvania, Philadelphia, PA 19104 and Harry S. Nick, Dept. of Biochemistry and Molecular Biology, University of Florida, Gainesville, FL 32610

The *E. coli* lactose operon has been the paradigm for gene regulation, and the structure of its repressor is of considerable interest because of the wealth of available genetic information. This tetrameric protein (360 amino acids/subunit) has evaded crystallization. However, detailed ^1H NMR studies have yielded a folded secondary structure for the first 51 amino acids (Kaptein *et al.*(1985) J. Mol. Biol., **182**, 179). Considerable genetic evidence and *in vitro* biochemical data indicate that these N-terminal amino acids comprise most if not all of the DNA interaction site. This has been challenged by *in vitro* data which suggest that operator DNA binding specificity resides entirely in tetramers missing the first 51 amino acids (Manly *et al.*(1984) J. Mol. Biol., **179**, 315).

The N-terminal DNA binding domain (headpiece) has always been isolated by cleavage with proteases yielding N-terminal fragments of 51-59 amino acids. Longer intact peptide fragments with DNA binding activity can not be obtained by this approach. In order to explore the repressor structure beyond the first 50 or so amino acid residues by ^1H and ^{15}N NMR spectroscopy, we have cloned the DNA sequence encoding various lengths of the *lac I* gene N-terminal domain into a vector system driven by the coliphage T7 RNA polymerase/promoter. In addition to the wild type sequence, we have generated single mutations at position 3 (Pro3 --> Tyr) and 61 (Ser61 --> Leu) as well as a double mutation in an N-terminal fragment 64 amino acids long. These mutations were chosen because they increase the DNA binding affinity of the intact *lac* repressor by a factor of 10^2-10^4. The production of these *lac* repressor fragments in the cell has been verified by radioimmunoassays. We have confirmed the binding of the wild type and mutant headpiece peptides both by *in vivo* footprinting and reduced β-galactosidase synthesis. These observations reinforce the usefulness of our approach to fully characterize the DNA binding region of the *lac* repressor. (Supported by Grants from the NIH)

M-PM-D10 THERMODYNAMIC CHARACTERIZATION OF THE BINDING OF E. COLI GAL-REPRESSOR TO ITS OPERATOR.
Elizabeth Jamison, Marie Pak and Michael Brenowitz. Department of Biochemistry, The Albert Einstein College of Medicine, Bronx, New York 10461.

E. coli gal-repressor regulates the activity of the *gal* operon by specifically binding to two sites in the absence of galactose. The location of these binding-sites is unusual in that the "external" site, O_E, is located upstream of the transcription start-site and the "internal" site, O_I, is located downstream; within the coding sequence of the first structural gene of the operon. It has been proposed that *gal*-repressor binds *cooperatively* to O_E and O_I causing the DNA between the sites to "loop" (Majumdar, A. & Adhya, S. (1984) Proc. Natl. Acad. Sci. 81: 6100-6104). Formation of this loop is thought to prevent binding of RNA polymerase through a mechanism involving steric inhibition. Studies of regulation *in vivo* support this model (Adhya, S., personal communication).

The *intrinsic* binding free energies, ΔG_E and ΔG_I, and the free energy of cooperativity, ΔG_{EI}, for the binding of *gal*-repressor to linear restriction fragments containing the wildtype operator or O_E^- or O_I^- mutants were examined *in vitro* using the quantitative DNase footprint titration method (Brenowitz, M., Senear, D.F., Shea, M.A. & Ackers, G.K. (1986) Proc. Natl. Acad. Sci. 83: 8462-8466). Under all solution conditions which have been tested $\Delta G_E = \Delta G_I \pm 0.2$ kcal/mol and, surprisingly, $\Delta G_{EI} = 0.0 \pm 0.2$ kcal/mol. Binding of *gal*-repressor is clearly non-cooperative. Possible explanations of the differences between the *in vivo* and *in vitro* results will be discussed. (Supported by NIH grant GM39929 and BRSG funds to the College of Medicine.)

M-PM-E1 EVIDENCE FOR EXCHANGEABLE PROTONS NEAR THE HEME OF FERROCYTOCHROME C AS DETECTED BY RESONANCE RAMAN DIFFERENCE SPECTROSCOPY. Jose A. Centeno[1,2] & Gerald T. Babcock*
[1]Departments of Chemistry, University of Puerto Rico, Mayaguez, P.R. 00708; Michigan State University, East Lansing, MI 48824-1322; [2]Department of Cellular Pathology, American Registry of Pathology, Armed Forces Institute of Pathology, Washington DC, 20306-2915.

Resonance Raman difference spectroscopy has been employed to probe the occurrence of H/D exchangeable sites near the heme chromophore of reduced cytochrome c. Frequency shifts of the metal atom oxidation state marker band at 1362 cm^{-1}(ν_4,C_a-N) and a porphyrin macrocycle core size related mode at 692 cm^{-1}(ν_7,δC_a-C_b-N), were detected. The low frequency spectrum, below 450 cm^{-1}, displays changes at 270 cm^{-1}, 350 cm^{-1}, 360 cm^{-1}, and 402 cm^{-1} upon use of deuterated buffers. The former Raman line is assigned to the out-of-plane pyrrole-substituent deformation mode, while the 360 cm^{-1} line may be ascribed to the $2\nu_{35}$ skeletal mode overtone, believed to be in Fermi resonance with the totally symmetric mode, ν_8, at 350 cm^{-1}. The 402 cm^{-1} line, which shifts down by 10 cm^{-1} when H_2O is substituted by D_2O, is assigned to an out-of-plane pyrrole folding mode based upon previous model compound assignments. Significant contributions from pyrrole rings III and IV, bearing the propionic acid side-chain peripheral groups, appears to be a determining factor in the resonance Raman intensity and frequency positions of these low-frequency modes. A comparison of the resonance Raman spectra of ferric cytochrome c in protonated and deuterated buffers resulted in intensity changes but no isotopic shifts were detected. This observation together with the detected changes in the oxidation state marker band, ν_4, are interpreted as indicating an increased electron density distribution in the porphyrin pyrrole ring's π-system upon isotopic substitution. (Supported by NIH Grant GM25480)

M-PM-E2 **COORDINATION CHEMISTRY AND MACROCYCLE CONFORMATION OF COFACTOR F_{430} OF METHYL-REDUCTASE AND RELATED NICKEL TETRAPYRROLES** **J. A. Shelnutt,[1] A. K. Shiemke,[2] R. A. Scott,[2] B. A. Crawford,[3] R. G. Alden,[3] M. R. Ondrias[3], [1]Sandia National Laboratories, Albuquerque, NM 87185, [2]University of Georgia, Athens, GA, [3]University of New Mexico, Albuquerque, NM.**

Methylreductase is the terminal enzyme of the reaction pathway leading to H_2 reduction of CO_2 to methane. The active site of methane reduction contains a nickel-tetrapyrrole cofactor, called F_{430}. Resonance Raman and UV-visible absorption spectroscopies have been used to investigate the axial ligation properties of F_{430} in solution and in the intact enzyme. In solution at low temperature, F_{430} is found to be hexa-coordinate with two water molecules acting as axial ligands. Between 0 and 65 C, F_{430} undergoes a transition from the bis-aquo complex to the tetra-coordinate complex. The strong temperature dependence of the binding affinity for H_2O may be physiologically relevant, since methylreductase is isolated from a thermophilic bacterium with optimum growth at 65 C. In the enzyme at room temperature, F_{430} is hexacoordinate; however, the enzyme site is unique in some fashion giving rise to an unusual Raman spectrum not observed for any common F_{430} axial ligand complex. The unique nature of the enzyme site may involve a special axial ligand or ligand geometry. Alternatively, a special macrocycle conformation might be involved. Using Raman spectroscopy we have observed multiple conformations of the tetrapyrrole macrocycle in a nickel-hydrocorphin related to F_{430}. Because of the out-of-plane macrocycle flexibility of such reduced tetrapyrroles, the low-temperature forms of the F_{430} analog are ascribed to ruffled conformers of the macrocycle. The conformations of the F_{430} analog are probably analogous to the planar and ruffled conformers of nickel porphyrins that coexist in solution.

***Supported by U. S. DOE Contract DE-AC04-76DP00789 and GRI Contract 5082-260-0767.**

M-PM-E3 VISIBLE EXCITATION RESONANCE RAMAN SPECTRA OF CYTOCHROME a IN CYTOCHROME c OXIDASE Jose A. Centeno[1,2] & Gerald T. Babcock*
[1]Departments of Chemistry, University of Puerto Rico, Mayaguez, P.R. 00708; *Michigan State University East Lansing, MI 48824-1322. [2]Department of Cellular Pathology, American Registry of Pathology, Armed Forces Institute of Pathology, Washington, DC 20306-2915.

To isolate the vibrations of cytochrome a from those of cytochrome a_3, we have employed visible excitation resonance Raman spectroscopy, in resonance with the zeroth vibrational level of the $Q_{(0-0)}$ electronic state of reduced cytochrome a^{2+} at 605 nm. With this laser excitation, the vibrations of cyt a^{2+} are markedly enhanced owing to its dominant contribution to the 605 nm α-band optical electronic absorption of reduced cytochrome c oxidase. We have studied the RR visible region of cyt a^{2+} under the influence of small perturbations near the heme a chromophore induced by the presence of deuterated buffers. Several of the high- and low-frequency formyl and vinyl vibrational modes display large isotopic shifts in the presence of deuterium atoms, indicating the important role of these side-chain peripheral substituents in determine the active structure of cyt a. A high frequency mode at 1615 cm^{-1} shifts down to 1611 cm^{-1} upon H/D exchange, suggesting a formyl contribution to this line, as previously predicted from α-band excitation studies of heme a model compounds. We have studied the depolarization ratio dependence of cyt a vibrational modes and found that a few modes exhibit characteristic anomalous polarization behavior, while the great majority of the visible excitation vibrations appear as polarized modes, approaching a value of 0.33. This is interpreted as arrising from a significant lowering in the molecular symmetry of the heme a macrocycle brought about by the unusual peripheral substituent pattern of heme a and strong cyt a...protein interactions.

M-PM-E4 SATURATION RAMAN SPECTROSCOPY OF PROTEINS.
Sanford A. Asher, J. Teraoka and P. A. Harmon, Department of Chemistry, University of Pittsburgh, Pittsburgh, Pennsylvania 15260.

The high power fluxes associated with typical UV excitation sources complicate UV resonance Raman (RR) studies of ground state species. Saturation of ground state intensities occur if the ground state population is depleted during the laser pulse.

We have developed models for saturation mechanisms, and explicitly explore the aromatic amino acid RR intensity dependence upon the incident laser power flux to learn about excited state interactions and relaxation processes.

We compare saturation between tryptophan-tyrosine dimers and mixtures of monomers to examine inter-residue interactions.

We also examine saturation of aromatic amino acid residues in heme and non-heme proteins to compare relaxation rates and the dependence of these rates upon protein conformation.

M-PM-E5 **Correlation between the alkaline Bohr effect and conformational changes of the heme group in the modified oxyHb -NES detected by resonance Raman spectroscopy**
Reinhard Schweitzer-Stenner, Dörte Wedekind and Wolfgang Dreybrodt
University of Bremen, Fachbereich 1 - Physics Department, 2800 Bremen, Fed. Rep. of Germany
The depolarization ratio dispersion (DPD) of two prominent Raman fundamentals (1375cm^{-1} and 1638cm^{-1}) of the modified oxyhemoglobin NES(N-ethyl succinimide) has been measured for pH-values between 6.0 and 8.5. Both modes exhibit a pH-dependence. The DPD are fitted to a fifth order time dependent perturbation theory. This yields parameters related to symmetry classified distortions of the heme. These depend on the pH-value and result as an effective value from the incoherent superposition of Raman intensity at distinct conformations of the heme. These distinct conformers are due to a distinct titration state of the protein. Hence a titration model is formulated relating each conformation to a set of distortion parameters. Fitting this model to the pH-dependent effective parameters reveals that the protonation of two amino acid residues with pK=6.5 and 8.2 affects the symmetry of the heme. These structural changes correspond to variations of the oxygen affinity. We applied the allosteric model of HERZFELD and STANLEY(J.Mol.Biol.82,231,1974) to O_2-binding curves measured at different pH-values. From this calculation we find the pK-values determining the Bohr effect are the same as those from the Raman data. By comparison with O_2-binding curves of HbA one assignes these pK to amino acids of the β-subunits (most probably HIS(FG5)β and LYS(EF6)β). The relation between heme distortions and O_2-affinity is rationalized in terms of orientational changes of the proximal histidine with respect to the heme core which effects asymmetric perturbations of the active site via interactions between the pyrrole nitrogens and the proximal imidazole thus affecting the binding properties of the Fe^{2+}-atom.

M-PM-E6 UV RESONANCE RAMAN ENVIRONMENTAL STUDIES OF TYROSYL AND TRYPTOPHYL RESIDUES OF MAMALIAN MYOGLOBIN USING A HIGH-REPETITION-RATE EXCIMER-BASED UV LASER.
P. J. Larkin, J. Teraoka, S. Song, and S. A. Asher, Department of Chemistry, University of Pittsburgh, Pittsburgh, Pennsylvania 15260.

UV Resonance Raman spectra of Horse and Sperm Whale myoglobin (Mb) excited at 225 and 240 nm, show well defined Raman bands between 600-1600 cm^{-1}, readily assigned to tyrosyl and tryptophyl residues. No interferences from phenylalanine vibrations occur at this wavelength. We compare the titration behavior of the resonance Raman spectra of the myoglobins to a stoichiometric mixture of aromatic amino acids between pH 6.80 and pH 13.30 in order to examine protein conformational changes. These studies require a high repetition rate (200 Hz) excimer laser-based UV Raman excitation source at low average power to avoid Raman saturation and/or interferences from photochemical transients which occur with a 20 Hz Nd:Yag excitation source.

We see titration behavior similar to that expected for the three tyr with pK_a values previously obtained from visible absorption spectroscopy. However, the tyr Raman cross sections change as residues titrate and the protein conformation changes. We see protein denaturation at high pH values which lead to large Raman intensity changes. We also observe a dependence of the Trp cross sections on protein conformation which reflect the local trp environment. We will discuss the environmental dependence of tyr and trp intensities and frequencies. We will also present UV resonance Raman studies of hemoglobin which characterize the differences in aromatic amino acid environment between R ⇄ T conformations important in the hemoglobin cooperativity mechanism.

M-PM-E7 X-RAY CRYSTALLOGRAPHY OF CYTOCHROME *c* UNDER PHYSIOLOGICAL CONDITIONS
M. Walter, S. Tykodi, A. Uhm, E. Westbrook, M. Sabat, E. Margoliash

It is now possible, for the first time in the history of cytochrome *c* x-ray crystallography, to arrive at an atomic structure under conditions representative of the physiological. Every previous x-ray diffraction study has utilized crystalline cytochrome *c* formed under non-physiological conditions at a minimal ionic strength of 7.5 molar. Experimental evidence chronicles the influence of the electrostatic environment upon many properties of the protein, some of which are influenced by the structure and are known to change as the ionic strength decreases below 200 mM. Consequently, every previously reported structure for cytochrome *c* reveals a protein which is not necessarily identical to that operating under physiological conditions.

As a first step in our investigation, we have successfully crystallized cytochrome *c* in a solution with an ionic strength of 30-40 mM. These crystals grow typically to dimensions of 0.2 x 0.4 x 1.0 mm in two to four weeks. The crystals belong to space group $P2_1$, with cell dimensions a = 37.3(5) Angstroms, b = 107.7(5) Angstroms, c = 56.0(3) Angstroms, β = 105.5(2) degrees. There are two monomers of cytochrome *c* per asymmetric unit, occupying 27% of the crystal volume. We have recorded 9,797 unique Bragg reflections, 87% of those possible, out to a resolution of 2.8 Angstroms. The symmetry R-factor for these data was 4.8% on intensity. These crystals clearly diffract to beyond 2.2 Angstroms, and are very stable in the x-ray beam.

We expect to successfully determine the structure of cytochrome *c* under physiological ionic conditions by the molecular replacement method. We have determined an unambiguous solution for the rotation function between the high-salt crystal and this low-salt form of cytochrome *c*, and there is promise for a successful translation solution to this structure.

(Supported by NIH grants GM19121 and GM29001, and DOE Contract No. W-31-109-ENG-38)

M-PM-E8 DYNAMICS AND ELECTROSTATICS IN SITE-SPECIFIC HUMAN Mb MUTANTS. S.G. Boxer, R. Varadarajan, D. Lambright, and S. Balasubramanian, Dept. of Chemistry, Stanford University, Stanford, CA 94305

Mutants of human Mb have been engineered to test specific hypotheses concerning residues which control the dynamics of ligand access to the heme pocket. Lys 45 → Arg (K45R) and Asp 60 → Glu (D60E) test the possible role of a salt bridge. Both k_{on} and k_{off} for CO for D60E were found to be identical to wild-type. For K45R k_{on} increased by a factor of 1.8, whereas k_{off} decreases by about 30%. These results suggest that a salt-bridge between residues 45 and 60 is not important for controlling ligand access in human Mb, while the residue at position 45 may play a role. Possible mechanisms to produce this change will be discussed, along with results from other mutants and ps NO geminate recombination kinetics (collaboration with J.-L. Martin and J. Petrich, ENSTA). Residue Val 68 (E11) has been changed to Ala, Asn, Glu and Asp (V68A, N, E, and D, respectively). In the ferric form, Glu is weakly coordinated to Fe as in Hb. Milwaukee, whereas the Asp side chain in V68D is too short to permit coordination without large conformational changes which are not observed. Isoelectric focussing data demonstrates that the carboxylate side-chains at position 68 in V68E and V68D are ionized in the ferric state, whereas reduction from Fe(III) to Fe(II) is accompanied by uptake of a proton. Large changes in the redox potential for the Fe(III)/Fe(II) couple are observed for V68E and V68D and the contributions of enthalpy and entropy changes have been quantitated (collaboration T. Zewert and H. Gray, Caltech). Apparent pK_a values for the buried Glu residue are obtained and used to provide an estimate for the polarity of the heme pocket at this site. Supported by NIH GM-27738

M-PM-E9 TIME-RESOLVED EMISSION SPECTRA AND CONCENTRATION DEPENDENCE OF THE PICOSECOND LIFETIMES OF UNLIGANDED HEMOGLOBIN. Enrico Bucci, Henryk Malak, Clara Fronticelli, and Joseph R. Lakowicz. Dept of Biochemistry, U. Md. Med. Sch, Baltimore MD 21201 We have used a 2 GHz fluorometer and front-face geometry for exploring the time-resolved characteristics of the emission of tryptophans of unliganded hemoglobin. The emission displayed ps and ns lifetimes at all wavelength between 313 and 380 nm. The lifetimes were independent of wavelength, and the fractional intensity of the ns components increased with wavelength. The time-resolved spectra revealed the presence of two distinct spectral emissions with peaks near 320 and 335 nm, corresponding to the ps and ns lifetimes respectively. A surprising finding was a blue shift of the spectrum corresponding to the emission in the ps time-range, during the first 100 ps of observation. Correspondingly the time-dependent center of gravity of the time-resolved spectra decreased to a minimum wavelength at 100 ps, followed by the increase produced by the increasing fractional intensity of the ns components. Another surprising observation was that the ps lifetime which is 5 ps at hemoglobin concentrations between 2 and 4 mg/ml increases with protein concentration to a maximum of 30 ps at 20 mg/ml. This concentration dependence was not present in CO hemoglobin which showed a ps lifetime of 25 ps. Addition of a bubble of CO to a 2mg/ml sample of deoxyhemoglobin converted the lifetime of the sample (5 ps) to that of CO hemoglobin (25 ps). These findings indicate a photodissociation of deoxyhemoglobin into subunits, upon illumination with laser light at 290 nm. Preliminary experiments conducted with hemoglobins intramolecularly crosslinked either between the alpha or between the beta subunits suggest that the photodissociation involves a separation of the alpha from the beta subunits.

M-PM-E10 PICOSECOND QUANTUM YIELDS AND KINETICS FOR O_2 AND CO HEMOGLOBIN AND MYOGLOBIN PHOTOLYSIS AT LOW TEMPERATURE. Mark R. Chance, Georgetown U., Department of Chemistry, Washington, D.C., Joel M. Friedman and Scott H. Courtney, AT&T Bell Labs, Murray, Hill, N.J., Mark Ondrias, Department of Chemistry, University of New Mexico, Albuquerque, New Mexico.

Ultrafast spectroscopy has been especially useful in identifying the primary events in photolytic processes, especially issues of quantum yields and geminate recombination. We have studied the photophysics of O and CO ligands with hemoglobin and myoglobin at low temperature, in an attempt to observe fast processes (Petrich et. al., Biochemistry, 1988, v. 27, p.4049.) using transient absorption techniques with a 30 ps photolysis pulse at 532nm. Our results show large apparent quantum yield differences for the two ligands at 10K and above, with an apparent yield for O photolysis of 0.6 and a yield for CO of 1.0. In addition, the photoproducts were stable at very low temperatures, evidencing little recombination. The apparently unphotolyzed portion of the O samples either did not photolyze under conditions of high powers (i.e. conditions where the CO samples were fully photolyzed) or recombined within the duration of the pulse. No rise times were observed, the absorbance changes were complete within the pulse duration. Transient absorption spectroscopy using a delay line showed fast geminate recombination for the O hemoglobin samples from 250K to 100K. Below 100K geminate recombination of CO and O hemoglobin was similar.

M-PM-E11 **Dynamics of Myoglobin with the Proximal Histidine-Iron Bond Broken**

Benjamin R. Cowen, David Braunstein, Hans Frauenfelder, Peter J. Steinbach, and Robert D. Young, Departments of Physics and Biophysics, University of Illinois, Urbana, Il 61801

Ascenzi et al. have shown that in sperm whale myoglobin (Mb) the proximal histidine (F8) protonates, causing the histidine-iron bond to break with a pK of 3.45[1]. With the proximal bond broken the room temperature carbonmonoxide (CO) association rate is about 20 times larger than that of Mb at pH 7. Their results raise the question as to whether the larger association rate is caused by a smaller enthalpic barrier at the heme. To answer this question we measured the rebinding kinetics of MbCO(pH3) in 75% glycerol/water following low-temperature flash photolysis. We monitored in the Soret from 10K to 280K and from 50 ns to 100 s. Below about 200K, the observed nonexponential kinetics is attributed to rebinding from the pocket, process I. The resulting distribution of enthalpic barriers for process I peaks at about 1 kJ/mol compared to 10 kJ/mol for Mb(pH7) and about 2 kJ/mol for protoheme. The pre-exponential for Mb(pH3) lies between that of Mb(pH7), ~10^9 s^{-1}, and that of protoheme, ~10^{11} s^{-1}. The proximal histidine bond in myoglobin contributes significantly to both the enthalpic and entropic barrier at the heme; thus it provides a mechanism by which the protein controls the ligand binding process.

1. Ascenzi, P., Brunori, M., Coletta, M. ,and Traylor, T.G. (1985) in *Structure and Motion: Membranes, Nucleic Acids & Proteins*, eds. Clementi, E., Corongiu, G., Sarma, M.H., and Sarma, R.H. (Adenine, Guilderland, NY), pp. 331-337

M-PM-E12 KINETIC COOPERATIVITY IN HEMOGLOBIN. Lionel P. Murray, Eric R. Henry, James Hofrichter, Naoya Shibayama, Takashi Yonetani, and William A. Eaton. Laboratory of Chemical Physics, NIDDK, NIH, Bethesda, MD; Department of Biochemistry and Biophysics, University of Pennsylvania School of Medicine, Philadelphia, PA; Department of Physics, Jichi Medical School, Tochigi, Japan.

We have employed time-resolved absorption spectroscopy in photodissociation experiments with nanosecond lasers to investigate the origin of cooperativity in the kinetics of carbon monoxide binding to hemoglobin. To study the kinetic properties of the beta subunit within an intact tetramer, the unreactive nickel(II) ion was substituted for iron in the alpha subunits. Lowering tne pH from 8.0 to 6.5 switches the population of diliganded $\alpha(Ni)\beta(Fe\text{-}CO)$ tetramers from mostly R-state molecules to mostly T-state molecules, as judged by the amplitudes of the fast and slow bimolecular rebinding phases. The geminate yield, which is the probability that the ligand rebinds to the heme from within the protein, is found to be 35% for the R-state, while for the T-state it is less than 1%. These results are very similar to what was found for the $\alpha(Fe\text{-}CO)\beta(Co)$ hybrid hemoglobin (Murray et al. Proc. Natl. Acad. Sci. USA 85, 2151-2155 (1988)). According to the simplest kinetic model, the results indicate that carbon monoxide enters the protein in the R and T quaternary conformations at the same rate; for both alpha and beta subunits the 60-fold decrease in the overall binding rate of carbon monoxide to the T state compared to the R state is almost completely accounted for by the decreased probability of binding after the ligand has entered the protein. The results also suggest that the low probability of binding in the T-state results from a decreased binding rate to the heme, and not from an increased rate of return of the ligand to the solvent.

M-PM-F1 SECONDARY STRUCTURE OF AN INTEGRIN RECEPTOR: PURIFIED PLATELET GLYCOPROTEIN IIb-IIIa. S. L. Helgerson, L. V. Parise,* and D. R. Phillips,* Chemistry Dept., Montana State Univ., Bozeman, MT 59717; *Gladstone Foundation Lab. and CVRI, UCSF, San Francisco, CA 94140.

Glycoprotein IIb-IIIa is the platelet cell membrane receptor for the adhesive proteins fibrinogen and fibronectin. GPIIb-IIIa is one of the integrin family of receptor proteins which bind the RGD peptide sequence common to the adhesive proteins. In human platelet cells, this interaction is important in the normal coagulation of blood and in the abnormal process of thrombosis associated with heart disease. The hypothesis is being tested that the binding of adhesive proteins triggers secondary events in the platelet cell through conformational changes in GPIIb-IIIa [1]. We have applied secondary structure prediction techniques and CD spectroscopy to GPIIb-IIIa. Based on the primary sequences for GPIIb and GPIIIa, the predicted secondary structure for the GPIIb-IIIa complex is 16% alpha-helix, 52% beta-sheet, 21% beta-turn, and 10% random coil using the Garnier-Osguthorpe-Robson algorithm, or 18% alpha-helix, 22% beta-sheet, 45% beta-turn, and 15% random coil using the Chou-Fasman technique. The CD spectrum from 190-250 nm of the purified GPIIb-IIIa complex in the detergent C12E8 shows a CD intensity at 222 nm of -4800 deg·cm^2/decimole. This indicates a low alpha-helical content. Analysis of the CD spectrum gives a secondary structure of 13% alpha-helix, 34% beta-sheet, 16% beta-turn, and 32% random coil using the Manavalan-Johnson variable selection CD basis set, or 19% alpha-helix, 35% beta-sheet, 3% beta-turn and 18% random coil using the Yang-Wu-Martinez CD basis set. The secondary structure prediction techniques and the CD spectrum analysis methods will be compared and contrasted.

[1] Parise et al. (1987) J. Biol. Chem. 262:12597-12602.

M-PM-F2 CELL SURFACE DISTRIBUTION OF Fc RECEPTORS II AND III ON LIVING HUMAN NEUTROPHILS BEFORE AND DURING ANTIBODY DEPENDENT CELLULAR CYTOTOXICITY. H.R. Petty, J.W. Francis, and C.L. Anderson,* Dept. Biol. Sci., Wayne State Univ., Detroit, MI and *Dept. Int. Med., Ohio State Univ., Columbus, OH.

Microscopic techniques have been employed to study the cell surface distributions of the immunoglobulin Fc receptors (FcR) II and III on living human neutrophils. Fluorescein- or rhodamine-conjugated monoclonal IgG or Fab fragments directed against FcRII and FcRIII were employed to label receptors. FcRII and III were found to be uniformly distributed at neutrophil surfaces during resting conditions. During neutrophil polarization and migration FcRII but not FcRIII preferentially accumulated at the uropod. Sheep erythrocytes (SRBCs) were opsonized with IgG and then incubated with neutrophils. When neutrophils were labeled prior to target addition, FcRII but not FcRIII were found to cluster at the target-effector interface. Little or no clustering of FcRs was observed if labeling was performed after target binding. SRBC oxidation was observed using Soret band illumination during transmitted light microscopy. Time-lapse studies of FcRII distribution and target oxidation were performed. FcRII formed clusters at target-effector interfaces prior to target oxidation. Three lines of evidence suggest that clustering is not a general plasma membrane response. Firstly, FcRIII do not cluster. Tannic acid-modified erythrocytes avidly bound to neutrophils but did not trigger clustering of FcRII. Furthermore, irrelevant neutrophil membrane labels were unaffected by the presence of IgG-opsonized erythrocytes. We suggest that FcRII clustering is one important component leading to the oxidative destruction of target cells.

M-PM-F3 MODULATION EFFECT BY ANF ON CA^{++}-DEPENDENT K^+ CHANNELS ACTIVATED BY ATP OR BRADYKININ IN BOVINE AORTIC ENDOTHELIAL CELLS (BAE). M. Chahine, R. Sauvé, P. Hamet*, and J. Tremblay*. Groupe de recherche en transport membranaire, Université de Montréal and *Institut de recherches cliniques, Montréal, Québec, Canada H3C 3J7.

It has been shown by Hamet et al. (1986) and recently by Leitman et al. (1988) that endothelial cells respond to atrial natriuretic factor (ANF) by a large increase in cGMP concentration. Although the relaxation of smooth muscle induced by ANF is currently associated with an increase in cGMP concentration, the contribution of endothelial cells to the effect of ANF is still not well understood. Recently, Sauvé et al. (1988) demonstrated in bovine endothelial cells the presence of Ca^{++}-dependent K^+ channels ($g_{K,Ca}$) which could be activated following P_2-receptor stimulation. Here we report that ANF at 50 and 100 nM increases the $g_{K,Ca}$ activity induced by ATP (10 µM) or bradykinin (10 nM), and this effect is mimiced by 8Br-cGMP (1 mM). In fact, in presence of ANF or 8Br-cGMP we observed an increase of the $g_{K,Ca}$ open probability. ANF was ineffective at concentrations less than 50 nM. In some experiments the effect of ANF was followed by an inhibition of $g_{K,Ca}$ activity induced by ATP. However, this effect could not be observed in presence of 8Br-cGMP. The specificity of ANF to induce an increase on $g_{K,Ca}$ activity was also established in some experiments performed in presence of cANF, an analog of ANF known to bind to ANF silent receptors (Maakc et al., 1987). Under these conditions, no effect on $g_{K,Ca}$ activity induced by ATP could be observed. Experiments carried out in inside-out configuration have failed to show any direct effect of cGMP on the $g_{K,Ca}$ activity at 4 µM calcium . This result suggests that ANF interferes with Ca^{++} homeostasis via a cGMP-dependent process leading on a sustained increase in cytosolic calcium concentration.

M-PM-F4 NANOSECOND DEPOLARIZATION STUDIES ON THE SEGMENTAL FLEXIBILITY OF MEMBRANE-BOUND IMMUNOGLOBULIN RECEPTORS FOR ANTIGEN David Holowka, Theodore Wensel*, Barbara Baird, Department of Chemistry, Cornell University, Ithaca NY and *Department of Biochemistry, Baylor College of Medicine, Houston, TX.

In order to probe the dynamic structures of cell surface-associated immunoglobulins that serve as receptors for antigen, time resolved fluorescence anisotropy measurements were carried out using a laser-based nanosecond fluorimeter and monoclonal anti-dansyl antibodies (Oi et al. Nature 307, 136, 1984). Anti-dansyl IgE bound to high affinity receptors on membrane vesicles from rat basophilic leukemia cells exhibit limited segmental flexibility that is manifested as a very restricted angular range of motion by the Fab segments. The segmental flexibility that is observed appears to be due largely to a fast component of motion with a rotational correlation time of 10 - 20 nsec which may correspond to the twisting of the whole Fab about its major axis. Inter-molecular crosslinking by a short bivalent hapten, N,N'-di-dansyl cadaverine, results in complete abrogation of segmental motion. Preliminary nanosecond depolarization studies have been carried out on membrane vesicles derived from a hybridoma cell line that expresses large numbers of surface IgG_1 with the same anti-dansyl combining site as the anti-dansyl IgE. Results indicate that surface IgG_1 that is anchored to the membrane via a C-terminal hydrophobic heavy chain sequence may have more restricted flexibility at its hinge region than the secreted IgG_1. The structural basis for this difference is currently under investigation.

M-PM-F5 PHOSPHORESCENCE ANISOTROPY STUDIES OF THE ROTATIONAL DYNAMICS OF IMMUNOGLOBULIN E-RECEPTOR COMPLEXES ON RAT BASOPHIL LEUKEMIA CELLS. Jeffrey N. Myers, Barbara A. Baird, and David A. Holowka, Cornell University, Dept. of Chemistry,Ithaca NY, 14853.

Aggregation of receptors for immunoglobulin E (IgE) on mast cells and basophils triggers cellular degranulation and the release of histamine in the allergic response. Crosslinking of IgE-receptor complexes by antigen or anti-IgE leads to a dramatic reduction in their lateral mobility, but the rotational mobility of these aggregates on the cell surface is unknown. In order to study the time-dependent changes in rotational motion of IgE-receptor complexes following external crosslinking, we have constructed a 'time-averaging' phosphorimeter that is capable of measuring the phosphorescence emission anisotropy of erythrosin conjugated to IgE on rat basophilic leukemia cells in suspension. Addition of polyclonal anti-IgE leads to a time-dependent increase in phosphorescence anisotropy that reaches a maximum value after 5-10 minutes at 25°C. A bivalent dinitrophenyl ligand that efficiently crosslinks the anti-dinitrophenyl IgE-receptor complexes on the cell surface causes an increase in phosphorescence anisotropy with a slower timecourse than that for anti-IgE. This instrumentation also allows us to probe changes in receptor interactions produced by other means. Preliminary data suggest that a guanine nucleotide-binding protein may be coupled to the receptor, directly or indirectly, as addition of GTP-γ-S, but not GDP-β-S, increases the rate of rotation of the IgE-receptor complexes. This instrument should allow us to probe changes in receptor interactions relevant to signal transduction.

M-PM-F6 ROLE OF Ca^{2+} IN THE REGULATION OF HORMONE RECEPTOR EXPOSURE DURING LYMPHOCYTE ACTIVATION. W. Jy and Lilly Y.W. Bourguignon, Department of Anatomy and Cell Biology, University of Miami Medical School, Miami, FL 33101 "(Intr. by Dr. Roobik Azarnia).

Ca^{2+} is known to be required for mitogen-mediated lymphocyte activation. In order to further define the regulatory role of Ca^{2+}, we have examined the activation events which occur following treatment with ionomycin (a Ca^{2+} ionophore) as compared to those occurring following concanavalin A (Con A) treatment of mouse splenic T-lymphocytes. Our results indicate that ionomycin and Con A induce the exposure of both IL-2 and insulin receptors on the surface of the lymphocytes within the first 5 min of treatment. The exposed insulin and IL-2 receptors have the following properties: 1) they consist of both high- and low-affinity receptors; and 2) they appear on the cell surface in small clusters (i.e. patches) or, occasionally, a large aggregate (i.e. cap). C-myc gene expression and DNA synthesis also occur in the ionomycin and Con A-treated lymphocytes when either IL-2 or insulin is present in the culture medium. Furthermore, the exposure of both hormone receptors can be inhibited by either EGTA (a Ca^{2+} chelator), bepridil (a Ca^{2+} channel blocker), W-7 (a calmodulin antagonist) or cytochalasin D (a microfilament inhibitor). Treatment with these inhibitors also blocks the expression of c-myc gene and DNA synthesis which occur at later times during IL-2 and insulin-induced activation of ionomycin- and Con A-treated lymphocytes. These findings suggest that a Ca^{2+} and calmodulin-mediated contractile system is involved in the exposure of certain hormone receptors which appear to be required for complete lymphocyte activation.

M-PM-F7 G PROTEIN βγ SUBUNITS ACTIVATE THE CARDIAC MUSCARINIC K CHANNEL VIA PHOSPHOLIPASE A_2. Donghee Kim, Deborah L. Lewis, Linda Grziadei, Eva J. Neer, Dafna Bar-Sagi, and David E. Clapham. Depts. Pharmacology, Physiology and Biophysics, Mayo Foundation, Rochester, MN, Cardiovascular Division, Brigham and Women's Hospital, Boston MA, Cold Spring Habor Laboratory, Cold Spring Habor, New York NY.

Acetylcholine binds the cardiac muscarinic receptor and activates an inwardly-rectifying K^+-selective channel ($I_{K.ACh}$) via a pertussis toxin-sensitive G protein. Recent studies have shown that both the α and βγ subunit of the G protein activate the K channel when applied to the intracellular surface of inside-out membrane patches. Since muscarinic receptor activation leads to generation of arachidonic acid in some cell lines and βγ activates PLA_2 in retinal rods, we tested the hypothesis that βγ activates $I_{K.ACh}$ via PLA_2. Purified bovine brain βγ subunit applied to inside-out patches of neonatal rat atrial membrane activated a 40 pS channel with a mean open time of 1 ms. Preincubation of atrial patches with affinity-purified antibody to PLA_2 completely blocked activation by βγ. The antibody did not block subsequent activation by GTPγS. Boiled antibody and control IgG prepared from preimmune serum did not block βγ-dependent activation. Arachidonic acid activated the K channel in cell-attached and less frequently in inside-out (10 μM) patches. Inhibitors of lipoxygenase (ETYA and NDGA) but not cyclooxygenase (indomethacin) blocked activation by arachidonic acid. Metabolites of arachidonic acid that activated the K channel were 5-HPETE, 12-HETE, leukotrienes B_4 and C_4. These results suggest that arachidonic acid derivatives may be second messengers that activate ion channels. We conclude that the βγ subunit of the G protein activates $I_{K.ACh}$ by stimulating the production of lipoxygenase-derived second messengers. SUPPORTED BY NIH GRANTS TO DK, EJN,DB-S, AND DEC.

M-PM-F8 **DEVELOPMENT OF A SPIN-LABELLED DERIVATIVE OF EPIDERMAL GROWTH FACTOR FOR ELECTRON PARAMAGNETIC RESONANCE OBSERVATIONS OF HORMONE-RECEPTOR INTERACTIONS.** L.A. Faulkner, A.H. Beth, P.S.R. Anjaneyulu, and J.V. Staros. Departments of Biochemistry and Molecular Physiology & Biophysics, Vanderbilt University School of Medicine, Nashville, TN 37232.

Epidermal growth factor (EGF) is a 53 residue mitogenic peptide hormone which acts by binding to specific receptors in the membranes of target cells. Binding of EGF to the receptor stimulates the activity of an intrinsic tyrosyl residue specific protein kinase. This transmembrane signaling event is followed by a variety of cellular responses culminating in mitosis. Linear and saturation transfer electron paramagnetic resonance methods are being employed to study the earliest events in signal transduction by directly observing binding of the hormone to the receptor and dynamics of receptor-ligand complexes.

The first step in our EPR studies has been to prepare a spin labeled derivative of EGF having "tight" motional coupling between the probe and the hormone while maintaining normal biological activity. We have used the bifunctional spin label bis(sulfo-N-succinimidyl) doxyl-2-spiro-4'-pimelate to prepare derivatives having the nitroxide probe covalently immobilized on the surface of the EGF molecule. Derivatives showing motional coupling, as indicated by a rotational correlation time of 2 nsec in aqueous solution at 20 °C, have been purified. We have shown these derivatives to be biologically active by competition binding assays with ^{125}I-EGF in cells and A431 cell vesicles and by stimulation of the kinase activity in autophosphorylation assays. Preliminary linear EPR observations of binding to solubilized receptors and to receptors in A431 vesicles demonstrate a two component signal resulting from EGF derivative free in solution and EGF relatively immobilized by interaction with receptors. Complete chemical characterization of the derivative, quantitative studies of binding kinetics and thermodynamics, and saturation transfer EPR studies of dynamics of receptor-ligand complexes are currently underway. Supported by: NIH CA43720 and DK31880.

M-PM-F9 SYNTHESIS OF TETRAMETHYLRHODAMINE LABELLED G-PROTEIN βγ SUBUNITS G. Kwon and R..R.Neubig. Dept. of Pharmacology, University of Michigan, Ann Arbor, Mi. 48109.

G proteins play an important role in transducing hormonal signals. Their distribution and interactions in the plasma membrane have been difficult to study. Fluorescence techniques provide one approach to these questions. Consequently we sought to prepare active fluorescent G-protein subunits..Purified βγ subunits from bovine brain G-proteins were labeled with the fluorescent sulfhydryl reagent iodoacetamidotetramethylrhodamine (TMR). The excess free dye was removed by the ultrafiltration, followed by further purification using HPLC gel filtration (GF 450 and GF 250) This technique resolved two peaks (retention times 17 and 19 min). Only the peak at 19 min. contained protein. The label comigrated entirely with the β subunit on SDS PAGE gel. (molecular weight, 35,000) The molar ratio of dye to protein was 0.09 to 0.13, measured by UV absorbance at 555 nm and amidoblack protein assay. To test the function of the TMR-βγ, the ability to form heterotimer with α_o was studied using sucrose density gradient sedimentation in CHAPS. The sedimentation of TMR-βγ was increased in the presence of alpha subunits. Both the protein peak and the measured TMR fluorescence shifted toward the bottom of the gradient. TMR-βγ will be a valuable tool to define the distribution and mobility of G protein subunits after activation not only in reconstituted membranes but also in intact cells. (Supported by HL-37551).

M-PM-F10 **TEMPERATURE-DEPENDENT LATERAL AND TRANSVERSE DYNAMICS OF THE EPIDERMAL GROWTH FACTOR (EGF) RECEPTOR FROM A-431 CELLS.** John L. Azvedo* and David A. Johnson, Division of Biomedical Sciences, University of California, Riverside, California 92521-0121.

Since growth factor control of EGF receptor kinase activity could be associated with a change in the receptor extracellular protrusion, we examined microaggregation-dependent changes in the extracellular protrusion of the EGF receptor using fluorescence resonance energy transfer (FRET) techniques. EGF was labeled with fluorescein isothiocyanate (FITC) and tetramethylrhodamine isothiocyanate (TRITC). Monoconjugated derivatives were separated from free label and unmodified EGF by gel filtration and high-pressure liquid chromatography. To evaluate the bioactivity of the derivatives, radionuclide displacement studies were performed. FITC-EGF and TRITC-EGF were as effective as native EGF in blocking [^{125}I] iodo-EGF from binding to A-431 cells. To demonstrate that EGF-occupied receptors reversibly microaggregate at elevated temperatures, equal concentrations of FITC- and TRITC- EGF were incubated at 4°C with plasma membrane-enriched fragments from A-431 cells, and FRET was measured at 4°C, 37°C, and again at 4°C. We observed more FRET at 37°C than at 4°C, suggesting that EGF-occupied receptors reversibly microaggregate at 37°C. To determine if the extracellular protrusion of the EGF receptor changes with microaggregation, we measured the transverse FRET between receptor-bound FITC-EGF and 5-(N-dodecanoylamino)-eosin partitioned into the lipid membrane at 4° and 37°C. The transverse distance between the lipid-membrane and the receptor-bound FITC-EGF was calculated to be about 67Å and did not change with temperature. We conclude that the extracellular protrusion of the EGF receptor does not change with microaggregation.

M-PM-F11 IDENTIFICATION AND ISOLATION OF THE PROSTAGLANDIN E_2 RECEPTOR FROM CARDIAC SARCOLEMMA. M. Michalak*, E.L. Wandler, K. Strynadka, W.M. Njue**, H.-J. Liu**, and P.M. Olley. Departments of Pediatrics, Biochemistry*, and Chemistry**, University of Alberta.

Despite considerable interest in the biological function of prostaglandin E_2 (PGE_2), a PGE_2 receptor has yet to be directly identified in any tissue. Bovine heart sarcolemmal (SL) vesicles contain high affinity binding sites for PGE_2. As the first step towards identification and isolation of the PGE_2 receptor in the heart we synthesized an azidophenacyl ester of PGE_2 (azido-PGE_2), which was used as a specific photoactive probe. Azido-PGE_2 competed with [^{3}H]PGE_2 binding to SL vesicles, although it was a less effective inhibitor of this binding than unlabeled PGE_2. Following photolysis, [^{3}H]azido-PGE_2 was incorporated into one protein band of about 100-kDa. Unlabeled PGE_2 competed with [^{3}H]azido-PGE_2 for incorporation into the 100-kDa polypeptide, indicating specificity of the [^{3}H]azido-PGE_2 for the PGE_2 receptor. The functional PGE_2 receptor was isolated from Chaps solubilized cardiac SL on a wheat germ agglutinin-affinity column followed by gel filtration HPLC. The purified receptor preparation contains a 100-kDa protein band. The 100-kDa PGE_2 receptor of the cardiac SL is a glycoprotein, which heavily stains with Concanavalin A, and over 20% of its mass consists of a carbohydrate. In conclusion, we report here the first identification and isolation of the PGE_2 receptor from the heart.

M-PM-G1 GTP-BINDING PROTEINS IN SQUID PHOTORECEPTOR MEMBRANES. P.R. Robinson*, S.F. Wood#, E.Z. Szuts#, A.Fein#, H.Hamm+, and J.Lisman*. *Brandeis Univ., Waltham, MA, #Marine Biol. Lab., Woods Hole, MA, + Univ. Ill. Col Med Chicago, Il

Squid photoreceptors contain two proteins (~38 and ~42 kD) that are ADP-ribosolyated by pertussis toxin in a light-dependent fashion. Several lines of evidence suggest that these proteins represent two distinct light-activated G-proteins. 1) Only the 38 kD protein is labelled by cholera toxin in a light-dependent manner. 2) Only the 42 kD protein crossreacts with the monoclonal antibody 4A. This antibody specifically recognizes the α subunit of the vertebrate photoreceptor G-protein. 3) The 42 kD protein is associated with the membrane fraction of a 100,000 x g centrifugation following a low salt wash, while the 38 kD protein is found in the soluble fraction. 4) This difference in solublity is also reflected in filter binding studies using $GTP\gamma S^{35}$: a light-dependent binding of the analog is found associated with both the pellet and soluble fractions after centrifugation following a hypotonic wash. 5) In membranes prepared by freezing, only the 42 kD protein is labelled by pertussis toxin. This work and the related work of Tsuda[1] indicate that there is more than one light-activated G-protein in invertebrate photoreceptors. The specific target enzymes for these have not yet been established. In squid photoreceptors there is a light-induced increase in both cGMP and IP_3. The possibility that these pathways are controlled by different G-proteins needs to be explored. 1.Tsuda,M.,(1987) Retinal Proteins.393-404.

M-PM-G2 PUTATIVE CALCIUM STORES WITHIN DISTAL SEGMENTS OF SQUID PHOTORECEPTORS. John P. Walrond and Ete Z. Szuts*. Colorado State University, Fort Collins, CO 80523 and *Marine Biological Laboratory, Woods Hole, MA 02543.

In squid photoreceptors, light induces the formation of inositol trisphosphate (IP_3), which is one of the putative messengers for invertebrate phototransduction. This messenger is believed to regulate the release of calcium from membrane-bound organelles. The relationship between light-induced IP_3 production and calcium release has been uncertain for squid vision, because putative calcium stores have not been observed in thin sections of aldehyde-fixed retinas. Here we report finding saccules in high voltage electron micrographs of thick sections (0.25-0.75 µm) of rapidly frozen and freeze-substituted squid receptors. The saccules are membrane-bound organelles which extend for several µm along the length of the distal segment, parallel to the rhabdom. They form an extensive membrane sheet, 60-80 nm from the microvillar openings, and so resemble the subrhabdomeral cisternae of Limulus ventral eyes that are known to sequester calcium. These findings suggest that the saccules are the calcium-storing organelles which interact with IP_3. Our biochemical experiments support this interpretation. IP_3 transiently releases ^{45}Ca from membrane fragments derived from homogenized squid distal segments. These studies indicate that some, if not all, the source of IP_3-mobilized calcium originates from intracellular stores in squid photoreceptors.

M-PM-G3 CHARACTERIZATION OF A 5-PHOSPHOMONOESTERASE OF INOSITOL TRISPHOSPHATE IN SQUID PHOTORECEPTORS. S.F. Wood*# and A. Fein+#.
*Boston Univ. Marine Program, #Marine Biological Laboratory, Woods Hole, MA 02543, and +Univ. of Conn. Health Center, Farmington, CT 06032.

Inositol (1,4,5)-trisphosphate (IP_3) is rapidly formed in response to light in squid photoreceptors where it is converted sequentially into IP_2 and IP_1, but not into IP_4. We have characterized this IP_3-metabolism by incubating squid photoreceptors with 10µM ^3H- or ^{32}P-labeled IP_3, then measuring the production of IP_2 and IP_1 or the production of free phosphate. The pathway is simpler than in other systems as no IP_3-kinase activity is detectable. The IP_3-phosphatase is a soluble enzyme (K_m=50 µM, pH_{opt}=7.0). Activation requires Mg^{++}(full) or Mn^{++}(partial) and 2,3 diphosphoglycerate inhibits activity (K_i = 5 mM). In competition experiments, only 1,4-IP_2(500µM) and 1,3,4,5-IP_4(100µM) block activity. In a mixture of ^3H-IP_3 (label on the inositol ring), and ^{32}P-IP_3 (on the 5-phosphate), both are hydrolyzed yet only free $^{32}PO_4$ is released with no formation of ^{32}P-IP_2, indicating that the IP_3-ase is specific for the 5-position. Using hydroxylapatite and DEAE-sepharose chromatography, we purified the enzyme 15-fold and separated the IP_3-ase from the IP_2-ase activity. The IP_3-ase is concentrated in the light-transducing distal segments of the receptors when compared to the whole retina, and thus is available to metabolize the IP_3 formed by light.

M-PM-G4 THE EFFECTS OF HEPARIN ON EXCITATION BY LIGHT AND IP_3 IN LIMULUS VENTRAL PHOTORECEPTORS. T.M. Frank and A. Fein. Physiology Department, University of Connecticut Health Center, Farmington, CT 06032

Heparin has been found to be a potent antagonist of inositol 1,4,5-trisphosphate (IP_3) induced calcium release in a number of in vitro preparations. Evidence that heparin appears to function by competing with IP_3 for IP_3 binding sites and that it has no effect on passive calcium efflux or Ca^{+2}-ATPase pump action, makes it an extremely useful tool for examining physiological effects attributed to IP_3 (Ghosh, et al., J Biol Chem 263: 11075, 1988). We utilized heparin to provide more information about the role of IP_3 in mediating excitation by light in Limulus ventral photoreceptors. These cells are excited by both light and IP_3, but the hypothesis that IP_3 is the messenger of light excitation is complicated by the fact that injection of calcium chelators abolishes the response to IP_3 but not to light. In this study, the effects of heparin on light and IP_3 excitation were determined by impaling single cells with two electrodes, one containing 100 μM heparin and the other containing 50 μM IP_3 (both dissolved in 100 μM K^+-aspartate, 10 mM Hepes, pH 7.0 injection buffer). Pressure injections of heparin produced a significant decrease in the intracellularly recorded responses to light and IP_3. These results provide support for the role of IP_3 in mediating excitation by light in these photoreceptors. This is also the first in vivo demonstration of the antagonistic effects of heparin on IP_3 activated calcium release.

M-PM-G5 CYTOPLASMIC CALCIUM CONCENTRATION MEDIATES LIGHT ADAPTATION IN SALAMANDER PHOTORECEPTORS. G.L. Fain*, H.R. Matthews, R.L.W. Murphy & T.D. Lamb, Physiological Laboratory, University of Cambridge, Cambridge CB2 3EG, U.K., and *Department of Ophthalmology, Jules Stein Eye Inst., UCLA School of Medicine, Los Angeles, California 90024.

To test the hypothesis that $[Ca^{2+}]_i$ is responsible for light adaptation in vertebrate photoreceptors, we minimized changes in $[Ca^{2+}]_i$ by reducing $[Ca^{2+}]_o$ to 0.3-3 μM and by simultaneously substituting the Na^+ in the Ringer with either guanidinium$^+$ or Li^+, which do not support Na^+/Ca^{2+} exchange. Responses to steps of light, which in normal Ringer showed an initial peak and prominant sag, became nearly monotonic in waveform in both rods and cones after switching to the low-Ca^{2+}/zero-Na^+ solution. The amplitude of the step response, which had a shallow dependence on light intensity in Ringer, increased much more steeply and saturated at a much dimmer intensity in low Ca^{2+}/zero-Na^+. The shape of the response-intensity (r-i) relation in low-Ca^{2+}/zero-Na^+ was the same for steps and for flashes, and the integration time (t_i) determined from the r-i relations was approximately the same as the t_i calculated from the small amplitude response to flashes. These results indicate that, when changes in $[Ca^{2+}]_i$ are prevented, photoreceptors sum responses to photons with an integration time which is invariant with the intensity or duration of illumination. The steady-state sensitivity of the photoreceptors, which in salamander normally decreases in proportion to background intensity (according to Weber's law), fell much more steeply in low-Ca^{2+}/zero-Na^+ and could be predicted simply from the derivative of the r-i relation for steps, as in response compression. Time-dependent changes in sensitivity after presentation of background light are also blocked upon switching to low-Ca^{2+}/zero-Na^+ solution. We conclude that Ca^{2+} is the messenger for light adaptation in both vertebrate rods and cones.

M-PM-G6 cGMP-GATED CHANNEL OF RETINAL RODS: STUDY OF ION TRANSPORT. Anna Menini & Vincent Torre. Dept. of Neurobiology, Duke Univ. Durham, NC 27710 and Dip. Fisica, Univ. di Genova, 16146 Genova, Italy. (Intr. by John W. Moore)

The membrane of retinal rod outer segments contains a high density of channels gated by cGMP that can be easily studied with excised patches in the inside-out configuration. In our experiments the patch pipette always contained 110 mM NaCl, 0.1 mM EDTA, 10 mM HEPES, pH 7.6 and the cytoplasmic ion composition was changed with a fast perfusion method. We studied macroscopic currents carried by various monovalent cations in low divalent solutions as a function of voltage and ion concentration. When the cation concentration at the cytoplasmic side of the membrane is 110 mM the measurement of reversal potential gives the following sequence of permeabilities: Li>Na>K>Rb>Cs, in agreement with B.J.Nunn (J.Physiol. 394:17P, 1987). However at +100 mV the efficacy in carrying the outward current is Na>K>Rb>Li>Cs.

Furthermore we studied the current carried by Na, K, Li as a function of ion concentrations and we found that the curves at +100 mV are very well-fitted by a Michaelis-Menten equation suggesting cation binding to one site inside the channel with a higher affinity for Li than for Na or K. Moreover the current in mixtures of Na and Li ions is a monotonic function of mole fraction. The results of these experiments can be well described by a one-ion pore.

M-PM-G7 DENSITY OF THE cGMP-SENSITIVE CATION CHANNELS IN ROD OUTER SEGMENT (ROS) PLASMA MEMBRANES: AN ESTIMATION FROM THE cGMP-INDUCED Ca-EFFLUX OF ROS VESICLES

Paul J. Bauer, Inst. of Biol. Information Processing, KFA, D-5170 Jülich, FRG

Previously, I reported experimental evidence suggesting that cGMP-sensitive cation channels and Na/Ca-exchanging proteins are restricted to the plasma membranes of ROS (1). Fusion of disk and plasma membranes by freezing and thawing increased about 8-fold the membrane fraction which contained the cGMP-sensitive channels and the Na/Ca-exchangers, thus lowering the density of these proteins by the same factor. Mild sonication (water bath) of the freeze-thawed suspension yielded vesicles with a mean diameter of 0.21 μm, and a mean surface of 0.035 μm^2. Since under these conditions each vesicle contains at most a few channels there should also be a distinct fraction of vesicles which contain no channels at all or only one (or a few) channels with the binding sites inside the vesicle. These vesicles will not display a cGMP-induced Ca-release. Experimentally, this vesicle fraction was found to be 0.76. From this value, one can estimate the mean number of channels/vesicle by assuming: (a) a Poisson distribution for the channels, (b) equal probability for both orientations of the channel with respect to the membrane surface, (c) that inactivation of the channel is not limiting for the Ca-release. With these assumptions, a mean value of 0.54 channels/vesicle is obtained, corresponding to a channel density of 15.4 channels/μm^2 in the fusionated membranes. Considering that the channels originate from the plasma membrane which comprises only 6 % of the total membrane surface of bovine ROS, the channel density in the plasma membranes (i.e. before fusion) can be estimated to 260 channels/μm^2.

(1) Biophys. J. 51 (1987) 16a; Biophys. J. 53 (1988) 473a; J. Physiol. 401 309

M-PM-G8 LATERAL DIFFUSION OF TRANSDUCIN PREDOMINATES ON THAT OF RHODOPSIN FOR THE R*-T COLLISION RATE IN THE VISUAL TRANSDUCTION CASCADE. Franz Bruckert, T.Minh Vuong and Marc Chabre. Biophysique Moleculaire et Cellulaire (UA 520 CNRS), LBio, DRF/CENG, BP 85, F38041 Grenoble.

The first amplifying step of the visual transduction cascade is the catalysis by R* of GDP/GTP exchange on transducins bound to the disk membrane surface. In vitro, with a ruptured rod plasma membrane, the slightly soluble T-GDP dilutes in the outside medium. Using near I.R. light scattering on oriented rods (Vuong et al. Nature 311:659 1984), we studied the dependence of the kinetics of T-GTP formation upon the surface concentration of T-GDP which was varied by diluting the ROS suspension and/or adding excess T-GDP in the solution. Analysis of the kinetics of the binding step demonstrated that the solubilized T-GDP rebinds too slowly to the membrane after a strong flash to take significant part to the cascade. In the intact cell, 99.7% of T-GDP is bound, the GTP concentration is high and the catalytic exchange step does not last longer than a millisecond. Solubility of T-GDP plays no role, but T-GTP is instantly released from the disk membrane.

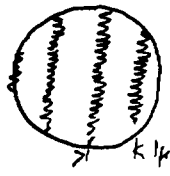

To analyse the contribution of the mobility of rhodopsin to the collision rate, measurements were made after excitation by a fringe interference laser flash that creates an inhomogeneous initial distribution of R*. For each given total number of R*, the kinetics were insensitive to the fringe pattern. If R* was the only, or the faster diffusing component for the multiple R*-T collisions, the kinetics should have been slowed down due to the time needed for R* to diffuse by half an interfringe. The absence of effect suggests that the peripherally bound transducin diffuses faster on top of the membrane than rhodopsin does in the lipid layer. This does not imply an "hopping model": the cytoplasmic surface layer is 100 time more fluid than the membrane lipids.

M-PM-G9 **LIGHT AND DARK ACTIVE PHOSPHODIESTERASE KINETIC PARAMETERS PROBED BY IBMX JUMPS: "CGMP CLAMP" IN SALAMANDER RODS.** W.H. Cobbs, Department of Biochemistry & Biophysics, University of Pennsylvania, Philadelphia, PA 19104-6059

After a jump into IBMX (I=5μM-mM), rod suction electrode dark current j increased and the photocurrent to a brief saturating flash was delayed. Onset of light-activated phosphodiesterase (PDE) inhibition was rapid: in I=200μM, the delay of the 1/e point of the photocurrent relative to a response in control ringer was maximal within 50 ms of the jump. The delay was described by $t=\tau \ln(1+I/Ki)$, τ=42 ms, Ki=300μM, expected if the arrival of light-activated PDE velocity were nearly exponential with time constant 42 ms. The initial rate of increase of j owing to dark-active PDE inhibition was half-maximal for I=200μM; the subsequent progress curve of j to steady state in darkness was kinked. The exponential time constant of the first portion was doubled between I=10μM and I=200μM. The second part grew larger and slower with increasing IBMX.

A step of background light coincident with an IBMX jump was chosen to just suppress the increase of current at steady state, after an initial transient. The transition from dark to light + IBMX occurred almost without change of membrane current when sufficient isomerizations from a 100μsec flash impulse were added at onset of the background. The ratio (flash isomerizations)/(background isomerization rate) gave the mean lifetime of excitation, presumably of G-GTP-PDE, under conditions of constant current, internal calcium and cGMP. Over 6 rods this value ranged from 0.55 - 1.0 sec, I=20-80μM, 22°C. Supported by NIH grant EY0-6192.

M-PM-G10 NUCLEOTIDE-DEPENDENT BINDING-RELEASE CYCLES OF MEMBRANE PERIPHERAL PROTEINS IN VISUAL EXCITATION/RECOVERY. Paul A. Liebman and Robert W. Zimmerman, Jr. Dept. of Anatomy, Univ. of Pennsylvania School of Medicine, Philadelphia, PA 19104.

$G_\alpha \cdot GTP$ release from and arrestin (A) binding to rod disk membranes is said to activate and quench PDE activation respectively in visual excitation and recovery. We describe here for the first time, direct measurement of stoichiometry and kinetics of the changes in distribution of all of the proteins of rods using rapid filtration through 0.2μm polyvinylfloride membrane filters after calibrated light flashes in the presence of 1mMGTP/2mMATP with 1-2 sec. time resolution. Filtrate proteins are separated and identified by PAGE and quantitated by gel densitometry. We found rapid light-activated release of both G_α and $G_{\beta\gamma}$, binding of $P_{\alpha\beta}$ and P_γ and slower binding of arrestin (48K protein). Each recovers in time proportional to rhodopsin bleached (R*). G and P movements are each amplified by factors over 100 v.s. R* while A moves stoichiometrically but unamplified with R*. Though each effect and its nucleotide dependence qualitatively agrees with expectation, several results conflict directly with widely accepted views. We find: 1) P_γ does not leave the membrane with $G_\alpha \cdot GTP$ and therefore $G_\alpha \cdot GTP \cdot P_\gamma$ elution cannot be an activation mechanism for $P_{\alpha\beta}$; 2) ATP-alone activation causes no G to leave the membrane but nevertheless vigorously activates P; 3) A cannot quench by binding P since one A would have to quench 100 or more P's. Supported by NIH EY00012 and 01583.

M-PM-G11 THE RESPONSE OF CONE PHOTORECEPTORS TO BRIGHT FLASHES OF LIGHT. Shaul Hestrin and Juan I. Korenbrot. Dept. of Physiology, Univ. Calif. San Francisco CA 94143.

Analysis of the response of photoreceptors to intense light flashes yields insight into the rate-limiting processes that underly phototransduction (Penn & Hagins, Biophys. J. 12:1073; Cobbs & Pugh, J. Physiol. 394:529). We measured the light responses of isolated tiger salamander cones with the tight-seal recording technique. At light intensities that bleached over 0.5% of the photopigment, we recorded a biphasic signal with no detectable latency and whose amplitude was proportional to the fraction of the bleached pigment and independent of the magnitude of the dark current. These properties indicate that this current (ERC) is analogous to the ERP and arises from charge displacement within the photopigment in the cone outer segment plasma membrane. The ERC is followed by the photocurrent, whose delay has a limiting value of 5-8 ms and which approaches saturation with an exponential time constant of 2-3 ms. Both this delay and this time constant are light-dependent. The features of this current are quantitatively similar to those measured in rods and reveal that the molecular events limiting the speed of the rising-phase of the photocurrent of these two receptor types are similar. The fast exponential was followed by a second, slower exponential component which had an amplitude of 1.5-3 pA and a time constat of 70-150 ms. This component was independent of light intensity and probably reflects the activity of a Na-Ca exchanger. Its time course was much faster than that of the corresponding current in rods, suggesting different kinetics of cytoplasmic Ca concentration changes between rods and cones (Yau & Nakatani, Biophys. J. 53:473a; Cobbs & Pugh, Biophys. J. 49:280a).

M-PM-G12 LIGHT ADAPTATION IN RETINAL RODS OF THE RABBIT. K. Nakatani and K.-W. Yau, Howard Hughes Medical Institute and Department of Neuroscience, Johns Hopkins University School of Medicine, Baltimore, MD 21205.

Amphibian rods actively adapt to light. This adaptation can be characterized by the following features: 1) the response to a flash of increasing intensity shows a progressively shorter time to peak, 2) the response to a step of light rises transiently to a peak and then relaxes to a lower plateau level, and 3) the flash sensitivity in the presence of a background light decreases according to an inverse relation with background intensity (see Baylor, Lamb & Yau, J. Physiol. 288, 589, 1979 and Baylor, Matthews & Yau, J. Physiol. 309, 591, 1980). This light adaptation has recently been shown to arise from a negative feedback action on the phototransduction cascade, mediated by a light-induced decrease in intracellular Ca^{++} (Matthews, Murphy, Fain & Lamb, Nature 334, 67, 1988; Nakatani & Yau, Nature 334, 69, 1988). Interestingly, primate rods scarcely show any of the above characteristics (Baylor, Nunn & Schnapf, J. Physiol. 357, 575, 1984). This raises the possibility of a fundamental difference between amphibians and mammals, or more generally between cold-blooded and warm-blooded animals. We have examined this question by studying the light-adapting properties of the rabbit rod using the suction-pipet recording method. We found that these cells behaved very much like their amphibian counterparts; active light adaptation was observed at both room temperature (20°C) and the body temperature of the rabbit (40°C). These results suggest that the behavior of primate rods is perhaps not typical of mammalian species.

M-PM-H1 **NMDA RESPONSES ARE MODULATED BY REDUCTION AND OXIDATION.** E. Aizenman, S.A. Lipton & R.H. Loring. The Children's Hospital and Harvard Medical School, Boston, MA.

The NMDA receptor is highly regulated: *a*) Mg blocks the ion channel linked to this receptor, *b*) glycine potentiates NMDA responses, and *c*) Zn blocks NMDA function by binding to a site different from the Mg and glycine sites. Here we report that NMDA responses in three different central neuronal preparations are subject to another modulatory mechanism: they are potentiated by a reducing agent, while oxidation decreases the magnitude of the responses. Electrical measurements were performed in the isolated chick retina by recording the D.C. potential between a suction electrode placed on the optic nerve and an electrode placed inside the eyecup solution. NMDA-induced (100 μM) responses in this preparation were potentiated 4.3±1.8 fold by treatment with 1-2 mM dithiothreitol (DTT; n=10). Oxidation with 0.1-1 mM dithio-bis-nitrobenzoic acid (DTNB) depressed or completely abolished the NMDA responses (81.6±24.1% decrease; n=7). DTT and DTNB had no effects on responses elicited by kainate, quisqualate, or AMPA (100 μM each). The potentiating effects of glycine, and the blocking effects of APV, MK-801, and kynurenate were apparent at all redox states in which a response was present. Whole-cell patch clamp experiments were performed in rat cortical neurons and retinal ganglion cells in culture. DTT (0.5-2 mM) potentiated NMDA-induced (10-200 μM) currents in both of these preparations (1.5±0.4 fold increase for cortical cells, n=7; 1.5±0.3 for ganglion cells, n=12). In addition, 0.1-1 mM DTNB decreased the NMDA response in both cortical and ganglion cells (22.9±12.9% decrease for cortical neurones, n=7; 49.4±9.4% for ganglion cells, n=4). The alternating reduction and oxidation cycle could be repeated indefinitely. Since the native redox state of the sites responsible for this phenomenon varies among neurons, an *in vivo* mechanism may exist which can strongly regulate NMDA receptor function by reduction or oxidation.

M-PM-H2 **TIGHT-SEAL WHOLE-CELL RECORDING OF EXCITATORY SYNAPTIC CURRENTS IN HIPPOCAMPAL THIN SLICES.** Pankaj Sah, Shaul Hestrin and Roger A. Nicoll. Depts. of Physiology and Pharmacology, UCSF, San Francisco, CA. 94143. Intr. by B. Katzung. Quantitative analysis of synaptic transmission in the mammalian CNS, using conventional microelectrodes, has been limited by technical difficulties. We have used the thin slice technique (F. Edwards, A. Konnerth & B. Sakmann, Pflügers Arch. 411:R149, 1988) to characterize the excitatory synapse between the Schaffer collaterals and CA1 pyramidal neurons. Whole cell recordings were obtained using patch pipettes (filled with CsF 130, HEPES 10, EGTA 10) from the exposed soma of neurons in the CA1 cell layer. The slice was perfused with oxygenated mammalian Ringer at 23°C. GABAergic inputs were blocked with 200 μM picrotoxin. Excitatory inputs were evoked by brief shocks delivered by a bipolar electrode positioned in stratum radiatum. We recorded excitatory synaptic currents in the range of 10 up to 300 pA. As previously described, (G. Collingridge, C. Herron & R. Lester, J. Physiol. 399, 283-300, 1988) synaptic currents were found to consist of a slow and a fast component with different pharmacology and voltage sensitivity. The slow component was selectively blocked by the specific NMDA antagonist APV, while the fast component was blocked by the quis/kainate antagonist CNQX. These antagonists were used to separate and characterise each of the components. Slow component: This component peaked in 20 - 30 ms and decayed exponentially with time constants of 70 - 200 ms. In the presence of 1.3 mM Mg^{++}, the peak I-V relationship had a region of negative slope resistance between –80 and –30 mV and reversed near 0 mV. Fast component: The fast component peaked in 3.5 - 8 ms and decayed exponentially with time constants of 5 - 15 ms. In the range –120 to +40 mV the time constant of decay was independent of voltage. The peak I-V relation was linear and reversed near 0 mV. These properties are similar to those mediated by NMDA and non-NMDA receptor components at glutaminergic synapses recorded in other preparations.

M-PM-H3 TWO DISTINCT QUISQUALATE RECEPTORS MEDIATE INCREASES IN $[Ca^{2+}]_i$ THROUGH DIFFERENT MECHANISMS IN MOUSE HIPPOCAMPAL NEURONS S.N. Murphy and R.J. Miller, University of Chicago, Chicago, IL 60637 (Intr. by E.W. Taylor)

Hippocampal neurons grown in monolayer cultures increased their $[Ca^{2+}]_i$ in response to quisqualate (QUIS), kainate (KA), and N-methyl-D-aspartate (NMDA) as analyzed using fura-2 based microflourimetry. In Ca^{2+} free medium QUIS caused a transient or oscillating increase in $[Ca^{2+}]_i$ not observed during applications of NMDA, KA, or a-Amino-3-hydroxy-5-methylisoxazole proponate (AMPA). Glutamate, ibotenate, and phenylephrine (PhE) caused similar increases of $[Ca^{2+}]_i$ in Ca^{2+} free medium which were not antagonized by substituting $[Na^+]_o$ with N-methyl-D-glucamine (NMDG) or simultaneous applications of the novel QUIS antagonist 6-Cyano-7-nitroquinoxaline-2,3-dione (CNQX). Sequential responses to QUIS in Ca^{2+} free medium could only be obtained when alternated with exposures to Ca^{2+} containing medium. QUIS responses following PhE induced $[Ca^{2+}]_i$ transients were also greatly reduced unless alternated with Ca^{2+} containing medium. This data supports the existence of a common intracellular Ca^{2+} pool mobilized by QUIS and PhE possibly by $InsP_3$. Not all hippocampal neurons responded to QUIS in Ca^{2+} free medium. However these neurons would often respond to QUIS and AMPA with a sustained increase in $[Ca^{2+}]_i$ when Ca^{2+} was returned to the medium. These QUIS induced sustained increases in $[Ca^{2+}]_i$ were completely blocked when $[Na^+]_o$ was substituted with NMDG or when voltage sensitive calcium channels were blocked using predepolarization in Ca^{2+} free medium with simultaneous 10 μM nitrendipine. CNQX was a potent antagonist of these sustained $[Ca^{2+}]_i$ increases with a Ke of 250 nM. This data supports a QUIS/AMPA/CNQX sensitive receptor that mediates membrane depolarization in these neurons. Thus QUIS could induce transient increases in $[Ca^{2+}]_i$ in Ca^{2+} containing medium without an accompanying sustained increase by simultaneous applications of CNQX. We conclude that in the hippocampus, distinct receptors mediate $[Ca^{2+}]_i$ mobilization and membrane depolarization in response to QUIS.

M-PM-H4 DOES THE FAST TRANSIENT GLUTAMATE ACTIVATED CURRENT "DESENSITIZE" OR "INACTIVATE?"

Cha-Min Tang, Reza Lankerian and Martin Morad. University of Pennsylvania, Dept. of Physiology, Philadelphia, PA.

Rapid step application of glutamate results in a fast transient current in hippocampal neurons. Using a novel perfusion technique which can "clamp" the external agonist concentration within one millisecond in combination with the outside-out patch clamp technique, we find that full activation of this channel is achieved within a couple of milliseconds. This transient current is mediated by a high conductance (35 pS) quisqualate sensitive channel. Following activation, the current decays with a time constant between 3 and 8 milliseconds. Conditioning pulse with subthreshold concentration of agonist decreases the amplitude of the transient current. Half-time of recovery from "desensitization" was about 100 milliseconds. The kinetics of activation, desensitization, and recovery from desensitization for this agonist-activated channel are thus very similar to kinetics of the gating of voltage activated channels. Our results suggest that desensitization may occur directly at a site closely associated with the channel.

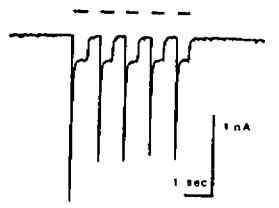

100 uM GLUT (WHOLE-CELL)

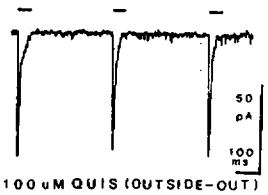

100 uM QUIS (OUTSIDE-OUT)

M-PM-H5 CONCENTRATION DEPENDENT EFFECTS OF α-NEUROTOXINS AT THE MUSCLE END-PLATE

Ronald J. Bradley, Neuropsychiatry Research Program, School of Medicine, University of Alabama at Birmingham, Birmingham, Al.35294

D-Tubocurarine causes a use-dependent fade in synaptic transmission at the neuromuscular junction. This fade could be due to the action of d-tubocurarine on a pre-synaptic ACh receptor (AChR) which modulates the release of ACh. This could not be a nicotinic AChR because it is known that α-neurotoxins from snake venom, which bind only to nicotinic AChRs, do not cause fade. Furthermore, electron microscope autoradiography has found no evidence for the existence of pre-synaptic nicotinic AChRs. In support of the work of others we indeed found that high concentrations of erabutoxin b (100-150 nM) from the venom of *Laticauda semifasciata* or α-neurotoxin I from the venom of Naja naja atra did not cause much fade of neuromuscular transmission in the rat diaphragm preparation. When these high concentrations were washed out of the bath thus rapidly reducing the toxin concentration, there was an immediate development of fade similar in all respects to the effects of d-tubocurarine. Similarly, very low concentrations of the toxin (5 nM), which required many hours to produce an effect, also caused fade which was identical to the effects of d-tubocurarine. These findings do not support the theory that tetanic fade is caused by pre-synaptic AChRs and suggest that fade could be caused by a use-dependent effect on the post-synaptic nicotinic AChR. The results suggest that there are two toxin binding sites possibly on the post-synaptic AChR. These are a high-affinity and a low-affinity site, which have equal rates of association but markedly different rates of dissociation. At low concentrations of toxin, binding to the high-affinity site could cause fade due to a use-dependent failure or desensitization of the AChR. At high concentrations of toxin the high-affinity and low-affinity sites would be bound and the AChR could not be activated. Therefore, use-dependent AChR failure would not be observed and the response would be evenly reduced without evidence of fade. The different concentration-dependent electrophysiological effects of the toxin were supported by binding studies with radioactive toxin which demonstrated two separate toxin binding sites on the post-synaptic AChR which have similar rates of association but differ markedly in their rates of dissociation. α-Bungarotoxin did not produce this use-dependent effect and in contrast has only one class of binding site to the post-synaptic AChR. Supported by NIH grant ES04295.

M-PM-H6 EXTERNAL HYDROGEN IONS AFFECT THE GATING AND PERMEABILITY OF NICOTINIC ACETYLCHOLINE CHANNELS. P.A. Pappone & G.L. Barchfeld, Department of Animal Physiology, University of California, Davis, CA 95616.

We used gigohm-seal patch clamp recordings to explore the effects of pH on the properties of nicotinic acetylcholine (ACh) channels in BC3H1 cells, a skeletal muscle-like cell line. Single-channel currents were measured in cell-attached patches on cells bathed with a high K solution to set E_m to 0 mV. The patch pipets contained a low ionic strength solution consisting of 10 or 20 mM CsCl, 5 mM Cs-HEPES, 1 mM Cs-EGTA, 250 mM sucrose, and 5 μM acetylcholine. Control measurements at an external pH of 7.2 gave an average single-channel conductance, γ, of 49$\pm$2 pS under these ionic conditions, measured from the slope of single-channel current-voltage relations at membrane potentials between -120 mV and -20 mV. Increasing the extracellular pH to 8.0 did not affect γ but decreasing external pH to 6.7 produced a 20% decrease in conductance in this voltage range, and further reduction in pH to 6.5 resulted in a conductance only 50-60% of that at neutral pH. No significant changes in the extrapolated reversal potential were seen with changes in pH, suggesting that channel selectivity was unaffected. Acid pH also changed channel kinetics. The frequency of channel events was reduced in low pH solution and channel mean open time, τ, measured at -100 mV approximately doubled in pH 6.7 solution from an average of τ = 2.2$\pm$0.3 ms to τ =4.6$\pm$1.0 ms. The long channel open times seen at low pH in unmodified ACh channels were absent when the cells were pretreated with trimethyloxonium (TMO), a specific methylating reagent which acts on carboxylic acids to convert them to a neutral ester. TMO modification reduced mean open times to about half their control values at pH 7.2. However, TMO modification eliminated the sensitivity of mean open time to pH, and τ was similar in modified membranes when measured at pH 7.2 or pH 6.7. Channel conductance was similarly reduced by low pH in modified and unmodified membranes. These results suggest that there is a titratable carboxylic acid group in ACh channels accessible to modification from the external face of the membrane that can influence channel gating properties. This work was supported by the American Heart Association, California Chapter, and grants NS07300 and AR34766 from the NIH.

M-PM-H7 SELECTIVE AND NON-SELECTIVE T_1 MEASUREMENTS OF BINDING CONSTANTS OF ACETYLCHOLINE AND ITS ANTAGONISTS TO SYNTHETIC AND GENETICALLY ENGINEERED PEPTIDES OF THE ACETYLCHOLINE RECEPTOR. Yigal Fraenkel*, Gil Navon*, Ami Aronheim† and Jonathan M. Gershoni.† *School of Chemistry, Tel Aviv University, Ramat Aviv, Tel Aviv 69978; †Department of Biophysics, Weizmann Institute of Science, Rehovot 76100, Israel.

The nicotinic acetylcholine receptor (AChR) is a ligand-regulated ion channel, composed of five subunits. Binding of acetylcholine to its α-subunits triggers channel opening. By systematically proteolyzing the α-subunit and checking fragments for toxin binding it was found that the region, α180-200 binds the inhibitor α-bungarotoxin(α-BTX). However due to the inadequacy of the methods for the detecting binding with K_d values exceeding 0.1 mM, binding of acetylcholine and other agonists to fragmented a subunits has not been directly demonstrated. In the present work we report such measurements, using selective and non-selective T_1 relaxation times of the ligands.

The amino acid sequence α184-200 was constructed and expressed by genetic engineering. Thus a bacterial fusion protein capable of binding α-BTX (trpE+α184-200) and a control bacterial protein with no binding capacity (trpE alone, Aronheim et al (1988) J. Biol. Chem. 263:9933) were subjected to NMR analysis. Binding constants for acetylcholine, nicotine, gallamine and d-tubocurarine to the recombinant α184-200 fusion protein were found to be: 2.4, 3.6, 0.15, and 0.24 mM respectively. For the non binding, control proteins, K_d values were always greater than 10 mM, and were regarded as background. Measurements were also performed for ligand binding to synthetic peptides corresponding to sequences α1-20, α128-143, and α184-200. Synthetic α184-200 showed similar binding constants to those obtained for its recombinant analogues, the other peptides showed only background binding.

M-PM-H8 IP3 MEDIATES m1 AND m3 MUSCARINIC RECEPTOR-ACTIVATED CALCIUM-DEPENDENT CONDUCTANCES **S.V.P. Jones, M.B. Goodman, J.L. Barker and *M.R. Brann. (Intr. by D. Gilbert)** Lab. of Neurophysiology and *Lab. of Molecular Biology, NINCDS, NIH Bethesda MD 20892.

Stimulation of muscarinic receptors has been shown to increase IP3, cAMP and arachidonic acid and to activate calcium-dependent conductances in A9 L cells transfected with m1 or m3 receptor cDNA. Whole-cell patch-clamp recordings of calcium-dependent potassium and chloride currents activated by ACh were blocked by addition of 200μM GTPγS to the intracellular pipette solution, suggesting the involvement of a G-protein. Overnight incubation in pertussis toxin (100ng/ml) did not alter the cholinergic activation of these conductances, indicating that the G-protein is pertussis toxin insensitive. ACh activation of the conductances could be mimicked by intracellular application of 10-100μM IP3; however, 100μM IP4 was without effect. Increasing intracellular free calcium to 1μM also mimicked the response. Optical measurements of intracellular calcium using the indicator dye Fura-2 demonstrated a rise in calcium on application of ACh, which could be blocked by 1μM atropine. Removal of extracellular calcium did not affect the initial ACh-induced calcium response but the calcium rise was markedly attenuated on further application of ACh. This attenuated calcium response was sufficient to support the electrical response, as removal of extracellular calcium had no effect on current amplitude. Local application of 5mM 8-bromo-cAMP and up to 50μM OAG elicited no electrical response and had no effect on ACh-induced currents. Application of PMA (10μM) did not elicit a response, but reduced the amplitude of the current response to ACh. In summary, the ACh-induced conductances can be mimicked by IP3 or by increased intracellular calcium. There is no contribution of extracellular calcium to the ACh-induced electrical responses.

M-PM-H9 ISOFLURANE RAPIDLY CHANGES THE KINETICS OF NICOTINIC ACETYLCHOLINE RECEPTOR CHANNELS. J.P. Dilger and R.S. Brett, Departments of Anesthesiology and Physiology and Biophysics, SUNY, Stony Brook, NY 11794-8480.

We have been studying the effects of the volatile general anesthetic isoflurane on the kinetic properties of single acetylcholine receptor (AChR) channels in BC3H-1 cells. Initially, we observed that isoflurane causes channels to occur in bursts of briefer than normal openings and showed that this behavior cannot be interpreted in terms of several popular anesthetic mechanisms [1]. Here, we report on patch clamp recordings made during rapid (ms) perfusion of ACh to outside-out patches [2]. In the absence of isoflurane, rapid application of 1 mM ACh to a patch containing several hundred AChRs gives rise to a current which develops quickly as channels are activated and decays with a time constant of 70 ms as the receptors desensitize (trace A). In the steady presence of 1.2 mM isoflurane (trace C), the agonist-induced current is reduced by 35% and the decay time constant decreases to 30 ms. The reduction in peak current may be a direct result of the shortening of the mean open and burst durations by isoflurane but the apparent acceleration of desensitization cannot be similarly explained. We examined the speed of onset of isoflurane's effects by simultaneously applying ACh and isoflurane to the patch (trace B). Clearly, the drug's action is as fast or faster than the time resolution of our perfusion system. On the basis of these and other experiments, we can assign lower limits of 10^6/M/s and 10^3/s to the apparent association and dissociation rate constants of isoflurane.

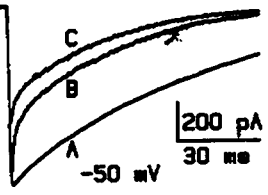

[1] Anesthesiology 69:161 (88). [2] Biophys J 50:987 (86).

Supported by NIH grant NS21581 (JPD)

M-PM-H10 THE STRUCTURE OF THE ACETYLCHOLINE RECEPTOR: INSIGHTS BASED UPON MODELLING STUDIES.
N.J. Vogelaar and S.I Chan, Department of Chemistry, California Institute of Technology, Pasadena, CA 91125.

The high-resolution structure of the acetylcholine receptor is not known at the present time. We have therefore undertaken modelling studies to arrange the transmembrane helices within the bilayer and to gain insights into the nature of the channel and its gating mechanism. The sequences of the receptor subunits were analyzed and transmembrane regions were designated. The residues of these transmembrane regions were examined with regard to their evolutionary conservation and variance. Conserved faces of the helices were positioned so that they were adjacent to other helices and variable faces were exposed to the lipid mileu. The best structure agreed well with the low-resolution receptor shape which was determined by Brisson and Unwin (Nature 315: 474-477, 1985). Biophysical aspects of this helical arrangement will be discussed as well as possible gating mechanisms of the ion channel. Specific residues which may be involved in the channel gating will be identified.

M-PM-H11 **ENERGY PROFILE FOR ION PERMEATION OF A PLAUSIBLE STRUCTURE FOR THE ACETYLCHOLINE RECEPTOR CHANNEL.**
G.Eisenman*, O. Alvarez+, A. Villarroel*, M. Montal#. *Physiol. and BRI, UCLA Med. School, L.A. CA 90024; +Fac.of Sciences, Biol. Dept., U. of Chile, Santiago, Chile; #Biol. and Physics Depts. UCSD, San Diego, CA 92093.

We apply Warshell's Protein Dipole Langevin Dipole procedure to calculate the energy profiles expected for ion permeation for a frozen pentameric structure proposed for the 23 residue segment, M2δ, of the Acetylcholine Receptor Channel by Oiki, Danho, Madison, and Montal (PNAS, in Press, coordinates provided by V. Madison). To remove some limitations of the Langevin procedure for modelling water molecules in narrow regions of a channel, we allow for a linear coordination of the ion by two water molecules. Computations for the neutral channel (and comparison with its polyglycine analogue) show the existence of such a large dipole field on the channel axis (see left figure for Cs) that the channel would be impermeable to cations or anions. This is due to summation of the fields from the 5 essentially parallel alpha helical M2 back bones and would presumably be opposed in the full channel by dipoles from oppositely oriented helices more distant from the channel axis. If partial dissociation of the rings of GLU 1, LYS 2 and ARG 23 residues is permitted under the influence of the dipole field (to produce charges of -3, +1, +2) the dipole potential is compensated and the energy profile permits permeation (right figure). This shows how dissociable residues can "buffer" helix dipole effects. The compensated energy profile for cations (or anions, not shown) exhibits three barriers and two sites, the internal site being formed by a ring of 5 -OH ligands from SER 8, the external site by 5 aromatic rings from PHE 16. The -OH ligands favor anions when the H's point toward the channel axis but favor cations when pointed away.

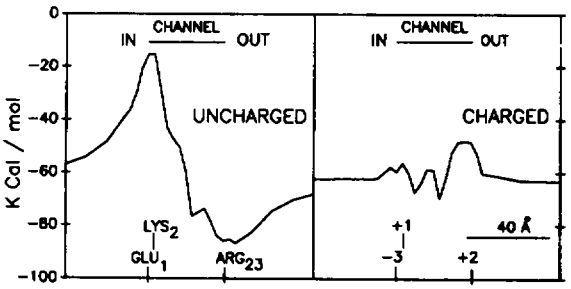

Supported by USPHS (GM24749,GM35981), NSF (BNS8411033), Fondecyt (1988-0451), Univ. of Chile DTI (B-2805/8812).

M-PM-H12 THE ACETYLCHOLINE RECEPTOR IS THE BEST THAT IT CAN BE.
Meyer B. Jackson, Department of Biology, UCLA, Los Angeles CA 90024.

As a result of natural selection one would expect that the acetylcholine receptor (AChR) has achieved a degree of perfection, and that it can transmit impulses to muscle fibers as rapidly as possible. The energetics and kinetics of activation of the AChR are evaluated in the context of optimal function of a synaptic receptor that is dedicated to rapid synaptic transmission. Physiological needs are used as the basis for estimating optimal values for the equilibrium constants of the liganded and unliganded closed to open channel equilibrium. An estimate of 13.4 kcal/mole was made of the maximum energy that can be derived from the binding of acetylcholine to a perfectly designed binding site. With these estimates it is then possible to evaluate receptor function. Application of the principle of detailed balance shows that with only one binding site the AChR will not be able to derive enough energy from acetylcholine binding to drive a sufficiently large change in the channel conformational equilibrium. This then provides a rationale for the existence of a second binding site, rather than the often invoked advantage of cooperativity. With two binding sites there is a considerable excess of binding energy, and consequently considerable flexibility in how binding energy can be utilized. It is shown that the AChR must have at least one binding site that binds acetylcholine weakly when the channel is closed. This is essential to rapid response termination. However, making the other binding site bind more tightly can enhance and accelerate the activation of the receptor. To optimize both response activation and termination the best solution is to make the two binding sites different in their binding affinities. This qualitatively reproduces an experimental observation (Jackson, J. Physiol. 397:555, 1988).

M-Pos1 SMOOTH MUSCLE ACTIVATION STUDIED WITH PEPTIDE PROBES AND CAGED-ATP G.J. Kargacin, T. Itoh, M. Ikebe and F.S. Fay Depts. of Physiology, U. Mass. Medical Center, Worcester MA and Case Western Reserve University, Cleveland OH

Myosin light chain kinase (MLCK), when activated by Ca-calmodulin, phosphorylates the 20kD light chains of smooth muscle myosin, a step believed necessary for activation of contraction and thought to be rate limiting in the activation process. We have tested these possibilities in vivo, by examining the actions of a proteolytic fragment of MLCK (IND-MLCK) and two synthetic peptides (SM-1 and RS-20) on shortening of skinned and intact single smooth muscle cells. When physiological levels of IND-MLCK, which is enzymatically active but unregulated by Ca-calmodulin, were added to skinned cells or injected into intact cells a rapid Ca-independent contraction occurred. Both SM-1, which is a pseudo substrate for the native kinase, and RS-20, which competitively inhibits Ca-calmodulin binding to the kinase, inhibited Ca-induced shortening of skinned cells and high-K contraction of intact cells even though Ca^{+2} (monitored with fura-2) rose to maximal levels. These results suggest that activation of MLCK is necessary and sufficient for shortening of smooth muscle. When photolysis of Caged-ATP was used to rapidly deliver ATP to skinned cells, a significant difference in initial shortening rate was seen between cells preincubated in IND-MLCK (light chains unphosphorylated before photolysis) or in ATP S (light chains phosphorylated before photolysis) suggesting that light chain phosphorylation is rate limiting in activation. No difference in the initial rate of shortening was seen when intact cells were injected with Ca^{+2} or IND-MLCK suggesting that the rate limiting step in smooth muscle activation occurs after the binding of the kinase. NIH HL14523

M-Pos2 EFFECTS OF A NOVEL PEPTIDE CALMODULIN ANTAGONIST ON HIGH-K^+ INDUCED $[Ca^{2+}]$ CHANGES IN SINGLE SMOOTH MUSCLE CELLS. T. Itoh, M. Ikebe, and F.S. Fay. Dept. of Physiology, U. Mass. Med. Ctr., Worcester, MA 01655

The physiological role of calmodulin in regulating Ca^{2+} movements in smooth muscle was studied by microinjection of a synthetic peptide calmodulin antagonist (RS20) into fura-2 loaded smooth muscle cells isolated from the toad stomach. RS20 corresponds to residues 493 to 512 of the smooth muscle myosin light chain kinase, a region which is believed to contain the calmodulin binding site. We studied its effects on resting $[Ca^{2+}]$ and on the kinetics of the $[Ca^{2+}]$ changes induced by high-K^+. Resting $[Ca^{2+}]$ (125 $\pm$ 25 nM ; n=35) was not changed after injection of RS20. When high-K^+ solution was briefly applied externally from a pipet, intracellular $[Ca^{2+}]$ was transiently increased (range from 200 to 700 nM, depending on the amplitude of the stimulus) and then declined to its original level. RS20 enhanced the peak $[Ca^{2+}]_i$ level attained by application of high-K^+ and prolonged the half time of the decline of the $[Ca^{2+}]_i$, but had no effect on the maximum rate of rise of $[Ca^{2+}]$. The enhanced $[Ca^{2+}]_i$ level attained in the presence of RS20 was apparently not due to a decrease in Ca^{2+} buffering by calmodulin. This followed from studies by equilibrium decays of $^{45}Ca^{2+}$ binding to calmodulin which revealed that RS20 slightly increased Ca^{2+} buffering in the physiological $[Ca^{2+}]$ range. These results suggest that Ca^{2+}-calmodulin may have a major effect on Ca^{2+} sequestering and/or extrusion mechanisms in smooth muscle cell. This work was supported by NIH grant #HL14523.

M-Pos3 EVIDENCE FOR AN INTERNAL LOAD IN SINGLE SMOOTH MUSCLE CELLS. D.Harris*, M.Yamakawa, and D.Warshaw, Physiol.& Biophys., U. of Vermont, Burlington, VT 05405.

The progressive decline in isotonic shortening velocity observed in single smooth muscle cells (Warshaw, J Gen Physiol 89:771, 1987) may be caused by an internal load or may reflect the time dependent modulation of inherent crossbridge cycling. To address this question, we determined whether the velocity of cell shortening in response to a step (10ms) reduction in force was a function of: 1) cell length; 2) the duration of contraction; 3) time following the step reduction in force. Single smooth muscle cells isolated from the gastric muscularis of the toad, Bufo marinus, were tied between an ultra-sensitive force transducer and piezoelectric length driver (Warshaw and Fay, J Gen Physiol 82:157, 1983) and stimulated electrically to produce maximum isometric force (Fmax). Isotonic shortening responses at force levels from 0.2Fmax to 0.75Fmax, showed dramatic slowing as the shortening progressed with time constants of 0.11-0.52s. However, when cells were subjected to a series of identical force steps from the same starting length, shortening responses were reproducible in terms of both the initial velocity of shortening and the slowing as the shortening progressed, suggesting that slowing of shortening velocity was not related to the time after the stimulation. In contrast, force steps made to the same force level (0.4Fmax) but from different starting lengths revealed that the velocity of shortening was determined by the cell length and not time after the force step. As the cell shortened at 0.4Fmax, shortening velocity slowed at 4.6Lcell/s/Lcell from an initial velocity of 0.2 Lcell/s. This dependency of shortening velocity on cell length supports the existence of an internal load that offers resistance to cell shortening and results in slowing of isotonic shortening velocity following a reduction in force. (Supported by NIH AR34872, HL35864, & AHA EI to DW)

M-Pos4 **DOES PROTEIN KINASE C REGULATE FORCE IN VASCULAR SMOOTH MUSCLE?** F.V. Brozovich, M.P. Walsh+ and K.G. Morgan. Harvard Medical School, Boston, MA 02215 and +University of Calgary, Calgary, Canada, T2N 4NI.

To determine the calcium sensitivity of single skinned vascular smooth muscle cells, isolation and skinning techniques for single cells from the ferret aorta were developed. Cells were isolated in Hanks solution containing elastase, collagenase and trypsin inhibitor. After isolation, the cells were plated onto glass coverslips and skinned in relaxing solution ([MgATP]=3mM, $[Ca^{2+}]=10^{-9}$ M) with 30 μg/ml added saponin. Cell length did not change during skinning and averaged 87±27 μm (x̄±sd, n=62). The single skinned cells were attached to microtools, one of which was connected to a force transducer. The cells were then activated by increasing the $[Ca^{2+}]$. Force began to develop at a $[Ca^{2+}]$ of about 0.05 μM and reached a maximum of 4.4±1.6 μN (n=36) at a $[Ca^{2+}]$ of about 0.5 μM. Data of relative steady state force vs. pCa ($-\log_{10}[Ca^{2+}]$) were fit to the Hill equation which yielded a pk=6.87±0.30 and N=2.3±1.4 (n=29). In a solution of pCa=7, the skinned cells developed an additional 2.5±0.5 μN (n=5) of force when stimulated with a phorbol ester, implying that protein kinase C was retained by the skinned cells. Adding a specific protein kinase C inhibitor (17 kd) to the calcium buffers depressed ($p<0.05$) the maximally Ca^{2+} activated force without changing the calcium sensitivity of force ($p>0.05$), and this depression of force could be reversed by the addition of an IgG anti-inhibitor to the solutions containing the protein kinase C inhibitor. These data suggest that in vascular smooth muscle, protein kinase C plays a role in the generation and maintenance of force. Supported by the NIH, HL-31704, and an AHA EI to KGM.

M-Pos5 EFFECTS OF CALCIUM AND TEMPERATURE ON ISOMETRIC TENSION TRANSIENTS FROM INTACT SINGLE SMOOTH MUSCLE CELLS. M. Yamakawa, D. Harris*, and D. Warshaw, Physiology & Biophysics, U. of Vermont, School of Medicine, Burlington, VT. 05405.

The fast and slow tension recovery phases in response to a small step length change in single smooth muscle cells from the toad stomach (J Gen Physiol 82:157, 1983) may be related to cross-bridge cycling kinetics. To relate these tension recovery phases to steps in the crossbridge cycle, we examined the effects of lowering extracellular calcium concentration $[Ca^{+2}]_o$ and temperature on tension transients. Single cells were tied between a force transducer and length driver in temperature controlled saline of either normal (1.8 mM) or low (0.18 mM) $[Ca^{+2}]_o$. At the peak of isometric force, following electrical stimulation, small, rapid (<=2.0% cell length in 3.6 ms) step stretches and releases were applied. In low $[Ca^{+2}]_o$ at 20°C, both the maximum stress and its rate of development were half those in normal $[Ca^{+2}]_o$. However, the rates of the tension recovery phases were comparable to those in normal $[Ca^{+2}]_o$ (Biophys J 53:189a, 1988). In normal $[Ca^{+2}]_o$ but at low temperature (~10°C), cells generated comparable maximum stresses following stimulation but 1.3 times slower than at 20°C. Tension recovery at 10°C was significantly slower than at 20°C, with rates of 20-50s^{-1} for the fast phase (apparent Q_{10} of ~2.0 for both stretches and releases) and 2-3s^{-1} for the slow phase (apparent Q_{10} of 1.5 for 2.0% releases but 0.8 for 2.0% stretches). We conclude that the tension transients do reflect crossbridge cycling kinetics and that these kinetics are insensitive to changes in $[Ca^{+2}]_o$. Although we can not assign specific steps in the crossbridge cycle to the fast tension recovery phase, the slow recovery phase suggests overall crossbridge cycling and a visco-elastic response of structures either external to or a part of the crossbridge. (Supported by NIH AR34872 & AHA EI to DW)

M-Pos6 PROTEIN KINASE C ACTIVATED PROTEIN PHOSPHORYLATION INHIBITS CONTRACTION IN SKINNED SMOOTH MUSCLE CELLS. Phyllis E. Hoar*, Janice Parente+, Michael P. Walsh+, and W. Glenn L. Kerrick*, Dept of Physiology and Biophysics*, Univ. of Miami FL 33101 and Dept. of Medical Biochemistry+, Univ. of Calgary, Calgary, Alberta Canada T2N4N1

An active Ca^{2+}- and diacylglycerol-independent fragment of chicken gizzard protein kinase C inhibits submaximal Ca^{2+}-activated contraction in skinned chicken gizzard cells, in agreement with the inhibition of actomyosin ATPase found by Nishikawa et al., J. Biol. Chem. 258:14069-14072, 1983. This inhibition occurs over a time course of approximately 30 minutes. During this same time approximately 1 mole of total phosphate per mole of myosin light chain-20 is incorporated. Incubation of the fibers for one hour allow up to 2 moles of phosphate to be incorporated into the myosin light-chain both in the presence and absence of Ca^{2+}. Pretreatment of skinned fibers with the protein kinase C fragment and ATPγS in the absence of Ca^{2+} had no effect upon the subsequent submaximal Ca^{2+}-activation of force, suggesting that protein kinase C does not thiophosphorylate myosin light-chains. These data show that myosin light chain phosphorylation by protein kinase C is associated with a reduction in the submaximal activation of contraction and thus may have a modulatory effect in intact smooth muscle. Supported by grants from the NIH (AR37447), American Heart Association and Affiliate, Muscular Dystrophy Association, and the Medical Research Council of Canada MT-9097.

M-Pos7 CALDESMON IS REQUIRED FOR THE ACTIVATION OF SMOOTH MUSCLE CONTRACTION IN SKINNED GIZZARD CELLS. W. Glenn L. Kerrick*, Michael P. Walsh+, Cindy Sutherland+ and Phyllis E. Hoar* (Intr. by D. Landowne), Dept. of Physiology and Biophysics*, Univ. of Miami Sch. of Medicine, Miami, FL. 33101 and Dept. of Medical Biochem.+, Univ. of Calgary, Calgary, Alberta Canada T2N4N1.

Caldesmon was extracted from skinned chicken gizzard muscle bundles in a high Mg^{2+} solution. The force which could be developed in extracted skinned gizzard cells decreased depending upon the extraction time. When the extracted skinned cells were incubated in a relaxing solution (pCa = 9.0 and 2 mM MgATP) containing the extracted proteins the ability of the fibers to contract was restored. If the extracted proteins were exposed to DTT their ability to recover the contraction was lost, but this effect of DTT could be reversed by treating the proteins with a Mn^{2+} solution. The effect of Mn^{2+} solution was to oxidize the caldesmon as judged by the change in its mobility on non-reducing SDS gels. The findings suggest that the ability of the extracted proteins to recover the loss of tension in extracted smooth muscle cells is dependent upon the oxidation state of the proteins. Addition of exogenous myosin light-chain kinase and/or calmodulin did not recover the ability of the cell bundles to develope force. When purified gizzard caldesmon was added back to the extracted fibers the ability of the fibers to produce Ca^{2+}-activated tension was partially recovered. These data suggest that caldesmon is required for the activation of smooth muscle contraction. Supported by NIH grant (AR37447), the American Heart Association and Florida Affiliate, and the Muscular Dystrophy Association and the Medical Research Council of Canada MT-9097.

M-Pos8 REGULATION OF ISOTONIC SHORTENING VELOCITY IN GLYCERINATED RAT UTERINE SMOOTH MUSCLE. Joe R. Haeberle, Timothy A. Sutton, and David R. Hathaway, Departments of Physiology/Biophysics and Medicine and the Krannert Institute of Cardiology, Indiana University School of Medicine, Indianapolis, IN.

It is well established that isotonic shortening velocity is dynamically regulated in smooth muscle; however, the mechanism of this regulation remains controversial. We have investigated the regulation of shortening velocity in chemically permeabilized (glycerinated) rat uterine smooth muscle. Relaxed muscles were first washed in a bath containing no ATP (pCa 8) and then incubated in a bath containing 100 mM thioATP (pCa 4.7) for 10 m to thiophosphorylate the 20 kDa myosin light chain (LC_{20}) to 1.0 mol/mol. Following washout of thioATP, the addition of 6 mM MgATP (pCa 8) produced a rapid and sustained contraction. The time-course of lightly-loaded shortening velocity ($V_{0.1}$) was measured by isotonic quick-releases to an afterload which was 10% of the anticipated peak isometric force. $V_{0.1}$ was determined as the slope of the length change between 1 and 2 s after the release. $V_{0.1}$ was 0.043 Lo/s at 10 s following the addition of MgATP and declined to 0.021 Lo/s by 10 m. The addition of Ca^{2+} (20 mM free) and calmodulin (30 μM) at 10 m had no effect on developed force or velocity. Incubation of the muscles with affinity-purified, polyclonal caldesmon antibody (22 μg/ml), prior to thiophosphorylation and contraction, depressed the velocity at 10 s to 0.021 Lo/s without changing the velocity at 10 m (0.023 Lo/s). These findings show that shortening velocity is regulated in the glycerinated rat uterine smooth muscle under conditions where LC_{20} phosphorylation is constant at 1.0 mol/mol. The inhibitory effect of caldesmon antibodies on the velocity transient suggests that caldesmon may regulate crossbridge cycling rates in contracting smooth muscle.

M-Pos9 CALCIUM-DEPENDENT MODULATION OF THE RELATIONSHIP BETWEEN ISOMETRIC STRESS AND MYOSIN LIGHT CHAIN PHOSPHORYLATION IN CHEMICALLY-PERMEABILIZED SMOOTH MUSCLE. Robert A. Forte, Judith A. Tanner, and Joe R. Haeberle, Departments of Physiology/Biophysics and Medicine and the Krannert Institute of Cardiology, Indiana University School of Medicine, Indianapolis, IN.

The latch state in smooth muscle is characterized by high levels of isometric stress with low levels of myosin light chain (LC_{20}) phosphorylation. Previous studies in our laboratory with smooth muscle permeabilized by glycerination showed, in contrast to findings in intact muscle, a linear dependence of isometric stress on LC_{20} phosphorylation; this relationship was the same during contraction and relaxation, and was unaltered by the presence or absence of Ca^{2+}. To determine if the prolonged incubation in glycerol (2 days) caused the loss or inactivation of a second regulatory process, we studied muscles which had been permeabilized by a 30-min exposure to the peptide ionophore alamethicin (30 μg/ml). The relationship between stress and LC_{20} phosphorylation in the presence or absence of Ca^{2+} was explored in this preparation. Contraction of muscles in the absence of Ca^{2+} (pCa 8) following thiophosphorylation of LC_{20} demonstrated an approximately linear dependence of stress on LC_{20} phosphorylation (81% of maximum stress at 0.73 mol/mol; 51% of maximum stress at 0.47 mol/mol; 35% of maximum stress at 0.12 mol/mol); this was similar to that seen previously with glycerinated muscles in either the presence or absence of Ca^{2+}. In the presence of saturating Ca^{2+} (pCa 4.7) and calmodulin (10 μM), however, the alamethicin-treated muscle developed 75% of maximum isometric stress with LC_{20} phosphorylation of only 0.15 mol/mol. This suggests that a calcium-dependent mechanism, which is either lost or inactive in the glycerinated muscles, modulates the relationship between isometric stress and LC_{20} phosphorylation in alamethicin-permeabilized muscles.

M-Pos10 OKADAIC ACID DECREASES CROSSBRIDGE CYCLING RATE IN PERMEABILIZED PORTAL VEIN OF THE RABBIT. M.J. Siegman, T.M. Butler and S.U. Mooers. Department of Physiology, Jefferson Medical College, Philadelphia, PA 19107

ATPase activity was determined in thin (50-60 μ) strips of permeabilized portal vein by measuring the rate of ^{3}HADP formation from ^{3}HATP. The average rate of energy usage was 246 $\pm$ 26 μM/min (n=10) in relaxing solution and 450 $\pm$ 49 μM/min (n=10) following the production of maximum active force in pCa 5. The myosin light chain was almost totally unphosphorylated in relaxing solution, and in pCa 5, 57 $\pm$ 10% was phosphorylated and 7 $\pm$ 2% was doubly phosphorylated. Subsequent treatment with the phosphatase inhibitor, okadaic acid (OA, 5 μM) in pCa 5 resulted in the maintenance of maximum force and phosphorylation of all of the light chain with 70 $\pm$ 3% double phosphorylation. Under these conditions, the suprabasal energy usage was only 27 $\pm$ 11% of that in pCa 5 alone, and there was a marked decrease in the rate of force redevelopment following a quick release. During comparable incubation times in pCa 5 without OA, ATPase activity and rate of force development declined slightly and there was some double phosphorylation. Washout of the OA results in dephosphorylation of the light chain to near initial values (only 15 $\pm$ 5% double phosphorylation) whereas ATPase remains depressed. These data suggest that the mechanism by which OA reduces crossbridge cycling rate is independent of its effect on myosin light chain phosphorylation. This mechanism, unmasked by the use of OA, may play a role in the normal regulation of crossbridge cycling rate in smooth muscle. (Supported by HL 15835 to the Penna Muscle Institute and AM 37598.)

M-Pos11 EFFECTS OF PHOTO-ACTIVATED RELEASE OF INTRACELLULAR CALCIUM IN GASTRIC AND COLONIC SMOOTH MUSCLE. Nelson G. Publicover and Frank A. Lattanzio. Departments of Physiology and Pharmacology, University of Nevada School of Medicine, Reno, NV 89557.

Intracellular electrical recordings from full-thickness segments of canine gastric and colonic smooth muscle reveal a rhythmic pattern of slow waves throughout most of the circular layer. Experiments were conducted to determine if the intracellular release of "caged" calcium alters the waveform and frequency of these slow waves. Tissues were incubated in the acetoxymethyl ester (AM) form of a "caged"-calcium compound, nitr-5. Ultraviolet light was used to release intracellular calcium at various times during the slow wave cycle. When tissues were incubated in 3 micromolar nitr for 1 hour, photo-activated release during the plateau phase of a slow wave caused a transient, partial repolarization. When the concentration of nitr and incubation time were increased to 15 micromolar and 2 hours, photolysis quickly caused slow waves to fully repolarize. The duration of spontaneous slow waves could be reduced from a mean of 6 seconds in tissues from the antral region of the stomach and 8 seconds in tissues from the proximal colon to less than 2 seconds. Photo-activated release of calcium during the interval between slow waves caused a hyperpolarization of up to 5 mV and delayed the occurrence of the next event. In gastric tissues, slow waves could be delayed for up to several minutes. These data support the hypothesis that both the repolarization phase of slow waves and the interval between slow waves are regulated by a calcium-activated potassium conductance.
(Supported by NIH grant DK32176.)

M-Pos12 MYOSIN LIGHT CHAIN KINASE PHOSPHORYLATION IN SMOOTH MUSCLE. J.T. Stull, L.-C. Hsu, and K.E. Kamm. Dept. Physiology, Univ. of Texas Southwestern Medical Center, Dallas, TX 75235.

Purified myosin light chain kinase (MLCK) from smooth muscle is phosphorylated by protein kinases; some of these phosphorylations alter Ca^{2+}/calmodulin (CaM) activation properties. For example, diphosphorylation (sites A and B) of MLCK in the absence of CaM by cyclic AMP-dependent protein kinase (PKA) results in a greater concentration of CaM required for half-maximal activation. Monophosphorylation in the presence of CaM (Site B) leads to no change in CaM activation properties. Site A phosphorylation by protein kinase C (PKC) also changes CaM activation properties. Phosphorylation of site A may contribute to smooth muscle relaxation by decreasing MLCK activity. We previously showed that an increase in cyclic AMP in smooth muscle did not change MLCK CaM activation properties. Others have shown that MLCK is phosphorylated in response to an agent that increases cyclic AMP. However, the sites of phosphorylation were not identified. We have used peptide mapping to identify sites phosphorylated in MLCK in smooth muscle.

Phosphorylation of MLCK in bovine tracheal smooth muscle was examined under conditions that activate PKA (isoproterenol; I) or PKC (phorbol 12, 13 dibutyrate; PDBu). Both I and PDBu cause relaxation of tracheal smooth muscle precontracted with carbachol (0.1μM). ^{32}P-labelled bovine tracheal smooth muscle strips were incubated in 1 μM I or 1 μM PDBu for 25 min, then quick-frozen. MLCK was immunoprecipitated with a monoclonal antibody from homogenates containing 100 mM $Na_4P_2O_7$, 100 mM NaF, 25 mM Tris, 250 mM NaCl, 10 mM EGTA, 5 mM EDTA, 1% NP-40, 50 μg/ml leupeptin and 1 mM PMSF at pH 8.8. After washing the immunoprecipitate, SDS-PAGE was performed. MLCK was excised and two dimensional peptide mapping performed after trypsin digestion. Purified ^{32}P-MLCK diphosphorylated by PKA was not dephosphorylated when added to tissue homogenates, and demonstrated two ^{32}P containing peptides (sites A and B). Site A was not phosphorylated in MLCK from tracheal tissues after I or PDBu treatments. These data indicate that site A phosphorylation of MLCK with the resultant change in CaM activation properties is not associated with relaxation produced by I or PDBu. (Supported in part by HL26043).

M-Pos13 MYOSIN PHOSPHORYLATION IN TRACHEAL SMOOTH MUSCLE. K.E. Kamm, L.-C. Hsu, Y. Kubota, and J.T. Stull, Department of Physiology, Univ. of Texas Southwestern Medical Center at Dallas, Texas, 75235.

Purified smooth muscle myosin can be phosphorylated at multiple sites on the light chain (LC) and heavy chain (HC) subunits by Ca^{2+}/calmodulin-dependent myosin light chain kinase (MLCK), protein kinase C (PKC) or other kinases. We previously found in bovine tracheal smooth muscle that LC was phosphorylated primarily in a single serine site by MLCK during both the initial and tonic phases of contraction produced by 10 μM carbachol (CCh). HC was phosphorylated to only very low values (5%) in both the resting and contracting trachealis muscle. HC is also phosphorylated in tracheal smooth muscle cells at confluence in culture.

We have extended these studies to include conditions that activate PKC in tracheal tissues by phorbol 12, 13 dibutyrate (PDBu). Myosin HC and LC were immunoprecipitated in homogenates of ^{32}P-labelled tracheal tissue. After washing the immunoprecipitates, SDS-PAGE was performed. LC was excised and two dimensional peptide mapping performed after trypsin digestion. Myosin HC was 6% phosphorylated under control conditions in bovine tracheal tissue. Treatment with CCh or PDBu resulted in no significant change. Control tissues had 9 ± 2% monophosphorylated LC with ^{32}P in the serine site phosphorylated by MLCK. CCh alone resulted in 42% ± 1% monophosphorylated LC after 25 min with ^{32}P only in the serine site phosphorylated by MLCK. PDBu alone resulted in 22 ± 3% monophosphorylated LC and 6% of the force produced by CCh. However, only 25% of the ^{32}P was in the MLCK serine site whereas 75% was in PKC serine site. PDBu plus CCh resulted in 27 ± 6% monophosphorylated LC with 18% of the force produced by CCh alone. About 60% of the ^{32}P was in the MLCK serine site with the remainder in the PKC serine site. CCh stimulation of tracheal smooth muscle results in phosphorylation of LC by MLCK with no significant increase in HC phosphorylation. PDBu appears to activate PKC as demonstrated by the peptide maps of LC, but changes in force with PDBu alone or plus CCh appear to be due to effects on LC phosphorylation by MLCK. PKC activation does not increase HC phosphorylation. (Supported in part by HL23096.)

M-Pos14 DIFFERENCES IN TEMPERATURE DEPENDENCE OF INTRINSIC TONE BETWEEN AORTA AND RENAL ARTERY. John Pawlowski, Kathleen G. Morgan. Harvard Medical School, Boston, MA 02215.

To investigate the mechanism of contractions of vascular smooth muscle induced by warming and cooling, stiffness measurements were compared to force measurements at a range of temperatures. Circular strips of ferret renal artery and aorta were prepared by removing the endothelium and attaching the strip at one end to a length driver and at the other end to a force transducer. The strips were set to slack length at room temperature and oscillations of <1% of the strip length applied to measure stiffness. From 0° to 37°, aortic strips showed a continuous increase in both force and stiffness. Force and stiffness were expressed as a percentage of the maximal change induced by 10^{-5}M phenylephrine at 37° C. Force and stiffness at 0° were 5.4±2.4% and 28.8±7.1% respectively and at 37° were 28.3±1.9% and 74.2±9.7% (n=25). In the renal artery, force and stiffness at 0° were 108.5±29.2% and 68.0±11.0% and at 37° were 60.6± 3.7% and 81.9±8.9%, respectively. Force for the renal artery had a nadir at 22.4° C with a mean value of 19.5±10.4% and was significantly lower than the force at 0° n=4 $p<0.5$. Phenylephrine produced a maximum force of .16 x 10^5 N/m^2 and maximum stiffness of .08 x 10^5 N/m^2 in renal artery and a maximal force of .75 ±.24 x 10^5 N/m^2 and a stiffness of .08±.03 N/m^2 in the aorta (n=6), which did not differ significantly. These data suggest that the drop in tone on cooling the ferret aorta is related to a decrease in the number of attached crossbridges but that the increase in tone on cooling renal artery involves processes other than the number of attached crossbridges. (Support: HL31704 and an AHA EI to KGM, GM 07592 to JP)

M-Pos15 FOUR-STATE MODELS AND REGULATION OF CONTRACTION IN SMOOTH MUSCLE. Carlos A. Lazalde & Lloyd Barr. Dept. of Physiology and Biophysics, University of Illinois, Urbana, IL 61801.

The initiation of contraction in smooth muscle (SM) requires phosphorylation (PH) of myosin light chain (MLC). In some SM's long term stress is maintained with very low levels of PH of MLC (I) but in others long term stress is correlated with relatively high levels of PH of MLC (II), (1). In the first group it appears that velocity of shortening is correlated with PH while in the other it does not. In some SM's calcium appears to be involved simply as a trigger for PH while in others it seems, in addition, it may be a regulatory factor by itself. We are investigating the behavior of a cyclic kinetic scheme where crossbridges (CB) exist in four states: M, PH-M, PH-XB and XB, where M indicates unattached and XB attached CB: M PH-M PH-XB XB M (III). From the analytical solution to III, it is clear that the evolution in time of any of the states or a linear combination of them depends on the eigenvalues of III which in turn depend on all transition rates (TR). With a suitable choice of TR's we are able to simulate experiments for SM's in I and II and calcium dependence of stress maintenance in the absence of PH. From the analytical solution it is possible to systematically fit III to skinned fiber experiments. We are currently exploring the implications of III in regard to velocity of shortening. (1) Chatterjee & Murphy, Science 221: 464, 1983; Kamm & Stull, AJP 249:C238, 1985; Haeberle et al., Pflugers Arch. 403:215, 1985; Siegman et al., Pflugers Arch. 401:385, 1984. (2) Lazalde & Barr, Abstracts 42nd Annual Meeting Soc. Gen. Physiol., 1988.

M-Pos16 FORCE, STIFFNESS AND SHORTENING SPEED IN RAT UTERINE SMOOTH MUSCLE. JL Smart and FJ Julian, Department of Anesthesia Research, Brigham & Women's Hospital, Boston MA, 02115.

This study examined the relationship between isometric force generation and stiffness together with lightly loaded shortening speed (LLSS) during electrically-induced contractions of the longitudinal layer of smooth muscle from non-pregnant rat uterus. Muscle strips were mounted between a servo motor and force transducer and held at the optimal length (Lmax) for maximal force generation (Fmax). Contractions were produced by electrical stimulation (30-50 mA, 60 Hz AC) for 10s. Stiffness ($\Delta F/\Delta L$) was measured by imposing a small amplitude (0.25% Lmax) 200 Hz sinusoidal length oscillation during the course of the contractions. LLSS measurements were made by imposing quick releases to a light load (~5% Fmax) at various times during the contraction. The stiffness to force ratio of 5 muscles was curvilinear with increased developed stiffness consistently leading active force generation. Maximal force and stiffness occured at 7.4 ± 1.0s and 8.6 ± 0.6s after onset of stimulation, respectively. Analysis of LLSS from force clamps imposed as early as 200 ms after onset of stimulation revealed values approximately 20% of peak LLSS. Maximal LLSS was observed from 1.25 to 1.5s after onset of stimulation which then declined to 75% of maximum during the remainder of the contraction. A lead of developed stiffness over developed force during the onset of contraction in smooth muscle may represent attachment of non- or low-force producing cross-bridges. In this study, LLSS and stiffness did not show the linear correlation nor temporal association which might have been expected based upon previously reported parallel changes in phosphorylation and speed of shortening (1,2) and correlation between phosphorylation and stiffness (3). Supported by NIH HD07008 (JLS) and HL35032 (FJJ). 1) Dillon et al., Science 211:495, 1981; 2) Kamm and Stull, AJP 249:C238, 1985; 3) Kamm and Stull, Science 232:80, 1985.

M-Pos17 CONTRACTION OF BOVINE TRACHEAL SMOOTH MUSCLE BY SUBSTANCE P. M.A. Corson, J.R. Sellers, R.S. Adelstein, and M. Schoenberg*, NHLBI & NIAMS*, Bethesda, MD 20892.

The contractile response of intact bovine tracheal strips to the peptide neurotransmitter Substance P (SP) was characterized. Reproducible dose-response curves were obtained for SP (0.3-30uM) in the presence of an inhibitor (PRMD 5uM) specific for SP's tissue protease. At low SP concentrations the isometric force response was almost completely abolished by inclusion of atropine (0.3uM), indicating mediation of contraction via SP-stimulated release of acetylcholine from pre-junctional nerve terminals; in contrast, at a near-maximal concentration (SP 10uM), the atropine-inhibited component of the force response was only 16%. Inclusion of antagonists for other airway smooth muscle receptors resulted in no further decrease in force. Under conditions whereby the muscles were activated by SP directly (SP 10uM, PRMD 5uM, atropine 0.3uM), peak tension was reached in 10 minutes, with a $t_{1/2}$ of approximately 2.5 minutes. Immunoblot analysis of the time course of myosin light chain (MLC) phosphorylation revealed an early increase to an incorporation of 0.3 to 0.4 mol phosphate/mol MLC, with subsequent decline when force was at steady state. Two-dimensional tryptic phosphopeptide analysis of MLC's revealed a single major phosphopeptide at both early and late times, migrating identically to that produced by myosin light chain kinase phosphorylation of MLC *in vitro*. These results indicate that: 1) SP mediates contraction of bovine trachea both directly and indirectly, and 2) under conditions where activation is via the direct mechanism, the tension and phosphorylation responses qualitatively resemble those seen with other previously characterized receptor-coupled physiologic agonists.

M-Pos18 ATP CONSUMPTION BY CROSSBRIDGE PHOSPHORYLATION AND CYCLING IN THE SWINE CAROTID MEDIA

Chi-Ming Hai and Richard A. Murphy. Section of Physiology and Biophysics, Division of Biology and Medicine, Brown University, Providence, RI 02912 and Department of Physiology, School of Medicine, University of Virginia, Charlottesville, VA 22908.

We have proposed the following crossbridge model to explain the regulation of contraction and the latch state in the swine carotid media (Am. J. Physiol. 254: C99-C106, 1988; A = actin, M = myosin, Mp = phosphorylated myosin; rate constants in s^{-1}). In this study, we analyze ATP consumption by: (1) crossbridge phosphorylation, and (2) cycling by calculating the crossbridge flux along the pathways in the model. The model predicted that more ATP is consumed for crossbridge phosphorylation than for cycling during steady-state isometric contraction. This is consistent with the observed low efficiency in doing work. Three factors contribute to the high economy of stress maintenance: (1) low cycling rate of phosphorylated crossbridges, (2) a 5-fold slower detachment rate of latchbridges (AM) compared with phosphorylated crossbridges, (3) a 4- to 5-fold lower concentration of crossbridges in smooth muscle compared with striated muscle. Supported by NIH Grant 5 PO1 HL-19242.

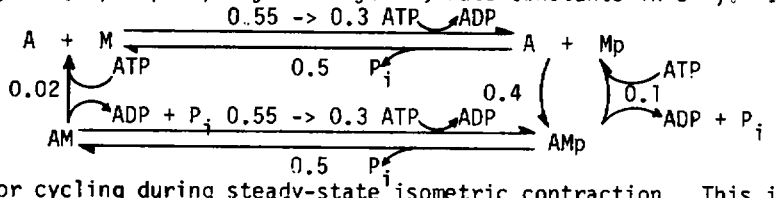

M-Pos19 SODIUM NITROPUSSIDE-INDUCED cGMP ELEVATION REDUCES MYOPLASMIC [Ca^{2+}], CROSSBRIDGE PHOSPHORYLATION, AND STRESS IN HISTAMINE STIMULATED SWINE CAROTID MEDIA. N.L. McDaniel, C.M. Rembold, and R.A. Murphy. Univ. of Virginia School of Medicine, Charlottesville, VA 22908.

We tested the hypothesis that cGMP elevation relaxes smooth muscle by reducing myoplasmic [Ca^{2+}]. Ca^{2+} (nM) as estimated by aequorin, myosin light chain phosphorylation (MP, mol P_i/mol MLC_2 by 2D gel electrophoresis), cGMP (pM/mg wet weight by radioimmunoassay), and stress ($\times 10^5$ N/m^2) were measured in tissues incubated in vitro at 37° C. Histamine (H, 10 μM)-induced contractions were associated with increases in [Ca^{2+}], MP, and small increases in cGMP. Sodium nitroprusside (SNP, 10 and 100 μM) added 10 minutes after histamine was followed by increased cGMP and decreased [Ca^{2+}], MP and stress. Data are presented as means ± SEM, * = $p < 0.05$ different from H control (collected 15 minutes after H addition = 5 minutes after SNP).

Treatment	[cGMP]	[Ca^{2+}]	MP	Stress
Basal	0.03 ± 0.01	77 ± 7	0.09 ± 0.01	0.11 ± 0.02
H control	0.07 ± 0.02	145 ± 12	0.35 ± 0.03	1.44 ± 0.12
H + 10 μM SNP	0.43 ± 0.10 *	129 ± 4 *	0.12 ± 0.02 *	0.50 ± 0.16 *
H + 100 μM SNP	1.24 ± 0.12 *	123 ± 8 *	0.15 ± 0.02 *	0.38 ± 0.05 *

Pretreatment with 100 μM SNP did not change resting [Ca^{2+}] but attenuated both the transient and sustained elevations in [Ca^{2+}] and force induced by 10 μM histamine. These data suggest that SNP-induced elevations in cGMP decrease myoplasmic [Ca^{2+}] and MP, thereby producing relaxation. Supported by Markey Trust 025, NIH Grants 5 PO1 HL 19242, 2T32 HL07355, and 5 RO1 HL38918.

M-Pos20 DYNAMIC STIFFNESS OF ISOMETRICALLY CONTRACTING ARTERIAL SMOOTH MUSCLE FROM THE SPONTANEOUSLY HYPERTENSIVE RAT (SHR). C.S. Packer, S.J. Moore-Renholzberger and R.A. Meiss. Indiana University School of Medicine, Indianapolis, IN 46223

Arterial smooth muscle (ASM) from SHR shortens more (↑ΔL), shortens faster (↑V_{max}), but relaxes at a slower rate than normotensive Wistar-Kyoto rat (WKY) ASM. In addition, ↑V_{max} has been reported at a time in contraction when "latch" bridges could be operative. However, maximal isometric force development (P_o) is unchanged in SHR ASM. Even though the number of available crossbridges per cross-sectional area of muscle may be unchanged (as reflected in the unaltered P_o), the dynamic stiffness may be changed due to increased crossbridge cycling rate as indicated by ↑V_{max}. The objective of this study was to compare the dynamic stiffness of SHR and WKY caudal arterial smooth muscle strips during isometric contraction and relaxation. We examined the amplitude of force responses to very small (~20 um; ~40 Hz sinusoidal length oscillations applied to contracting and relaxing muscle. Inherent stiffness of isometrically relaxing WKY muscle was anomalously high ($p<0.05$). Comparison of SHR (n=7) with WKY (n=6) mean Stress/Strain versus Force (N/cm^2) curves revealed that the SHR muscle was less stiff ($p<0.05$) than the WKY muscle throughout both contraction and relaxation except at very low levels of developed force (i.e. except at onset of contraction and near completion of relaxation). These results imply differences between SHR and WKY dynamic crossbridge behaviour (attachment, detachment, etc.). Faster cycling bridges may spend less time attached and this could contribute to diminished dynamic stiffness.

Supported by the Canadian Heart Foundation and NIH Grant DK 34385.

M-Pos21 PHOSPHATASE INHIBITORS INCREASE SHORTENING CAPACITY, BUT NOT VELOCITY, IN SKINNED TRACHEAL SMOOTH MUSCLE. Siow-Kee Kong and Newman L. Stephens, Dept. of Physiology, University of Manitoba, Winnipeg, MB. R3E 0W3, Canada.

Previous reports have shown that increased airway smooth muscle shortening capacity is usually associated with increased velocity of shortening. In this study we report that under some circumstances, in skinned smooth muscle, shortening capacity is not dependent on shortening velocity. Canine tracheal smooth muscle (TSM) strips were skinned in buffer solution containing 1% Triton X-100, pH 7.0, at 25°C for at least two hours. The skinned smooth muscle can develop either isometric or isotonic contraction in a contracting buffer solution containing 10^{-5}M Ca^{++} and 2mM MgATP. The maximal shortening velocity (Vmax) of the skinned TSM can be obtained from quick-release experiments. Skinned TSM strips treated with NaF and p-Nitrophenyl phosphate disodium (PNPP), the phosphatase inhibitor and substrate, developed isometric tensions that were not different from controls. Vmax of the treated and control skinned TSM showed no significant difference. ATPase assay also showed that both PNPP and NaF did not have any effect on myofibrillar ATPase activity. However, the shortening capacity of treated skinned TSM at optimal length was about 20 to 25% more than that of the control counterpart. These results indicate that shortening capacity and velocity of skinned smooth muscle can function independently. The increased shortening capacity of the treated skinned TSM could be due to the increased phosphorylation of certain cytoskeletal proteins. It is speculated that these mechanisms could underlie the increased shortening capacity we have reported in airway smooth muscle from a canine model of allergic bronchospasm. (Supported by funds from the Amer. Counc. for Tobacco Research)

M-Pos22 ENDOTHELIN-INDUCED CONTRACTIONS OF SWINE CAROTID ARTERIES. S. Moreland and R.S. Moreland. The Squibb Institute for Medical Research, Department of Pharmacology, Princeton, NJ and Bockus Research Institute, Graduate Hospital, Philadelphia, PA.

Endothelin, a newly discovered peptide believed to be synthesized and released by endothelial cells, has potent vasoconstrictor activity (Yanagisawa *et al.*, Nature 332:411, 1988). If endothelin is the endothelial derived contracting factor, it is important to understand the intracellular events associated with activation by this agonist. The goals of this study were to examine the relationships between stress, myosin light chain (MLC) phosphorylation and maximal shortening velocity (V_o) during endothelin activation, and to determine if endothelin-induced contractions are supported by phosphorylated crossbridges or latchbridges. Strips of swine carotid media (≈ 180 μm thick) were mounted for determination of stress, V_o, and MLC phosphorylation levels. Endothelin (0.3 to 10 nM) induced concentration dependent contractions (ED_{50} = 1.5 ± 0.1 nM, n = 5) which were dependent on the presence of extracellular calcium. The maximal stress developed in response to 10 nM endothelin (2.3 ± 0.2 x 10^5 N/m^2, n = 11) was approximately equal to that developed in response to 110 mM KCl. Stimulation with KCl resulted in an immediate, but transient, increase in MLC phosphorylation and V_o concomitant with stress development. Later in the contraction, while stress was maintained, both MLC phosphorylation and V_o decreased to suprabasal levels. In contrast, endothelin caused a monotonic increase in MLC phosphorylation which peaked within 5 min of stimulation and remained high during the entire stimulation period (0.36 ± 0.03 mol P_i/mol MLC, n = 22). Even so, V_o remained low during the course of the contraction (range of 0.029 ± 0.005 to 0.041 ± 0.004 L_o/sec, n = 6). Thus, endothelin-induced contractions of intact swine carotid arteries represent a physiological situation in which changes in V_o do not parallel changes in MLC phosphorylation. If latchbridges are defined as slowly cycling crossbridges capable of supporting high levels of stress, the results of this study demonstrate that endothelin activates latchbridges. This study was supported, in part, by funds from the NIH, HL 37956 (RSM).

M-Pos23 E-AZA-ATP AS A PROBE OF THE ACTIVE SITE OF TURKEY GIZZARD MYOSIN. Leslie E. Sommerville and David J. Hartshorne. Bates College, Department of Chemistry, Lewiston, ME 02420 and University of Arizona, Department of Animal Science, Muscle Biology Group, Tucson, Az 85721.

Smooth muscle myosin can undergo a transition from a folded, 10S state, to an extended 6S state. Increased ATPase activity has been correlated with the this 10S to 6S transition. We have used the fluorescent ATP analog, E-aza-ATP, to probe the active site of turkey gizzard myosin. On addition of stoichiometric amounts of E-aza-ATP to myosin there was a rapid rise in the E-aza-ATP fluorescence. This enhanced emission was about 2 fold (maximum = 480 nm) and 6 fold (maximum = 460 nm) greater than unbound E-aza-ATP for E-aza-ATP bound to 10S and 6S myosin respectively. Under the conditions of these experiments all of the E-aza-ATP was bound, therefore the spectral differences reflect structural changes at the active site. The E-aza-ATP fluorescence intensity decreased as a single exponential for both 6S and 10S myosin with a rate constant of 0.095 sec^{-1} and 0.012 sec^{-1} respectively, at 25°C. These rate constants correlated with rate constants for the decrease of enhanced tryptophan fluorescence (10S; 0.01 sec^{-1} and 6S; 0.1 sec^{-1}) when stoichiometric amounts of E-aza-ATP were added and the turnover number for P_i when saturating amounts of E-aza-ATP were added (10S; 0.01 nmol/sec - mol active site and 6S; 0.08 nmol/sec - mol active site) at 25°C. The rates of hydrolysis of E-aza-ATP and ATP are quantitatively different but qualitatively E-aza-ATP and ATP appeared to bind in a similar way. E-aza-ATP was found to be a good probe for both, kinetic and structural changes, at the active site of turkey gizzard myosin. This work was supported by NIH Grants HL23615 and HL20984 (to D.J.H.) and NIH Postdoctoral Training Grant HL07249 (to L.E.S.).

M-Pos24 RELATIONSHIP BETWEEN LIGHT CHAIN PHOSPHORYLATION, FILAMENT ASSEMBLY AND ACTIN-ACTIVATED ATPase OF BLADDER MYOSIN. Mathew Samuel*, and Samuel Chacko, Department of Pathobiology, University of Pennsylvania, Philadelphia, PA 19104. (Introduced by Dr. R.E. Davies).

The effects of myosin phosphorylation, and filament formation on actin-activated ATPase was investigated using swine urinary bladder myosin which was phosphorylated at various levels using endogenous kinase prior to purification. Myosins at different levels of phosphorylation were reconstituted with smooth muscle actin or actin-tropomyosin (molar ratios M:A, 1:40; Tm:A, 1:6) and the ATPase activity was measured at varying free Mg^{2+} concentrations. On raising the free Mg^{2+} from 0.5 mM to 4 mM, the actin-activated ATPase activity increased at all levels of phosphorylation, resulting in a linear correlation between phosphorylation and actin-activated ATPase. Tropomyosin caused a 2-3 fold potentiation of actin-activated ATPase at all levels of phosphorylation. The difference in the acitivity between unphosphorylated myosin and myosin phosporylated to 50% decreased on raising the free Mg^{2+} from 4 mM and at 8 mM, the correlation curve was flat until the level of phosphorylation reached 50%. The ATPase activity increased linearly between 50% and 100% phosphorylation, indicating that at high Mg^{2+}, the actin-activated ATPase of the myosin increased only when both heads of the myosin became phosphorylated. At Mg^{2+} concentration of around 8 mM, the assembly of myosin filament, as determined by turbidity and sedimentation, was similar. In conclusion, the relationship between phosphorylation and actin-activated ATP hydrolysis is linear at low levels of free Mg^{2+}. The negative cooperativity, evident at high Mg^{2+} concentration, may be related to the filament assembly, which is compatible with low level of actin activation. Supported by NIH grants DK 3970 and HL 22264.

M-Pos25 PHOTOLABELLING OF GIZZARD MYOSIN WITH 3'-O-N-METHY ANTHRANILOYL-8-N_3-ATP. S. Maruta and M. Ikebe, Department of Physiology and Biophysics, Case Western Reserve University, Cleveland, OH 44106.

3'-O-(N-methyl anthraniloyl)-8-azido-ATP (Mant-8-N_3-ATP) was used as a photoprobe of the ATPase active site of smooth muscle myosin. Mant-8-N_3-ATP is known to form syn conformation with respect to the N-glycoside bond between adenine and ribose groups while ATP forms anti conformation. Mant-8-N_3-ATP was hydrolyzed by gizzard myosin, however, the properties of the hydrolysis are distinct from ATP. The rate of hydrolysis of Mant-8-N_3-ATP was little in the presence of EDTA and was much faster (10 times) than that of ATP in the presence of Mg^{2+} at high ionic strength. In the presence of either Mg^{2+} or Ca^{2+}, the 6S-10S transition of gizzard myosin was induced by Mant-8-N_3-ATP as is induced by ATP. However, the hydrolysis of Mant-8-N_3-ATP was not significantly affected by the 6S-10S transition while the hydrolysis of ATP was markedly influenced by the 6S-10S transition. In the presence of Mg^{2+}, gizzard myosin was irradiated with Mant-8-N_3-ATP in both the 6S and 10S conformations. In both conditions, 27 kDa fragment derived from the 29 kDa fragment of tryptic S-1 containing the N-terminus of heavy chain was labelled, and this labelling was completely inhibited by the addition of ATP. In contrast, Mant-8-N_3-ATP was incorporated to the C-terminal 20 kDa fragment of tryptic S-1 of skeletal muscle myosin. In the 10S conformation, the amount of incorporation to the 27 kDa fragment was about 2 times more than in the 6S conformation. Relatively large ATP independent binding to the 17 kDa light chain was also observed. The results suggest that the conformation of the active site of smooth muscle myosin is different from that of skeletal muscle myosin. (Supported by NIH, AHA, and Syntex).

M-Pos26 STABILITY OF STRUCTURAL DOMAINS OF SMOOTH MUSCLE MYOSIN ROD.

L. King*, S. S. Lehrer & J. Seidel, Boston Biomedical Research Institute, Boston MA. *Current Address, Department of Biochemistry, Chang Gung Medical College, Taiwan, Republic of China.

Gizzard myosin rod, an α-helical coiled-coil, shows two thermal and GdmCl-induced helix unfolding transitions in solutions containing 0.6M NaCl at neutral pH, monitored by circular dichroism (CD) at 222 nm. The first thermal transition which has a midpoint at 47° corresponds to ≈ 30 % helix loss. The second transition at 53° in which the helix is completely lost, is extremely sharp with a 10 % - 90 % span of 1°. To obtain information about the location of the unfolding domains and the nature of the intermediates, the single Cys of each chain located 43 amino acid residues from the head-rod junction (Yanagisawa et. al., J. Mol. Biol. 198, 143, 1987) was labeled with acrylodan, an environmentally sensitive fluorescence probe. The fluorescence spectral change was monitored at increasing temperature and [GdmCl]. It was found that the spectrum experiences a ≈ 10 nm blue shift associated with the first thermal and GdmCl transition. These data indicated that the Cys is located in the least stable part of the rod. The lack of a red spectral shift expected if acrylodan were exposed to solvent indicates that the environment of the labeled Cys in the unfolded region of the intermediate is not in a random coil conformation. (Supported by NIH).

M-Pos27 STABILITY AND PHOTOCHEMICAL PROPERTIES OF VANADATE TRAPPED NUCLEOTIDE COMPLEXES OF GIZZARD MYOSIN IN THE 6S AND 10S CONFORMATIONS. Douglas G. Cole and Ralph G. Yount, Biochemistry/Biophysics Program, Washington State University, Pullman, WA 99164-4660

The stability and photochemical properties of vanadate (V_i) trapped nucleotide complexes of the 6S and 10S conformations of gizzard myosin have been studied. The half-lives of both the 6S myosin•MgADP•V_i and 10S myosin•MgADP•V_i complexes in the dark are on the order of several days. Irradiation of the 6S or 10S complexes with UV light for 5 min photomodified the enzyme and destabilized the complexes. The photomodified 6S complex released nucleotide within minutes as has been observed in comparable experiments with skeletal myosin subfragment 1 (S1) (Grammer, J.C., Cremo, C.R., and Yount, R.G. (1988) *Biochemistry* **27**, in press). The photomodified 10S complex, however, was more stable and released nucleotide with a half-life of several hours. This slow off-rate is likely related to the known stable trapping of MgADP•P_i on 10S myosin (Cross, R.A., Cross, K.E., and Sobieszek, A. (1986) *EMBO J.* **5**, 2637). Reduction of photomodified 6S and 10S myosins by NaB^3H_4 resulted in the incorporation of ^3H into the protein. Similar experiments with S1 and NaB^3H_4 have led to the identification of Ser-180 as the photomodified amino acid (Grammer, J.C., Cremo, C., and Yount, R.G., these abstracts). Further characterization of the 10S V_i complex and photomodified enzyme are in progress. Supported by MDA and NIH (DK 05195).

M-Pos28 DIGESTION OF VASCULAR SMOOTH MUSCLE MYOSIN WITH CALPAIN II: IDENTIFICATION AND CHARACTERIZATION OF A NEW MYOSIN SUBFRAGMENT-1. R. C. Turner, P. McClelland, and D.R. Hathaway, Department.of Medicine, Indiana University School of Medicine, Indianapolis, IN 46202.

Vascular smooth muscle contains large amounts of calpain II (CDP), a Ca^{2+}-dependent thiol protease. In an effort to identify potential endogenous substrates of the protease, we have examined the effects of CDP on vascular myosin (VM). Both the heavy chain (HC) and the regulatory light chain (LC_{20}) were cleaved by CDP. LC_{20} was preferentially cleaved to yield an 18 kDa major fragment that remained bound to myosin. The cleavage site was identified by electroblotting the 18 kDa fragment from SDS gels onto PVDF paper and sequencing the transferred protein by automated gas phase methodology:

S*-S*-K-R-A-K-A-K-T*-T-K–↓–K-R-P-Q-R-T**-S**-N-V...

The location of the cleavage site between lysine residues 11 and 12 suggested that proteolysis by the CDP should selectively remove labeling of LC_{20} by PKc (*, PKc sites) while preserving the sites that are phosphorylated by myosin light chain kinase (**, MLCK sites). When LC_{20} was labeled by phosphorylation with PKc in the presence of [^{32}P]ATP, conversion of LC_{20} to the 18 kDa fragment was associated with loss of the [^{32}P] label. On the other hand, when labeling with MLCK was performed, CDP digestion of LC_{20} did not result in the loss of [^{32}P] label. The relationship between CDP digestion of myosin and actin-activated ATPase activity was determined. A progressive increase in actin-activated ATPase activity was associated with the generation of a low-salt soluble 65 kDa fragment of the HC. Following purification, this HC fragment contained the 18 kDa LC_{20} fragment and the essential light chain (LC_{17}). Its subunit composition and molecular weight resembled myosin subfragent-1 and a V_{max} of 2.2 sec^{-1} with a K_{app} for actin of 356 μM was determined. The amino terminus of the "CDP"-S1, like that generated from VM digested with Staphlococcal V8 protease, was unblocked although the amino terminal sequences of the two species of S1 were different:

"CDP"-S1: I-N-N-P-V-A-Q-A....
"V8" - S1: F-L-F-V-D-K-N-F....

We conclude that vascular calpain II can digest smooth muscle myosin producing a unique S1 species with a regulatory light chain that is devoid of PKc phosphorylation sites.

M-Pos29 TEMPERATURE DEPENDENCE OF P_i RELEASE FROM THE 10S CONFORMER OF SMOOTH MUSCLE MYOSIN.
D. Applegate, E. Harper*, K. D'Abreu*. Mt. Sinai Sch. of Med., N.Y., N.Y. 10029.

Cross et al. (EMBO.J. 5, 2637-2641, 1986) have shown that the 10S conformer of dephosphorylated gizzard smooth muscle myosin can effectively "trap" the products of ATP hydrolysis, ADP and P_i. The "trapped" products apparently stabilize the 10S conformer, inhibiting unfolding of the myosin molecule. Using protocols for kinetic measurements similar to these authors, we have found that the rate of release of P_i from the 10S conformer is strongly influenced by temperature. For example, under our experimental conditions, (0.15M KCl, 1mM $MgCl_2$, 1mM EGTA, 10mM Imid., pH 7.3, 1.1uM myosin), the $t_{\frac{1}{2}}$ for product release at 20°C and 30°C, respectively, are 60 and 10 minutes. Our preliminary data for rate constants for P_i release determined at temperatures ranging from 15°C to 33°C yield a linear Arrhenius plot. The activation energy calculated from the slope is surprisingly high (approximately 20 kcal/mole).

Measurements of light scattering at 90° were used to assess the influence of temperature on the rate of reassembly of filaments from folded myosin monomers following the removal of excess ATP. For all temperatures tested, there is a striking similarity between the kinetics of product release and filament re-assembly. The data provide strong support for the suggestion of Cross et al. (1986) that product release is an obligatory step preceding incorporation of a particular myosin molecule into a growing filament. Further, these data suggest that the stability of the folded species of smooth muscle myosin is highly temperature dependent. (Supported by NIH grant 1R29DK40154-01).

M-Pos30 TWO DIMENSIONAL ISOELECTRIC FOCUSING/GLYCEROL-UREA ELECTROPHORESIS RESOLVES PHOSPHORYLATION STATES AND ISOFORM TYPES OF THE MYOSIN 20 KD LIGHT CHAIN IN ARTERIAL SMOOTH MUSCLE.
B.D. Gaylinn and R.A. Murphy. Department of Physiology, School of Medicine, University of Virginia, Charlottesville, VA 22908.

Both one (urea-glycerol) and conventional two dimensional (IEF-SDS) gel electrophoretic systems are used to assay phosphorylation of the myosin regulatory light chain (LC_{20}). Urea-glycerol gels resolve one band corresponding to each phosphorylation state of LC_{20} (un-, mono-, and diphosphorylated) in the swine carotid media. IEF-SDS gels display the un- and monophosphorylated forms of the major LC_{20} isoform plus more acidic "satellite spots". These satellites contain a mixture of the diphosphorylated major LC_{20} isoform plus a coelectrophoresing minor nonmuscle-like LC_{20} isoform. The location of this minor LC_{20} isoform on urea-glycerol gels has been unclear. We resolved LC_{20} species that coelectrophorese on the convention gel systems by using two dimensional gels incorporating IEF followed by urea-glycerol electrophoresis. The new 2-D gel system demonstrates that the bands on one dimensional urea-glycerol gels each contain a mixture of the two LC_{20} isoforms that had previously been detected by the IEF-SDS gel system. Thus, phosphorylation measurements by the 1-D system give a weighted average of phosphorylation in both myosin isoforms, while the 2-D IEF-SDS system gives phosphorylation of the major isoform alone. Fortunately quantitations by the two techniques are equivalent due to the low abundance and similar phosphorylation levels of the minor isoform. Supported by USPHS grant 5-P01-HL19242.

M-Pos31 N-ETHYLMALEIMIDE-MODIFIED MYOSIN CREATES AN INTERNAL LOAD USING THE NITELLA-BASED IN VITRO MOTILITY ASSAY
Seiji Umemoto and James R. Sellers, NHLBI, NIH, Bethesda, MD 20892

We have been using the Nitella-based in vitro motility assay to study the regulation of smooth muscle and nonmuscle myosin movement. This system (Sheetz et al., Meth. Enzymol. 134, 531, 1986) appears to be a correlate of the unloaded shortening velocity of muscle fibers. In order to study the ability of these myosins to generate force in this in vitro assay, we used skeletal muscle myosin which was extensively modified with N-ethylmaleimide (NEM). This reaction results in a myosin that no longer hydrolyzes MgATP yet retains high affinity binding to actin. It has been proposed that its binding affinity for actin is similar to the affinity of myosin for actin in the absencse of ATP. We found that NEM treatment of skeletal muscle myosin completely abolished the ability of this myosin to move beads. When NEM-modified myosin was mixed with either skeletal muscle myosin or phosphorylated smooth muscle myosin, the velocity of the respective unmodified myosin was decreased. Varying the percentage of NEM-labelled myosin from 0 to 100% decreased the velocity in a dose dependent manner. A 50% decrease in velocity of skeletal muscle myosin is obtained when the percentage of NEM-modified myosin is about 30%. In contrast, a 50% decrease in the velocity of phosphorylated turkey gizzard smooth muscle myosin is not reached until the percentage of NEM-modified myosin is 50%. These data suggest that phosphorylated smooth muscle myosin may be capable of generating higher force per crossbridge than does skeletal muscle myosin.

M-Pos32 AGGREGATION OF CHICKEN GIZZARD MYOSIN IN A NEW 3-DIMENSIONAL, QUASI-CRYSTALLINE LATTICE DETECTED IN THIN SECTIONS.

S.S. Margossian, J.R. Sellers, S.C. Watkins and H.S. Slayter. Montefiore Medical Center, Bronx, NY 10467; NHLBI, NIH, Bethesda, MD 20892; and Dana Farber Cancer Institute, Boston, MA 02115

The ability of chicken gizzard myosin to form ordered aggregates was investigated under a variety of conditions. Paracrystals with 13.5 nm periodicity were obtained with control unphosphorylated myosin in buffers containing 10-20 mM $MgCl_2$ in the presence or absence of ATP. Aggregates of sidepolar filaments were formed by both phosphorylated and unphosphorylated myosins in 0.3 M KCl, pH 6.0, which upon sectioning, revealed a new pattern. The molecules associated through the heads forming a 20 nm thick plane with the tails projecting out radially established by immunoelectron microscopy of the preparations labelled with anti-S1 and anti-LMM antibodies coupled to gold. Frequently, these filaments were aligned with similar structures, generating a 2-dimensional crystalline sheet, with a head-to-head spacing of 210 nm. Unphosphorylated myosin, on the other hand, aggregated to form a 3-dimensional lattice with a 270 nm period. Oppositely directed myosin molecules were stacked on each other producing ribbon-like strips held together through non-covalent interactions between heads to generate a crystalline lattice. The planes corresponding to heads were 60 to 80 nm thick. Neither Mg^{++} nor ATP were essential for this unique form. Myosin with heavy chains cleaved at a single site by the myopathic hamster protease, could form the 2-D sheets, but not the 3-D lattice.

(Supported by NIH grant HL 26569 to SSM)

M-Pos33 PRIMARY SEQUENCE OF *DROSOPHILA MELANOGASTER* CYTOPLASMIC MYOSIN SUBFRAGMENT-1

Andrew S. Ketchum, C. Todd Stewart, and Daniel P. Kiehart, Department of Cellular and Developmental Biology, Harvard University, Cambridge, MA 02138.

We have sequenced the subfragment-1 region of the gene that encodes the non-muscle myosin heavy chain in *Drosophila melanogaster*. This is among the first metazoan cytoplasmic myosins studied at the primary sequence level, and it contains extensive homologies to other known myosins. Regions responsible for actin binding, ATPase activity, and light chain binding in the myosin protein show extensive homology with other myosins (Warrick and Spudich, Ann. Rev. Cell Biol., 3:379-421, 1987).

The ATP binding sequence (GESGAGKT) matches exactly all other known myosin sequences and is similar to other ATP binding proteins (e.g. *E. Coli* recA and adenylate kinase) and the overall 25kD/50kD/20kD domain structure is also evident. Interestingly, regions that are not well conserved among myosins are not well conserved between *Drosophila* non-muscle and muscle myosins.

The *Drosophila* subfragment-1 region has two cysteine residues that correspond to the SH1 and SH2 reactive sulfhydryl residues. This contrasts protozoan cytoplasmic myosin subfragment-1 regions which only have a cysteine at the SH2 position. (Supported by National Institute of Health grants GM33830 to D.P.K. and 2R01 GM33830-04 to A.S.K.).

M-Pos34 SOLUTION X-RAY SCATTERING STUDIES OF RABBIT MYOSIN SUBFRAGMENT-1.
M.GARRIGOS(*) and P. VACHETTE, (*)Service de Biophysique, Département de Biologie, CEN Saclay, 91191 Gif sur Yvette cedex, FRANCE; L.U.R.E,Bat 209 D, Université Paris-Sud 91405 Orsay Cedex, FRANCE. (Intr.by M.LE MAIRE).

We have studied rabbit myosin chymotryptic subfragment-1 (EDTA-S1) by Small-angle X-ray scattering (SAXS) using the D-24 station at the L.U.R.E synchroton radiation facility in Orsay.All protein samples were dialysed against Imidazole 50mM pH7.2, NaCl 0.1M, DTT 2mM, MgCl2 2mM and then applied on a TSK 3000 SW column equilibrated with the same buffer at room temperature. Protein samples were used immediately after being eluted from the HPLC column. The radius of gyration (Rg) and the intensity at the origin (Io) were obtained from a linear regression on a Guinier plot of the background-corrected intensities ranging from $1/70nm^{-1} < s < 1/16nm^{-1}$ (where $s=(2\sin\theta)/\lambda$, 2θ is the scattering angle and $\lambda=1.608$Å.). A 4mg/ml solution of ATCase (Mw=306Kd) from Escherichia coli was used as a reference to derive a value for the Mw of S1 samples. SAXS data for EDTA-S1 (at 20°C) showed no significant dependence of Rg values over the concentration range investigated (4 to 7mg/ml). We found Rg=(37±1)Å for EDTA-S1, a value significantly different from that found in previous studies (Rg=33Å, Mendelson, Nature(1982), 298.665). Such difference might be related to the HPLC purification step performed just before the X-ray experiment. Average Mw deduced from Io values from seven experiments at different protein concentrations was (100±7)Kd in good agreement with Mw determined by sedimentation equilibrium (Mw=106Kd). SAXS results on papain S1 as well as results obtained in the presence of bound MgATP on both S1 preparations will also be presented.

M-Pos35 MYOSIN FILAMENT ASSEMBLY PROBED WITH MONOCLONAL ANTIBODIES. Stephanie A. Silos and Donald A. Winkelmann, Department of Pathology, Robert Wood Johnson Medical School, Piscataway, New Jersey 08854.

Three anti-rod monoclonal antibodies were used to probe the interactions involved in myosin filament assembly, stability and structure. The epitopes defined by two of the antibodies (10F12.3 and 8G12.5) have been mapped to the S2 subfragment, and the epitope for the third (5C3.2) maps to the LMM subfragment, very near to the C-terminus of the rod. Myosin filaments (1 μm long) were formed by stepwise dilution of adult chicken pectoralis myosin to physiological salt conditions. Myosin was either incubated for 30 min. with IgG antibody prior to filament formation, or preformed filaments were incubated with antibody for periods of up to 24 hours. Electron microscopy revealed that the anti-LMM antibody (5C3.2) blocks normal filament assembly by forming stable core filaments, 0.27 μm long. This antibody does not appear to periodically label filaments, but does cause a slow depolymerization of long filaments to short 'cores'. The anti-S2 antibody, 10F12.3, also blocks filament assembly, forming 0.34 μm core filaments with a distinct labeling pattern which distinguishes them from the anti-LMM 'cores'. This anti-S2 antibody periodically labels long filaments with an apparent repeat of 14 nm and often bends filaments but does not cause depolymerization. In contrast, anti-S2 8G12.5 does not interfere with normal filament assembly or stability but does periodically label filaments. These results support the view that myosin filament formation is the consequence of multiple types of bonding interactions. The anti-LMM (5C3.2) and anti-S2 (10F12.3) antibodies block assembly at nucleation by forming stable core structures which do not undergo further elongation. This demonstrates the separability of the nucleation and elongation interactions. Furthermore, our observations confirm the conclusions of others concerning the importance of the C-terminus of the LMM subfragment in myosin filament assembly, and extend these observations by demonstrating that antibody binding to sites along the S2 subfragment can also destabilize post-nucleation assembly interactions.
(Supported by grants from the NIH and the MDA)

M-Pos36 VANADATE-PROMOTED PHOTOCLEAVAGE AT THE ACTIVE SITE OF MYOSIN SUB-FRAGMENT-1 (S1). Jean C. Grammer, Christine Cremo and Ralph G. Yount, Biochemistry/Biophysics Program, Washington State University, Pullman, WA 99164-4660.

Vanadate (Vi) forms a stable transition state-like complex with MgADP at the active site of myosin or S1. The S1·MgADP·Vi complex has a $t_{1/2}$ of days in the dark but is decomposed in min. by irradiation with light between 300-400 nm (J. Grammer, C. Cremo and R. Yount (1988) *Biochemistry* **27**, in press). Irradiation of the Vi complex specifically oxidizes the β–hydroxyl of Ser-180 in the consensus ATP binding sequence **GESGAGKT** to an aldehyde with concomitant release of Vi and ADP. Reduction of the aldehyde group with NaB^3H_4 places ^3H specifically on Ser-180. Formation of the [^{3}H]S1·MgADP·Vi complex and subsequent irradiation releases Vi and ADP and part of the ^3H as ^3H_2O. The photomodified S1 retraps MgADP and Vi but at a slower rate. Irradiation of this new complex releases Vi, ADP and the remaining ^3H as ^3H_2O with specific cleavage of the 95 kDa heavy chain into 21 kDa (NH_2 terminal) and 74 kDa (COOH terminal) fragments. These results indicate that further oxidation of the aldehyde form of Ser-180 leads to cleavage of the polypeptide backbone. Experiments are in progress to characterize the chemical nature of the cleavage. Supported by MDA and NIH (DK O5195).

M-Pos37 EXPRESSION AND SITE-DIRECTED MUTAGENESIS OF CHICKEN MYOSIN LC2 LIGHT CHAIN.
Lakshmi D. Saraswat and Susan Lowey, Rosenstiel Basic Medical Sciences Research Center,Brandeis University, Waltham, MA 02254.

The 19-kd light chain (LC2) is important in regulating the enzymatic activity of myosin in invertebrates and in smooth muscles. In order to study putative conformational changes in LC2, we have synthesized the chicken skeletal muscle light chain in Escherichia coli, and constructed three mutants in which either Pro-2, Ser-73 or Pro-94 has been replaced by cysteine. The LC2-encoding cDNA was isolated from clone L10/λgt11 (Reinach and Fischman, 1985) and ligated to the bacterial expression vector pKK233-2. Oligonucleotide-directed mutagenesis was carried out in M13mp19 single-stranded phage DNA. All cloned mutants were sequenced in their entirety to confirm that no changes other than the cysteine residues had occurred. Although full length, immunologically reactive LC2 could be synthesized using the pKK233-2 vector, the yield was poor and the light chain was readily cleaved in the N-terminal region during its isolation. To improve the yield, the LC2 cDNA was transferred to a vector containing the T7 RNA polymerase/promoter system (Tabor and Richardson, 1985), and grown in a protease-deficient strain of E. coli. In this system, a high level of expression of LC2 was obtained, and the protein could be isolated without proteolysis. The synthetic light chain can be bound to chicken myosin heavy chain after removal of native LC2 by immunoaffinity chromatography. By labeling the sulfhydryl residues in the mutant light chains with iodoacetamido fluorescein, it should be possible to map the location of the chain in the myosin head with anti-fluorescyl antibodies, as well as detect possible changes in the conformation of the light chain by fluorescence spectroscopy.

M-Pos38 Immunohistochemical examination of type 2B to type 2A transformation in chronically stimulated rabbit muscles.

K. Mabuchi, F. A. Sreter, and J. Gergely. Dept. of Muscle Res., Boston Biomedical Research Institute, Boston, MA, Depts. of Neurology and Anesthesia, Mass. General Hosp., and Dept. of Biol. Chem. and Mol. Pharmacol. and Dept. of Anesthesia, Harvard Med. School, Boston MA, 02114.

It has been documented that chronic indirect stimulation transforms fast-twitch mucles to slow-twitch mucles. In normal tibialis anterior (TA) muscles there exist two types of fast-twitch fibers--type 2B and type 2A. It has been suggestd that transformation of type 2Bto type 2A fibers precedes that of fast to slow fibers (Sreter et al., Exp. Neurol. 75, 95, 1982). Using monoclonal antibodies (McAbs) capable of distinguishing myosins in type 1, type 2A and type 2B fibers, we studied the transformation by phasic pattern (40Hz, 2.5 sec tetanus and 7.5 sec resting) of type 2B fibers to type 2A and type 1 fibers. After 3 days of stimulation number of fibers reactive with anti-type 2A myosin McAb were clearly increased.in the core region of TA. At day-6 almost all fast fibers contained type 2A myosin and some fibers in the core also contained both type 2A and type Imyosins, After 2 weeks type 1 myosin was present in peripheral fibers. By 4 weeks the type 2B to type 2A transformation was complete. Even when more than 90% of the fibers became type 1, a few type 2B fibers persisted in TA muscles stimulated for 7-8 weeks. No fibers reacted with both anti-slow and anti-type 2B McAbs at any stage of transformation. These observations indicate tat slow myosin cannot be expressed in type 2B fibers and type 2B fibers become type 2A fibers before changing to type 1 fibers. (Supported by grants from NIH (HL 5949) and MDA).

M-Pos39 TETRAMERIC VANADATE AND UV LIGHT CLEAVES MYOSIN SUBFRAGMENT-1 HEAVY CHAIN AT TWO SITES.
C. CREMO, J. GRAMMER, G. T. LONG AND R. G. YOUNT, BIOCHEMISTRY/BIOPHYSICS PROGRAM, WASHINGTON STATE UNIVERSITY, PULLMAN WA 99164-4660.

In the presence of mM concentrations of vanadate, UV light promotes cleavage of the S1 heavy chain at 2 distinct sites. One site (V1) is identical to the previously described active site cleavage at or near serine-180 (C. Cremo, J. Grammer and R. Yount (1988) Biochemistry 27, in press; also see abstract these meetings, J. Grammer et al.). Cleavage at the second site (V2), to give 75 kDa NH_2-terminal and 20 kDa COOH-terminal peptides, does not appear to be affected by nucleotides or divalent cations as does the V1 site. ^{51}V-NMR experiments indicate that the tetrameric species of vanadium $(V_4O_{13})^{-6}$ binds to S1 whereas no binding of either the monomeric $(VO_4)^{-3}$ or dimeric $(V_2O_7)^{-4}$ species could be detected. These results suggest that the bound tetrameric vanadate cleaves the S1 heavy chain upon irradiation with UV light. Irradiation of vanadate in Tris buffer without S1 caused a rapid decrease in the tetrameric vanadate signal. Concurrently there was a slower decrease in the remaining vanadium signals (mono, di and penta vanadate), indicating that UV light reduces V(V) species to relatively stable compounds in the V(IV) oxidation state. Vanadate irradiated in the absence of buffers did not appear to be reduced, suggesting a role for the Tris buffer to stabilize the V(IV) species. These reduced forms of vanadium were apparently not competent to cleave S1 as pre-irradiation of the buffered vanadate solutions decreased the extent of cleavage.

M-Pos40 TRYPSINOLYSIS ENHANCES ANTIBODY ACCESSIBILITY TO MYOSIN S1 EPITOPES. K. N. Rajasekharan and M. Burke, Department of Biology, Case Institute of Technology, Case Western Reserve University, Cleveland, OH 44106.

Limited trypsinolysis of skeletal myosin subfragment 1 (S1) results in the cleavage of the heavy chain at two sites of about 27 kDa and 75 kDa from the N-terminus. These cleavages - particularly the one at the 25/70 kDa site - have been shown to increase the accessibility of the N-terminus of the heavy chain to site specific anti-N-terminus antibodies and this increase has been suggested to result from an enhanced flexibility of the N-terminus brought about by the trypsinolysis [Chen, T. Liu, J. & Reisler, E., Biochem. Biophy. Res. Comm., 147, 369-374 (1987)]. We now show that the tryptic cleavage results in a more general increase in the accessibility of the antigenic epitopes on the cleaved myosin S1. On competitive ELISA experiments with immobolized S1, tryptically cleaved S1 was found to compete more effectively compared to intact S1 for monoclonal antibodies raised against epitopes located on the 27-kDa and 50-kDa segments of S1. Thus the increase in epitope accessibility upon tryptic cleavage is seen to manifest also on regions located further away from the N-terminus. If the increased epitope accessibility could be equated to an increase in the flexibility in that region, then the trypsinolysis seems to increase the flexibility in regions of the 27-kDa and 50-kDa segments of S1. The binding of actin did not affect the above observations. The mild denaturation of S1 by methanol or by heating was found to increase the accessibility of epitopes in the 50-kDa segment to anti-50-kDa MAb but not that of the epitopes in 27-kDa segment to anti-27-kDa MAb. (Supported by NIH grant NS151319)

M-Pos41 A CONSENSUS SEQUENCE FOR MYOSIN ROD

Richard D. Ludescher, Department of Food Science, Cook College, Rutgers University, New Brunswick, NJ 08903

A consensus amino acids sequence of myosin rod has been generated by comparing published sequences of mematode, rabbit (skeletal and cardiac), chicken, rat, and human myosin. This approach attempts to identify regions of specific function in the coiled coil in which amino acids are conserved. In a continuous stretch of 1098 residues, beginning with a conserved proline (P 850 in nematode numbering), 39% of the amino acids are identical in the six sequences and an additional 21% are similar (all but one identical with a conservative substitution for the odd residue). Only one deletion, which occurs at position 919 (nematode numbering) of the skeletal sequence, is necessary to align the sequences.

There are several interesting features to the consensus sequence. The only tryptophans found in the rod sequences are fully conserved at sites W1383 and W1468 (both hydrophobic d sites in the heptad analysis). Three of the four "skip" residues, necessary to maintain the proper heptad repeat, are identical (E1397, E1594, and G1819). The fourth skip residue, G1819, is one of a fully conserved GLY-GLY pair (G1819-G1820) that is embedded in a stretch of 21 residues (1808-1828) of which 81% are identical. The two arginines that are thought to delimit the proteolysis sensitive hinge of rabbit skeletal myosin, R1138 and R1291, are fully conserved. There is also a 77 amino acid region with only 21% identical and 10% similar amino acids centered around the putative hinge/LMM junction at R1291. Although the heptad repeat sites e and g, which are thought to interact via charges, show high charge conservation (39% of the sites), the charges appear to pair in a random fashion and like-charge pairs actually outnumber the unlike-charge pairs 15 to 12.

M-Pos42 INTERMOLECULAR ASSOCIATION BETWEEN MYOSIN HEADS ON RELAXED THICK FILAMENTS FROM SCALLOP & FISH STRIATED MUSCLES. R.J.C. Levine, P.D. Chantler, R.W.Kensler & R.G. Yount., Dept. Anatomy, Med. College Pa, Philadelphia PA 19129 & Biochemistry/Biophysics Program, Wash. State Univ., Pullman WA.

Using the bifunctional agent, $Bis_{22}ATP \cdot V_1$ to cross-link the active sites of the 2 myosin heads in each surface subunit on Limulus thick filaments, we previously showed that these heads originate from axially sequential myosin molecules (J.Cell Biol. 107:in press,'88), confirming the predictions of 3-D reconstructions of relaxed thick filaments from chelicerate arthropod muscles (Stewart et al. J. Cell Biol. 101:402,'85; Crowther et al. J.Mol. Biol. 184:429,'85). We have now used the same cross-linker to examine the situation on thick filaments from Aequipecten and fish striated muscles; available reconstructions of these filaments are not at a resolution sufficient to predict if the 2 heads /helical subunit are of inter- or intramolecular origin.

Experimental filaments with good relaxed helical order were first exposed to rigor buffer to remove bound ATP, then incubated, first on $Bis_{22}ATP$ alone, then on cross-linker plus V_1, and finally exposed to 0.6M KCl. Control filaments were either exposed to high salt from the relaxed state, or were treated as the experimentals, but were incubated on rigor buffer plus 2mM DTT (severs the -SS- in the cross-linker)prior to exposure to high salt. Both scallop and fish filaments that had their active sites cross-linked retained all surface myosin even after 15' on 0.6M KCl, whereas high salt caused severe disruption of control filaments. These results suggest that intermolecular association between myosin heads arising from axially sequential molecules occurs on these filaments, too. Supported by USPHS grants: AR33302, AR 30442, HL 15835 to The Penna. Muscle Institute & AHA grant 870688.

M-Pos43 DEVELOPMENTAL MYOSIN HEAVY CHAIN SPECIES IN THE AVIAN PECTORALIS MAJOR MUSCLE.
J.I. Rushbrook, C. Weiss and T.-T. Yao. Department of Biochemistry, SUNY Health Science Center at Brooklyn, New York 11203.

Myosin heavy chain species in the developing avian pectoralis major muscle have been explored using high resolution anion-exchange chromatography of chymotryptic subfragment-1 (S-1) species. At 15 days in ovo, four major S-1(LC1) species were identified. One of these became the predominant form in the 19 day in ovo - 1 day post-hatch period. This peri-hatching species then gave way to the post-hatch form, the major species between 8 days - 20 days post-hatch. The adult form generally was apparent at 20 days post-hatch and constituted about 30% of the total at 32 days post-hatch. The structural relationships among the various species are being investigated using HPLC of cyanogen bromide fragments followed by N-terminal amino acid sequencing.

M-Pos44 FORMATION AND CHARACTERIZATION OF SMOOTH MYOSIN 20 kDa LC AND SKELETAL MYOSIN HYBRIDS. LOCATION OF PHOTOCROSSLINKS FROM THE LIGHT CHAIN CYS-108 AND THE HEAVY CHAIN.
Morita, J., Rajasekharan, K. N., Ikebe, M., Mayadevi, M., and Burke, M. Department of Physiology and Biophysics and Department of Biology, Case Western Reserve University, Cleveland, OH 44106.

Experiments are described to enable smooth myosin 20 kDa light chain and endogeneous DTNB light chain to be exchanged into skeletal myosin in a stoichiometric fashion. The resulting myosin hybrids retain their actin-activated MgATPase activities. Unlike the situation in smooth myosin, dephosphorylation of the smooth light chain in the skeletal hybrid does not bring about the 6S to 10S transition suggesting that this transformation may also depend on the nature of the heavy chain subunit. DTNB and smooth 20 kDa light chains pre-modified at their cysteinyl residues with 4-(N-maleimido)benzophenone can also be exchanged stoichiometrically into skeletal myosin and, on subsequent photolysis of the isolated myosin, photocrosslinking between these light chains and the heavy chains can be detected by SDS PAGE analysis. By immuno-peptide mapping with a monoclonal antibody to the N-terminal 23 residues of the skeletal heavy chain, it is found that the crosslink is made to sites in the heavy chain located more than 95 kDa from the N-terminus.(Supported by grants from NIH, AHA and Syntex)